이학박사 학위논문

Regulation of osteoclastogenesis by lipoteichoic acid and adiponectin

리포테이코산과 아디포넥틴에 의한 파골세포의 분화 조절

2015 년 2 월

서울대학교 대학원

치의과학과 면역 및 분자미생물 전공

양 지 현

Regulation of osteoclastogenesis by lipoteichoic acid and adiponectin

by

Jihyun Yang

Under the supervision of

Professor Seung Hyun Han, Ph. D.

A Thesis Submitted in Partial Fulfillment of

the Requirements for the Degree of

Doctor of Philosophy

February 2015

School of Dentistry

Graduate School

Seoul National University

ABSTRACT

Regulation of osteoclastogenesis by lipoteichoic acid and adiponectin

Jihyun Yang

Department of Dental Science, Major of Immunology and Molecular Microbiology in Dentistry, School of dentistry, Seoul National University
(Supervised by Professor **Seung Hyun Han, Ph. D.**)

Objectives

Bone homeostasis is maintained by a balance between bone-resolving osteoclasts and bone-forming osteoblasts. Osteoclasts are derived from monocyte/macrophage lineages of hematopoietic stem cells, whereas osteoblasts are derived from mesenchymal stem cells which are likely to differentiate into adipocytes. Because the differentiation of osteoclasts and osteoblasts is important for maintaining appropriate bone metabolism, disruption of the differentiation can result in bone diseases such as bacteria-induced bone destruction and osteoporosis. Bacterial infection triggers inflammatory bone destruction resulting from excessive osteoclast differentiation, and microbe-associated molecular patterns (MAMPs) expressed on bacteria are known to induce inflammatory responses. Lipoteichoic acid (LTA) is considered as a major virulence factor expressed on the cell wall of Gram-positive bacteria, but little is known about its effect on the osteoclastogenesis. On the other hand, osteoporosis is known to be a representative bone disease accompanying reduced bone mass with increased bone marrow adiposity. Adiponectin is the member of adipokines secreted primarily from adipocytes and plays an important role in the regulation of metabolic processes, but its role in osteoclastogenesis is still uncertain. In the present study, the roles of LTA and adiponectin in the regulation of osteoclastogenesis and the action mechanisms were investigated.

Methods

Ethanol-inactivated wild-type and LTA-deficient *Staphylococcus aureus* were prepared and LTA was purified from *S. aureus*. Mice were intraperitoneally administered with ethanol-inactivated bacteria. Mouse calvarial bone was implanted with collagen sheet soaked in LTA and/or a synthetic peptide Pam2CSK4 mimicking Gram-positive bacterial lipoproteins. Bone marrow-derived macrophages (BMMs) were prepared from stroma-free bone marrow cells (BMs) by incubating with macrophage colony-stimulating factor (M-CSF), and the BMMs were further differentiated into osteoclasts by incubating with M-CSF and receptor activator of nuclear factor κB ligand (RANKL) in the presence or absence of the activated bacteria or LTA. Committed osteoclast precursors were prepared from BMMs by incubating with RANKL and M-CSF. The committed osteoclast precursors were stimulated with LTA and/or osteoclast-inducing factors, such as bacteria, Pam2CSK4, lipopolysaccharide (LPS), TNF-α, and RANKL, in the presence of M-CSF.

To investigate the role of adiponectin in osteoclastogenesis, wild-type and adiponectin-deficient mice were used. Osteoblast precursors were isolated from the calvaria of one-day-old mice and incubated with ascorbic acid and β-glycerophosphate to induce osteoblast differentiation. For induction of adipocyte differentiation, osteoblast precursors were incubated with dexamethasone, insulin, and 3-isobutyl-1-methylxanthine. BMMs were prepared from stroma-free BMs by incubating with granulocyte/macrophage colony-stimulating factor (GM-CSF) for M1 macrophages or M-CSF for M2 macrophages. To examine osteoclast differentiation, the BMMs were incubated with M-CSF and RANKL or co-cultured with osteoblast precursors. RANKL-induced bone destruction was made by intraperitoneal administration or by implantation on mouse calvarial bone.

Bone parameters of the femur and the calvaria were analyzed by micro-computed tomography. Osteoclast differentiation and bone resorption capacity were evaluated by enumerating tartrate-resistant acid phosphatase (TRAP)-positive multinucleated cells (MNCs) and by measuring the areas of resorption pits. Expression of cell surface proteins, such as TLR2, CD14, c-Fms, RANK, and TREM2, was analyzed by flow cytometry. Osteoblast differentiation was evaluated by staining with alkaline phosphatase and Alizarin Red S. Adipocyte differentiation was evaluated by staining with Oil

Red O. Expression of RANKL, OPG, IL-6, TNF-α, and IL-10 in the culture supernatants, the bone marrow extracellular fluids, or the serum was measured by enzyme-linked immunosorbent assay. Intracellular signaling pathways were determined by Western blotting, electrophoretic mobility shift assay, or immunoprecipitation.

Results

LTA-deficient *S. aureus* augmented massive bone destruction compared with wild-type *S. aureus*. Consistently, the LTA-deficient *S. aureus* increased the number of TRAP-positive MNCs. LTA alone affected neither differentiation of committed osteoclast precursors nor bone destruction. However, LTA inhibited differentiation of BMMs into TRAP-positive MNCs in response to RANKL. In contrast, LTA augmented phagocytic and inflammatory potential of the BMMs. The inhibitory effect of LTA on RANKL-induced osteoclastogenesis was mediated by attenuated activation of ERK, JNK, and AP-1 through toll-like receptor 2 (TLR2) with partial involvement of MyD88. In addition to BMMs, LTA also inhibited differentiation of committed osteoclast precursors into TRAP-positive MNCs triggered by *S. aureus*, Pam2CSK4, LPS, TNF-α, or RANKL. The inhibitory effect of LTA was not altered in the osteoclasts derived from mice lacking TLR2. LTA suppressed activation of both MAPKs and actin polymerization. Taken together, these results suggest that LTA inhibits not only M-CSF/RANKL-mediated osteoclastogenesis from macrophages through TLR2-dependent pathways but also osteoclastogenesis from committed osteoclast precursors triggered by TLR ligands, pro-inflammatory cytokines, and RANKL through TLR2-independent pathways.

Adiponectin-deficient mice exhibited a decrease of bone mass but, instead, an increase of bone marrow adiposity. Bone histomorphometric analysis also demonstrated that the bone of adiponectin-deficient mice showed an increase of bone resorption, a decrease of bone formation, and an increase of adiposity formation. Concordant with the *in vivo* results, adiponectin-deficient osteoblast precursors were scarcely differentiated into osteoblasts but, instead, efficiently differentiated into adipocytes. However, unlike the *in vivo* results, adiponectin-deficient BMMs were hardly differentiated into TRAP-positive MNCs. Both formation of bone resorption pits and DNA-binding activities of AP-1 and NFATc1 were reduced in the adiponectin-deficient BMMs. The

weak osteoclastogenic potential of the adiponectin-deficient BMMs was associated with properties of M1 macrophages. M1 macrophages were barely differentiated into osteoclasts by attenuating activation of NFATc1 conferred by the increased expression of IRF5. However, when adiponectin-deficient BMMs were co-cultured with adiponectin-deficient osteoblast precursors, the number of TRAP-positive MNCs was increased. In addition, a RANKL/OPG ratio was up-regulated under the same condition. The up-regulated RANKL/OPG ratio was also observed in bone marrow extracellular fluid of adiponectin-deficient mice. Indeed, RANKL-induced bone destruction was facilitated in the adiponectin-deficient mice. These results suggest that adiponectin is an important factor inhibiting osteoclastogenesis by down-regulation of RANKL/OPG ratio, consequently contributing to an increase of bone mass.

Conclusion

Controlling the osteoclastogenesis is important for an efficient treatment or prevention of bone diseases. Therefore, it is important to identify the molecular targets controlling osteoclastogenesis and to characterize their regulatory mechanisms for osteoclastogenesis. The present study demonstrated the inhibitory roles of LTA and adiponectin in osteoclastogenesis. Although LTA alone affected neither osteoclast differentiation from committed osteoclast precursors nor bone mass, LTA inhibited not only M-CSF/RANKL-induced osteoclast differentiation from macrophages but also TLR ligands, TNF-α, and RANKL-induced osteoclastogenesis from committed osteoclast precursors, consequently resulting in suppression of bone resorption. Adiponectin deficiency enhanced osteoclast differentiation by down-regulation of RANKL/OPG ratio and also attenuated osteoblast differentiation by skewed differential potential of osteoblast precursors toward adipocytes. Conclusively, LTA and adiponectin might be important factors capable of inhibiting osteoclastogenesis and could be potential target molecules controlling bone diseases accompanying excessive generation of osteoclasts.

Keywords: Osteoclast, Macrophage, Committed osteoclast precursor, Lipoteichoic acid, Adiponectin

Student number: 2008-30634

CONTENTS

List of Figures

List of tables

Abbreviations

α-MEM	alpha-minimum essential medium
AP-1	activator protein 1
APC	allophycocyanin
APN	adiponectin
BMP6	bone morphogenetic protein 6
BMM	bone marrow-derived macrophage
BSA	bovine serum albumin
BSP	bone sialoprotein
CD	cluster of differentiation
CREB	cAMP response element-binding protein
CTR	calcitonin receptor
DMSO	dimethyl sulfoxide
EDTA	ethylenediaminetetraacetic acid
EMSA	electrophoretic mobility shift assay
ELISA	enzyme-linked immunosorbent assay
ERK	extracellular signal-regulated kinase
FBS	certified fetal bovine serum
FITC	fluorescein isothiocyanate
GM-CSF	granulocyte/macrophage colony-stimulating factor
HBSS	Hanks' balanced salt solution
HEPES	4-(2-hydroxyethyl)-1-piperazineethanesulfonic acid
HRP	horseradish peroxidase
H&E	hematoxylin and eosin
IBMX	3-isobutyl-1-Methylxanthine
Ig	immunoglobulin
IGF-1	insulin-like growth factor-1
IFN-γ	interferon-γ
IRF	interferon regulatory factor
JNK	c-Jun N-terminal kinase

LB	Luria-Bertani
LPS	lipopolysaccharide
LTA	lipoteichoic acid
MALDI-TOF	matrix assisted laser desorption/ionization time-of-flight
MAMP	microbe-associated molecular pattern
MAPK	mitogen-activated protein kinase
M-CSF	macrophage colony-stimulating factor
MFI	Mean fluorescence intensity
MMP9	matrix metalloproteinase 9
MNC	multinucleated cell
MTT	3-[4,5-dimethylthiazol-2-yl]-2,5-diphenyltetrazolium bromide
MyD88	myeloid differentiation primary response gene 88
NF-Kb	nuclear factor-kappa B
NFATc1	nuclear factor of activated T cells 1
NLR	NOD-like receptor
OASS	osteoclast activity assay substrate
OPG	osteoprotegerin
OCN	osteocalcin
OCCAR	osteoclast-associated receptor
PAM2	PAM2CSK4
PBS	phosphate-buffered saline
PE	phycoerythrin
PVDF	polyvinylidene difluoride
PerCP	peridinin Chlorophyll Protein Complex
PGN	peptidoglycan
PPAR γ	peroxisome proliferator-activated receptor γ
PRR	pattern-recognition receptor
RANK	receptor activator of nuclear factor κB
RANKL	receptor activator of nuclear factor κB ligand
RBC	red blood cell
RT-PCR	reverse transcription-polymerase chain reaction
S1P	sphingosin-1-phsophate

SDS	sodium dodecyl sulfate
STAT	signal transducer and activator of transcription
TGE	Tris-Glycine-EDTA
TGF-β	transforming growth factor-β
Th	helper T lymphocyte
Treg	regulatory T lymphocyte
TRAP	tartrate-resistant acid phosphatase
TREM-2	triggering receptor by expressed myeloid cells-2
TLR	toll-like receptor
WT	wild-type

Chapter I. Introduction

1. Bone and osteoclastogenesis

1.1. Bone remodeling

Bone is an important tissue responsible for structural support, protection of organs, hematopoiesis, and storage of inorganic elements. Bone remodeling is tightly regulated through a balance between bone-resolving osteoclasts and bone-forming osteoblasts to maintain bone homeostasis (Fig. 1) [1]. Under environmental changes such as hormonal changes and mechanical stress, hematopoietic stem cells can differentiate into osteoclast precursors [2]. The osteoclast precursors attach to the bone surface and further differentiate into osteoclasts that possess bone resorption capacity [3, 4]. At the end of the bone resorption phase, the mature osteoclasts secret bone morphogenetic protein 6 (BMP6) and sphingosin-1-phsophate (S1P) to recruit osteoblast precursors that are derived from mesenchymal stem cells. As the bone matrix is degraded, growth factors such as insulin-like growth factor-1 (IGF-1) and transforming growth factor-β (TGF-β) are released to promote osteoblast differentiation [5, 6]. Unlike osteoclasts, osteoblasts are responsible for bone formation and mineralization by producing bone matrix proteins such as type I collagen, bone sialoprotein (BSP), and osteocalcin (OCN) [2]. After the mineralization, some of the osteoblasts are converted into lining cells or osteocytes [1]. Several reports have demonstrated that bone remodeling is controlled by internal factors such as hormones, adipokines, and cytokines, and external factors such as microbes and microbial components [2]. Also, bone remodeling can be regulated by adjacent cells in the bone microenvironment such as adipocytes, B lymphocytes, and T lymphocytes [2].

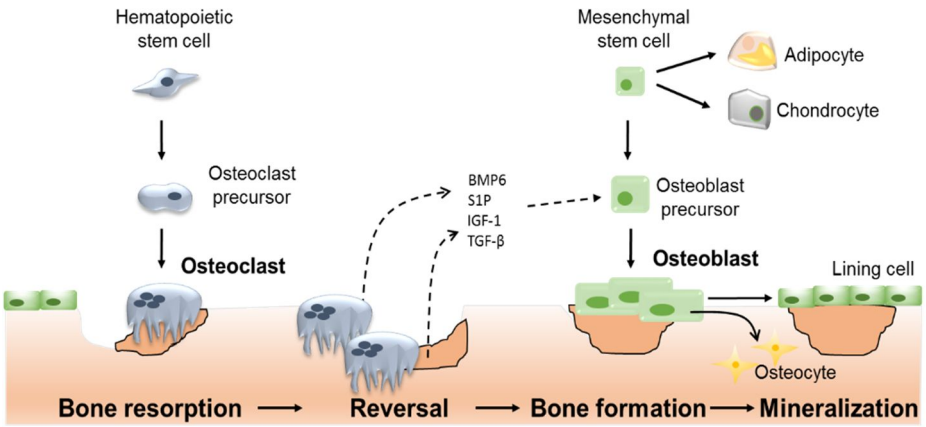

Figure 1. Bone remodeling

Bone remodeling is a lifelong process involving sequential steps of bone resorption, reversal, bone formation, and mineralization. Upon exposure to external or internal stimuli, osteoclasts are differentiated from monocytes/macrophages of hematopoietic cell lineages and degrade bone matrix by producing proteolytic enzymes. At the end of the bone resorption phase, osteogenic factors such as BMP6, SP-1, IGF, and TGF-β are secreted from the osteoclasts and the bone matrix to recruit mesenchymal stem cells and promote osteoblast differentiation. After mineralization, some of the osteoblasts are converted into lining cells or osteocytes. BMP6, bone morphogenetic protein 6. S1P, sphingosin-1-phsophate. IGF-1, insulin-like growth factor-1. TGF-β, transforming growth factor-β.

1.2. Bone diseases

Regulation of osteoclasts and osteoblasts are pivotal for appropriate bone remodeling [2]. Thus, disruption of osteoclast and/or osteoblast differentiation can result in a variety of bone diseases [7]. Notably, excessive generation of osteoclast is frequently found in several bone diseases. For instance, osteoporosis is the most common bone disease [8, 9]. Osteoporosis is considered as a significant public health problem worldwide because of increasing life expectancy and aging [8, 9]. It is characterized by reduced bone mass through excessive bone resorption and attenuated bone formation. Also, increased bone marrow adiposity is known to be a typical feature of osteoporosis [8], because vacant bone marrow space generated by excessive bone resorption is occupied by adipocytes [8, 9]. Since both adipocytes and osteoblasts are derived from common mesenchymal cell lineages, the increased bone marrow adiposity is associated with skewing differentiation potential of mesenchymal cells into adipocytes rather than osteoblasts [8]. Inflammatory bone diseases such as arthritis, osteomyelitis, and periodontitis are also accompanied by excessive bone destruction [10]. Notably, bacterial infections often cause various inflammatory bone diseases [11]. Osteomyelitis is the one of inflammatory bone diseases caused by bacterial infection, in particular *Staphylococcus aureus* [12]. It occurs commonly in children and elderly people [12]. Recently, osteomyelitis is known to be one of the most frequent infections of the diabetic patients with a foot wound [13]. Since excessive generation of osteoclasts is frequently found in several bone diseases, osteoclasts and their precursors can be exposed to distinct factors present in the pathological conditions resulting in uncontrolled osteoclastogenesis. Therefore, understanding their effects on osteoclastogenesis is important to control the mechanism of bone diseases and developing target molecules for bone diseases.

1.3. Osteoclastogenesis

Osteoclasts are specialized multinucleated cells (MNCs) with bone resorptive capacity [4]. Macrophage colony-stimulating factor (M-CSF) and receptor activator of nuclear factor κB ligand (RANKL) are required for osteoclast differentiation and activation, and they are largely produced from osteoblasts (Fig. 2) [4]. M-CSF supports proliferation, differentiation, and survival of osteoclast precursors. On the other hand, RANKL activates osteoclast differentiation through intracellular signaling pathways such as mitogen-activated protein kinases (MAPKs), nuclear factor-kappa B (NF-κB), and cAMP response element-binding protein (CREB) followed by induction of master transcription factors such as c-Fos and nuclear factor of activated T cells 1 (NFATc1) [14, 15]. RANK-RANKL signaling can be inhibited by osteoprotegerin (OPG) that is an antagonistic decoy receptor for RANKL and secreted from osteoblasts [3, 16]. Also, osteoclastogenesis requires co-stimulatory signal through osteoclast-associated receptor (OSCAR) and triggering receptor by expressed myeloid cells-2 (TREM2) [17, 18]. The co-stimulatory signal efficiently activates NFATc1 by sustaining CREB activation via calcium oscillation [18, 19]. The activated NFATc1 elicits development of mature osteoclasts by augmenting tartrate resistant acid phosphatase (TRAP), cathepsin K, and matrix metalloproteinase 9 (MMP9) [20].

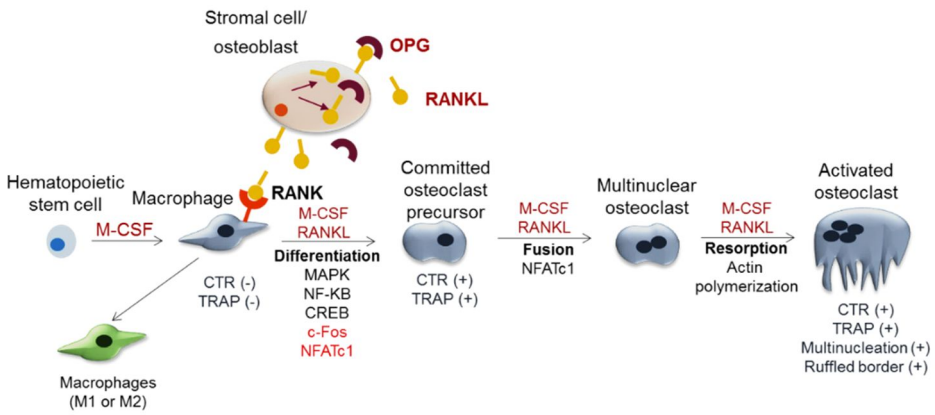

Figure 2. Osteoclastogenesis

Osteoclasts are differentiated from macrophages of hematopoietic cell lineages. Osteoclast precursors, macrophages, are able to polarize toward inflammatory M1 macrophages or anti-inflammatory M2 macrophages. Osteoclastogenesis consists of multiple steps, including differentiation of macrophages into committed osteoclast precursors, fusion of the mononuclear osteoclast precursors into multinuclear osteoclasts, and activation of osteoclasts to resorb bone. M-CSF and RANKL are primarily secreted from stromal cells and osteoblasts, and they facilitate osteoclastogenesis. Inhibition of this process occurs through the action of the soluble OPG secreted from stromal cells and osteoblasts. Expression of CTR and TRAP is absent in the macrophages but is gradually is increased during osteoclastogenesis. M-CSF, macrophage-colony stimulating factor. RANKL, receptor activator of nuclear factor κB ligand. CTR, calcitonin receptor, TRAP, tartrate resistant acid phosphatase.

1.3.1. Macrophages

Osteoclasts are differentiated from macrophages of hematopoietic cell lineages [14]. Macrophages act as major immune cells playing phagocytosis, cytokine production, and antigen presentation in the innate immune responses as well as osteoclast precursors [14]. The macrophages are able to polarize toward M1 or M2 macrophages for an effective response to the environmental changes (Table 1) [21, 22]. In steady state, macrophages exhibit M2-like cells with anti-inflammatory activity in response to M-CSF secreted from fibroblasts and stromal cells [23, 24]. Upon bacterial or viral infections, however, macrophages are exposed to granulocyte/macrophage colony-stimulating factor (GM-CSF), IFN-γ, or lipopolysaccharide (LPS), and the cells are rapidly polarized toward inflammatory M1 macrophages [21, 23]. The M1 macrophages trigger inflammatory responses by inducing pro-inflammatory cytokines and producing reactive oxygen species [25]. In contrast, anti-inflammatory M2 macrophages are activated by parasitic products such as IL-4 and IL-13 as well as parasitic infection [21, 22]. In addition, M2 macrophages are induced by IL-10, TGF-β, and glucocorticoids. The M2 macrophages participate in immune suppression and tissue remodeling [21, 22]. Several reports have demonstrated that various transcription factors are associated with macrophage polarization [21]. For instance, M1 macrophages are induced by interferon regulatory factor 5 (IRF5), IRF8, or STAT1, while M2 macrophages are activated by IRF4 or PPARγ [21]. Among the transcription factors, IRF5 is crucial for macrophage conversion capable of repolarizing from M1 to M2 or from M2 to M1 macrophages, because IRF5 induces M1-specific genes but inhibits M2-specific genes [26]. With respect to the osteoclastogenesis, M-CSF-induced M2 macrophages have been used as general osteoclast precursors [27, 28] although the different subtypes of macrophages can possess osteoclastogenic potential.

Table 1. M1 and M2 macrophages

	M1 macrophage	M2 macrophage
Stimuli	GM-CSF IFN- γ IFN-γ + LPS	M-CSF IL-4 or IL-13 (M2a) Immune complex + LPS (M2b) IL-10 (M2c)
Transcription factors	IRF5 IRF8 STAT1	IRF4 PPARγ STAT6
Secondary products	IL-6^{high} IL-12^{high} IL-23^{high} IL-10^{low} Arginase II iNOS	IL-6^{low} IL-12^{low} IL-23^{low} IL-10^{high} Arginase I
Phenotypes	cluster of differentiation 86 (CD86)^{high} CD80^{high} MHC class II^{high} CD206^{low}	CD86^{low} CD80^{low} MHC class II^{low} CD206^{high}
Functions	Inflammatory responses Host defense Killing of intracellular pathogens High phagocytic capacity Secretion of degradative enzymes Promotion of Th1 response	Anti-inflammatory responses Resolution of inflammation Anti-parasitic function (M2a) Tissue repair Matrix remodeling Promotion of Th2 response (M2a) Expansion of Treg

1.3.2. Macrophages and committed osteoclast precursors

During RANKL-induced osteoclastogenesis, macrophages sequentially differentiate into committed osteoclast precursors followed by osteoclasts [29]. Committed osteoclast precursors are TRAP-positive and mononucleated cells. Two types of osteoclast precursors, macrophages and committed osteoclast precursors, possess different osteoclastogenic properties. For instance, differentiation of macrophages into osteoclasts is likely to be inhibited by microbes and their components [30]. In contrast, committed osteoclast precursors tend to efficiently differentiate into osteoclasts in response to microbes and their components [31]. In addition, two types of osteoclast precursors have different immunological properties. The committed osteoclast precursors possess weak phagocytic and inflammatory capacities compared with the macrophages [29, 31, 32]. Recently, proportion of the osteoclast precursor subtypes is poorly investigated in the bone microenvironment.

1.3.3. Regulation of osteoclastogenesis

Several reports have demonstrated that osteoclastogenesis is regulated by several factors such as internal factors, external factors, and interactions with adjacent cells in the bone marrow [33]. Among them, the effect of cytokines on osteoclastogenesis has been well demonstrated [28]. For instance, inflammatory cytokines such as TNF-α, IL-1, and IL-6 are reported to directly activate osteoclastogenesis through activation of NFATc1 in osteoclast precursors [28]. Also, the inflammatory cytokines can indirectly induce osteoclast differentiation and activation through up-regulation of RANKL with down-regulation of OPG in osteoblasts [28]. In contrast, anti-inflammatory cytokine, IL-10, inhibits osteoclastogenesis through not only suppression of TREM2 expression on osteoclasts [34] but also OPG up-regulation in osteoblasts [28]. Beside cytokines, osteoclastogenesis can be regulated by adipokines secreted from bone marrow adipocytes at pathological conditions such as osteoporosis accompanying increased bone marrow adiposity [8]. In addition,

osteoclastogenesis can be controlled by microbes and their components upon bacterial infection.

2. Microbes and lipoteichoic acid (LTA)

2.1. Microbial regulation of osteoclastogenesis

Microbes constitutively interact with host and regulate immune responses. For instance, normal flora in skin, intestinal tract, and oral cavity are reported to play important roles in development of immune system [35], regulation of metabolism [36], and suppression of pathogenic microbial growth [35]. On the other hand, microbial infections activate inflammatory responses and cause a variety of infectious diseases such as sepsis, pneumonia, and inflammatory bone diseases. Among microbes, Gram-negative bacteria including *Escherichia coli* and *Aggregatibacter actinomycetemcomitans* and Gram-positive bacteria such as *S. aureus* and *Enterococcus faecalis* are closely associated with inflammatory bone disease [11, 37]. Bone and joint infections commonly enhance osteoclastogenesis but reduce osteoblastogenesis, subsequently leading to inflammatory bone diseases such as osteomyelitis, septic arthritis, and periodontitis [11, 38]. Although bone is generally resistant to bacterial colonization, breach of the host epithelial barriers such as wound or surgery can cause bacteremia [11]. The bacteria can spread to the bone via bloodstream resulting in disruption of bone remodeling [11]. Upon infection, the host recognizes and response to microbe-associated molecular patterns (MAMPs) expressed in microbes.

2.2. Effect of MAMPs on osteoclastogenesis

Microbes possess various MAMPs such as LTA, lipoproteins, LPS, and peptidoglycan (PGN), and flagellin [39]. MAMPs are recognized by pattern-recognition receptors (PRRs) such as the Toll-like receptors (TLRs) and NOD-like

receptors (NLRs) to activate immune responses [40]. As described in Table 2, previous reports have demonstrated that each TLR recognizes distinct MAMPs. One of the best-characterized MAMP is LPS of Gram-negative bacteria [40]. LPS is recognized by TLR4 triggering myeloid differentiation primary response gene 88 (MyD88)-dependent and independent signaling pathways [40]. On the other hand, LTA of Gram-positive bacteria is recognized by TLR2 triggering MyD88-dependent signaling pathways [39]. Diacylated lipoprotein preferentially expressed on Gram-positive bacteria is recognized by TLR2/TLR6 heterodimer, whereas triacylated lipoprotein expressed on Gram-negative bacteria is recognized by TLR2/TLR1 heterodimer [40]. Osteoclasts and their precursors are reported to express various TLRs, therefore, their differentiation and activation can be regulated by MAMPs [30].

As shown in Table 2, macrophages and committed osteoclast precursors differently respond to MAMPs. Most MAMPs inhibit RANKL-induced osteoclast differentiation from macrophages but induce osteoclast differentiation from committed osteoclast precursors in the absence of RANKL [30, 31, 41, 42]. Since osteoclast differentiation is regulated by osteoblasts through production of RANKL and OPG, the osteoclast precursor (BMs or macrophages)-osteoblast precursor co-culture has been used as a representative *in vitro* model to mimic dynamic *in vivo* conditions in the bone microenvironment [43]. In the co-culture system, osteoclast differentiation is enhanced by bacterial lipoproteins, LPS, flagellin, and CpG motif though up-regulation of RANKL with down-regulation of OPG in osteoblasts [31, 42, 44, 45]. Indeed, previous reports have demonstrated that bacterial lipoproteins and LPS augment bone loss *in vivo* [42, 46]. Therefore, it is crucial for examination of the effect of MAMPs on osteoclastogenesis and bone metabolism with various *in vitro* systems and verification of the result with *in vitro* through *in vivo* experiments.

Table 2. Effect of MAMPs on osteoclastogenesis and bone resorption

MAMPs		*In vitro* (osteoclastogenesis)			*in vivo*	Ref.
		Macrophages	Committed osteoclast precursors	Osteoblast/ osteoclast coculture	Bone loss	
TLR2 ligand	**LTA**	↓	unknown	unknown	unknown	[47]
TLR2/6 or TLR1/2 ligand	**lipoproteins**	↓	↑	↑	↑	[42, 48]
TLR2 ligand	**PGN**	↓	↑	unknown	unknown	[30, 49]
TLR4 ligand	**LPS**	↓	↑	↑	↑	[30, 31, 46]
TLR3 ligand	**dsRNA Poly(I:C)**	↓	unknown	unknown	unknown	[30]
TLR5 ligand	**Flagellin**	↓	No effect	↑	unknown	[45]
TLR7 ligand	**ssRNAs R848**	↓	unknown	↓	unknown	[50]
TLR9 ligand	**CpG motif of unmethylated DNA**	↓	↑	↑	unknown	[30, 41, 44]

2.3. LTA

Gram-positive bacteria are often associated with bacterial bone and joint diseases. Remarkably, *S. aureus* is clinically responsible for 80–90% of pyogenic osteomyelitis accompanying the excessive bone destruction [12]. Upon bacterial infection, its ability to cause inflammatory bone disease depends on the potency of adherence to bone tissue, induction of inflammation, and disruption of the balance between osteoclasts and osteoblasts, all of which are affected by MAMPs expressed on the cell wall of Gram-positive bacteria such as LTA, lipoproteins, and PGN. Among MAMPs, LTA of Gram-positive bacteria is considered as the counterpart of LPS of Gram-negative bacteria because of structural similarities and inflammatory potential in that (i) LTA is composed of hydrophobic glycolipid and hydrophilic polysaccharide as LPS [51] and (ii) both LPS and LTA can induce the production of inflammatory mediators such as TNF-α and iNOS [52]. However, LTA differs from LPS in that (i) D-alanine and lipid moieties of LTA are important for the immune responses, while LPS contains lipid A which is essential for immunological properties, (ii) LTA is sensed mostly by TLR2, while LPS is recognized by TLR4 [39], and (iii) LTA alone cannot induce septic shock, while LPS is sufficient to do so [53]. Despite its importance, LTA has received less attention than LPS because commercially available LTA preparations often contained structurally damaged LTA and/or biologically active impurities including LPS [51, 54]. Therefore, it is necessary to investigate the effect of LTA on osteoclastogenesis using highly pure and structurally intact LTA to clearly understand the regulation of bone metabolism by Gram-positive bacterial infection.

3. Adipokines and adiponectin

3.1. Adipokines

Adipokines, protein hormones primarily secreted from adipocytes, are classified into two groups: anti-inflammatory and inflammatory adipokines [55-57]. The anti-inflammatory adipokines, such as adiponectin and omentin-1, are abundantly expressed under physiological conditions but slightly expressed by increasing adiposity [55]. Anti-inflammatory adipokines inhibit production of pro-inflammatory cytokines contributing to immune suppression [55]. In contrast, most adipokines belong to the inflammatory adipokines including leptin, resistin, and chemerin [57]. The inflammatory adipokines are highly induced by increasing adiposity and play important roles in the development of chronic inflammation leading to metabolic syndrome such as obesity and diabetes [57]. Besides their immunological functions, the anti-inflammatory and inflammatory adipokines are able to modulate lipid metabolism as shown that adiponectin, omentin-1, and leptin except chemerin inhibit adipocyte differentiation [58, 59]. Indeed, the adipokines have been reported to affect bone metabolism because their receptors are expressed on osteoclasts, osteoblasts, and their precursors [60]. As summarized in Table 3, leptin is known to inhibit osteoclast differentiation [61, 62] and to promote osteoblast differentiation [63]. In contrast, chemerin induces osteoclast differentiation but attenuates osteoblast differentiation [64, 65]. Omentin-1 inhibits differentiation of both osteoclasts and osteoblasts [66].

Table 3. Effect of adipokines on bone metabolism

Adipokines	Source(s)	Receptor(s)	Bone metabolism	Ref.
Leptin	Adipocytes	Leptin receptor	Osteoblast ↑ Osteoclast ↓ Bone mass↑	[59] [61] [67]
Resistin	PBMCs Adipocytes	Adenylyl Cyclase-Associated Protein 1	Osteoblast ↑ (weak) Osteoclast ↑	[68]
Chemerin	Adipocytes	Unknown	Osteoblast ↑ Osteoclast ↓	[64, 65]
Adiponectin	Adipocytes	AdipoR1 AdipoR2	Osteoblast ↑ Osteoclast (controversial) Bone mass (controversial)	[69-74]
Omentin-1	Stromal vascular cells	Unknown	Osteoblast ↓ Osteoclast (no effect on M-CSF/RANKL-induced osteoclastogenesis) Osteoclast ↓ (in osteoblast-osteoclast coculture system)	[66]

3.2. Adiponectin

Among adipokines, adiponectin is considered to be a crucial factor capable of controlling metabolic processes as shown in hypoadiponectinemia is one of risk factors for developing metabolic syndrome [75]. In addition, adiponectin has been suggested to be a crucial mediator in osteoporosis accompanying increased bone marrow adiposity, because its production is decreased by increasing adiposity. Adiponectin was reported to induce osteoblast differentiation but to inhibit osteoclast differentiation [70, 76, 77]. In addition, adiponectin-administered mice showed increased bone mass by attenuating bone resorption and promoting bone formation [78]. However, previous studies have shown that adiponectin-deficient mice exhibited normal bone mass [71, 72], except a slight increase of bone mass in a certain age [72], or showed increased bone mass in young mice but decreased bone mass in aged mice [73]. Accordingly, the precise role of adiponectin in bone metabolism is still controversial.

4. Aims of this study

Understanding the regulation of osteoclastogenesis is required for an efficient treatment or prevention of the bone diseases accompanying excessive osteoclastogenesis such as bacteria-induced bone diseases and osteoporosis. Thus, it is important to identify the molecular targets controlling osteoclastogenesis and to characterize their regulatory mechanisms for osteoclastogenesis. The aim of the present study is to investigate the roles of LTA and adiponectin in osteoclastogenesis and the underlying molecular mechanisms. Under the research aim, (i) the effect of LTA on osteoclastogenesis was investigated using both LTA-deficient *S. aureus* mutant strain and LTA isolated from *S. aureus*, and the action mechanisms were further elucidated. Also, (ii) the effect of adiponectin on bone metabolism was investigated using adiponectin-deficient mice and the action mechanisms were further investigated.

Chapter II. Materials and Methods

1. Reagents and chemicals

Recombinant murine M-CSF, GM-CSF, and RANKL, IL-10, and IFN-γ were obtained from PeproTech (Rocky Hill, NJ, USA). Recombinant murine IL-4 and commercial ELISA kits were obtained from R&D Systems (Minneapolis, MN, USA). Pam2CSK4 and ultrapure *E. coli* O111:B4 LPS were obtained from Invivogen (San Diego, CA, USA). Murine alpha-minimum essential medium (α-MEM), certified fetal bovine serum (FBS), Hanks' Balanced Salt solution (HBSS), and 4-(2-hydroxyethyl)-1-piperazineethanesulfonic acid (HEPES) were obtained from Gibco-BRL (Grand Island, NY, USA). Ascorbic acid free α-MEM was purchased from Welgene (Daegu, Republic of Korea). An osteoclast activity assay substrate (OAAS) and osteo assay 96-well plates were purchased from Osteogenic Core Technologies (Chunan, Korea) and Corning Inc. (Corning, NY, USA), respectively. Fluorescein isothiocyanate (FITC)-conjugated Dextran (MW 40,000) was obtained from Molecular Probes (Eugene, OR, USA). BCA protein assay kit was purchased from Pierce (Rockford, IL, USA). Fluorescent dye-conjugated antibodies and isotype antibodies were purchased from BioLegends (San Diego, CA, USA) unless otherwise indicated. Specific antibodies used for flow cytometry analysis were as follows: purified rat anti-mouse CD16/CD32 antibody, rat allophycocyanin (APC)-conjugated anti-mouse c-Fms antibody, rat phycoerythrin (PE)-conjugated anti-mouse RANK antibody, rat FITC-conjugated anti-mouse CD11b antibody, rat peridinin Chlorophyll Protein Complex (PerCP)-conjugated anti-mouse F4/80 antibody, armenian hamster PE-conjugated anti-mouse CD3ε antibody, rat PE-conjugated anti-mouse CD45R/B220 antibody, and rat FITC-conjugated anti-mouse CD14 antibody. Rat PE-conjugated anti-mouse TLR2 antibody was obtained from eBioscience (San Diego, CA, USA). Antibodies specific to IRF-5 and TREM-2 were obtained from Abcam (Cambridge, UK). Fluorescent dye-conjugated isotype antibodies were used FITC-conjugated rat

immunoglobulin (Ig) $G2_{a,\kappa}$ antibody, FITC-conjugated rat $IgG2_{b,\kappa}$ antibody, PE-conjugated rat $IgG2_{a,\kappa}$ antibody, PE-conjugated rat $IgG2_{b,\kappa}$ antibody, PE-conjugated armeninan hamster IgG antibody, PerCP-conjugated armeninan hamster IgG antibody, PerCP-conjugated rat $IgG2_{a,\kappa}$ antibody, PerCP-conjugated rat $IgG_{2b,\kappa}$ antibody, and APC-conjugated armeninan hamster IgG antibody. For Western blot analysis, phosphorylated and non-phosphorylated forms of primary antibodies (p38 kinase, EKR, JNK, and CREB) were obtained from Cell Signaling Technology (Beverly, MA, USA). Antibodies specific to NFATc1 and c-Fos were purchased from Santa Cruz Biotechnology (Santa Cruz, CA, USA). Horseradish peroxidase (HRP)-conjugated secondary antibodies specific to mouse IgG, rabbit IgG, and goat IgG were purchased from SouthernBiotech (New Orleans, LA, USA). Trizol reagent, Alexa Fluor 488-conjugated phalloidin, Hoechst 33258, fluo-4 acetoxymethyl (AM), pluronic acid F127, and probenecid were obtained from Molecular probe (Carlsbad, Ca, USA). PRO-PREP was obtained from Intron Biotechnology (Seoul, Korea), and skim milk and mouse anti-gelsolin antibody were purchased from BD Biosciences (Sparks, MD, USA). Protein G agarose and polyvinylidene difluoride (PVDF) membranes were obtained from Millipore (Bedford, MA, USA). ECL Plus reagent was obtained from Neuronex (Pohang, Republic of Korea). [γ-^{32}P]-dATP was purchased from Perkin Elmer (Waltham, MA, USA). Non-Idet P40 and dispase were obtained from Roche Applied Science (Mannheim, Germany). Type I collagenase and 1α,25-dihydroxyvitamin D_3 were purchased from Wako Pure Chemical (Osaka, Japan) and Enzo life science (Farmingdale, NY, USA), respectively. Sodium dodecyl sulfate (SDS), Tween-20, and bovine serum albumin (BSA) were obtained from Amresco (Solon, OH, USA). Red blood cell (RBC) lysing buffer, ascorbic acid, β-glycerophosphate, dexamethasone, insulin, 3-isobutyl-1-Methylxanthine (IBMX), a leukocyte acid phosphatase-staining kit, a leukocyte alkaline phosphatase kit, 3-[4,5-dimethylthiazol-2-yl]-2,5-diphenyltetrazolium bromide (MTT), and antibody specific to β-actin were obtained from Sigma-Aldrich Inc. (MO, USA).

2. Experimental animals

All experiments were approved by the institutional Animal Care and Use Committee of Seoul National University. Six- to twelve-week-old C57BL/6 mice were purchased from Orient Bio (Seongnam, Korea) and housed with food and water under specific pathogen-free conditions. TLR2-deficient, MyD88-deficient, and adiponectin-deficient mice on the C57BL/6 background were used in some experiments. Dr. Shizuo Akira, of Osaka University, Osaka, Japan, kindly provided the TLR2- or MyD88-deficient mice. Adiponectin-deficient mice were kindly provided by Dr. Young Yang, of Sook Myung University, Seoul, Korea.

3. Preparation of ethanol-inactivated *S. aureus*

S. aureus RN4220, LTA-deficient mutant (Δ*ltaS*), and its complementary strain (Δ*ltaS* strain containing a plasmid harboring the *ltaS* gene, pS*ltaS*) were kindly provided by Dr. Bok Luel Lee (Pusan National University, Busan, Korea). *S. aureus* RN4220 was grown in Luria-Bertani (LB) media as a parent strain, whereas Δ*ltaS* and p*SltaS* strain were grown in LB media containing 50 μg/ml of kanamycin. *S. aureus* RN4220 were incubated at 37°C with shaking at 200 rpm until mid-log phase (A600, 0.6), whereas *ΔltaS* and pS*ltaS* was incubated at 30°C because of temperature sensitivity [79]. Bacteria were incubated with at 180 rpm for 18 h, harvested, and washed three times with phosphate-buffered saline (PBS). The bacterial cells were inactivated with 70% ethanol in PBS at room temperature with vigorous shaking for 2 h. After extensive washing of bacterial cell pellets, the complete inactivation was confirmed by plating and culturing onto a LB agar plate at 37°C for 24 h. No bacterial colony was observed on the plate.

4. Preparation of LTA

Highly pure and structurally intact LTA was isolated from *S. aureus* ATCC 29213, *Bacillus subtilis* ATCC6633 (American Type Culture Collection, Manassas, VA, USA), and *Lactobacillus plantarum* KCTC 10887BP (Korean Collection for Type

Culture, Daejeon, Korea) as described previously [80]. Briefly, bacteria were disrupted in 0.1 M sodium citrate buffer (pH 4.7) by ultrasonification. LTA-containing fractions were isolated by N-butanol extraction followed by chromatography with octyl-Sepharose column CL-4B and DEAE-Sepharose FastFlow column. Structural identity of LTA was confirmed using high-field nuclear magnetic resonance and MALDI-TOF mass spectrometry. The purified LTA was not contaminated with endotoxins, proteins, or nucleic acids.

5. Cells

5.1. M-CSF/RANKL-mediated osteoclast differentiation from macrophages

Six- to fourteen-week-old mice were used for preparation of macrophages as osteoclast precursors. Bone marrow cells (BMs) were obtained by flushing the marrow space of tibiae and femurs from mice with PBS. After removal of RBC with RBC lysing buffer, the BMs at 2×10^6 cells/ml were plated in 5 ml/dish on a 90 mm petri dish and incubated in α-MEM supplemented with 10% heat-inactivated FBS, 100 U/ml of penicillin, and 100 μg/ml of streptomycin in a humidified incubator at 37°C with 5% CO_2 overnight. Non-adherent cells (stroma-free BMs) were harvested, plated in 10 ml/dish on a 90 mm petri dish at 5×10^5 cells/ml, and then further incubated with 10 ng/ml of GM-CSF for M1 macrophages or 20 ng/ml of M-CSF for M2 macrophages for 5 days. Bone marrow-derived macrophages (BMMs) were used as osteoclast precursors. In some experiments, BMMs differentiated with M-CSF at 1.5×10^4 cells/ml were plated in 200 μl/well on a 96-well culture plate and incubated further incubated with 100 ng/ml of LPS plus 20 ng/ml of IFN-γ for M1 or with 20 ng/ml of IL-4 or 20 ng/ml of IL-10 for M2 macrophages in the presence of 20 ng/ml of M-CSF for 24 h. For preparation of peritoneal macrophages, peritoneal cells were isolated from peritoneal cavity by injecting with 5 ml of ice-cold PBS and retrieving from wild-type and adiponectin-deficient mice. The cells were plated on a 90 mm petri dish, incubated for 2 h, and then adherent cells as peritoneal macrophages were harvested. For osteoclast differentiation, macrophages

at 1.5×10^5 cells/ml were plated in 200 μl/well on a 96-well culture plate and further incubated with 20 ng/ml of M-CSF and 40 ng/ml of RANKL for 2-3 days.

5.2. Osteoclast differentiation from committed osteoclast precursors

For preparation of committed osteoclast precursors, stroma-free BMs were incubated with 20 ng/ml of M-CSF for 5 days. BMMs were further incubated with 20 ng/ml of M-CSF and 40 ng/ml of RANKL for 30-40 h. After washing with culture media, the committed osteoclast precursors at 1.5×10^5 cells/ml were plated in 200 μl/well on a 96-well culture plate and stimulated with 100 μg/ml of inactivated bacteria, 30 μg/ml of LTA, 1 μg/ml of LPS, 0.1 μg/ml of Pam2CSK4, 0.2 μg/ml of TNF-α, or 0.1 μg/ml of RANKL in the presence of 20 ng/ml of M-CSF for 24 h.

5.3. Isolation of calvarial osteoblast precursors

The calvaria were obtained from 1-day-old mice and digested in 5 ml of L-ascorbic acid-free α-MEM culture medium containing 0.1% type I collagens and 0.2% dispase for 15 min at 37°C with vigorous shaking. After repeating the digestion procedure six times, the cells isolated by the all digestions except first time were combined and filtered with a tissue strainer. The collected cells were plated in 10 ml/dish on a 100 mm dish at 5×10^4 cells/ml and incubated for 3 days. Adherent cells were harvested and then kept frozen until use.

5.4. Osteoclast differentiation by co-culture of osteoblast precursors with osteoclast precursors

Calvarial osteoblast precursors at 2.5×10^4 cells/ml were plated in 400 μl/well on a 48-well culture plate and incubated for 6 h. Then, M-CSF-induced BMMs at 2.5×10^5 cells/ml were added and co-cultured with 50 nM 1α,25-dihydroxyvitamin D_3 for 7 days. The media were half changed with fresh culture medium containing 50 nM 1α,25-dihydroxyvitamin D_3, every 3 days.

5.5. Differentiation of calvarial cells into osteoblasts or adipocytes

Calvarial cells at 3×10^4 cells/ml were plated in 400 μ/well on a 48-well culture plate and grown until fully confluent in ascorbic acid free-α-MEM. The cells were incubated with osteoblast induction medium (50 μM ascorbic acid and 10 mM β-glycerophosphate) or adipocyte induction medium (1 μM dexamethasone, 0.5 mM IBMX, and 5 μg/ml of insulin) for 7 to 21 days. The media were half changed with fresh media containing the differentiation factors, every 3 days.

6. Cell staining

6.1. TRAP staining

Osteoclast differentiation was verified by staining for TRAP, a marker of osteoclasts. Cells were fixed with a fixative solution containing 26% citrate, 66% acetone, and 8% formaldehyde for 2 min and washed with distilled water two times. Then, the fixed cells were stained with the leukocyte acid phosphatase staining kit following the manufacturer's instructions. TRAP-positive and MNCs with three or more nuclei (TRAP-positive MNCs) were enumerated as mature osteoclasts under an inverted-phase-contrast microscope (Olympus CKX41, Japan) [81].

6.2. Alkaline phosphatase (ALP) staining

Osteoblast differentiation was verified by staining for ALP. At day 7 after the initial incubation with osteoblast induction medium, calvarial cells were fixed with a fixative solution for 2 min, washed, and stained with the ALP staining kit following the manufacturer's instructions. Images of the stained cells were obtained with an inverted phase-contrast microscope.

6.3. Alizarin Red S staining

Alizarin Red S staining was performed to determine an ability of calcium deposits as osteoblast function. After 21 days from the initial incubation with osteoblast induction medium, calvarial cells were fixed with 4% paraformaldehyde for 30 min, washed, and then stained with 2% alizarin red S (pH 4.2) for 45 min.

Images of the stained cells were obtained with an inverted phase-contrast microscope. To quantify Alizarin Red S, its precipitate was dissolved in 20% methanol and 10% acetic acid for 15 min, and then an absorbance was measured at 450 nm using a microtiter plate reader (Versa-Max, Molecular Devices, Sunnyvale, CA, USA).

6.4. Oil Red O staining

Oil Red O staining was performed to determine adipocyte differentiation. At day 21 after the initial incubation with adipocyte induction medium, calvarial cells were fixed with 4% paraformaldehyde for 30 min, washed, and stained 0.3% Oil Red O for 1 h. Images of the stained cells were obtained with an inverted phase-contrast microscope. To quantify Oil Red O, its lipid droplet was dissolved in isopropanol for 15 min and measured by spectrophotometric analysis at 500 nm.

7. *In vitro* bone resorption assay

BMMs at 2.5×10^5 cells/ml were plated in 200 μl/well on a 96-well calcium phosphate-coated culture plate and incubated with 20 ng/ml of M-CSF and 40 ng/ml of RANKL for 2 days to prepare committed osteoclast precursors or 4 days to differentiate to osteoclasts. Committed osteoclast precursors were washed with culture media and stimulated with 30 μg/ml of LTA and/or 0.1 μg/ml of Pam2CSK4 in the presence of 20 ng/ml of M-CSF for 4 days. To lyse the cells, the calcium phosphate-coated plate was treated with 5% sodium hypochlorite for 10 min, washed with distilled water, and dried. The resorbed pit area was photographed using an inverted phase-contrast microscope and measured using ImageJ software (version1.44; National Institutes of Health, USA).

8. Micro-computed tomography (micro-CT) analysis

The femurs were isolated from ten- to fourteen-week-old mice and scanned by a high-resolution micro-CT at 7 μm resolution (Skyscan1172 scanner; Skyscan, Kontich, Belgium). Scanned images were reconstructed by an NRecron program

(Skyscan) and analyzed using Dataviewer 1.3.2 program (Skyscan) followed by a CT-analyzer program (Skyscan). Bone parameters were analyzed in 1 mm region in length, starting from 0.5 mm below the distal femoral growth plate, to determine trabecular bone volume, trabecular number, trabecular thickness, and trabecular separation. In a separate experiment, the calvaria were subjected to micro-CT at 12 μm resolution and bone volume was analyzed in 3 mm diameter circle centered on an anterior fontanelle using the CT-analyzer program. Three dimensional images of the femurs and the calvaria were obtained using a CT-vol program (Skyscan).

9. Bone histomorphometric analysis

The femurs were fixed in 4% formalin for 7 days and then decalcified with 10% ethylenediaminetetraacetic acid (EDTA) for 15 days. Preparation of 5 μm paraffin-embedded tissue section was performed at the Clinical Research Institute of Seoul National University Hospital (Seoul, Korea). After TRAP- and hematoxylin and eosin (H&E) staining, bone histomorphometry of the femurs was analyzed with Osteomeasure software (Osteometrics, Decatur, GA, USA).

10. *In vivo* bone resorption assay

10.1. Trabecular bone resorption assay

Six- to fourteen-week-old mice were used for the experiments. Mice were intraperitoneally administered with 20 μg per mouse of GST-RANKL or 4 mg per mouse of inactivated bacteria, twice a four-day interval. At day 7, right femur was isolated, scanned with the micro-CT, and analyzed with the CT-analyzer program.

10.2. Calvarial bone resorption assay

Six- to eleven-week-old mice were used for the experiments. After intraperitoneal administration of avertin in 2-methyl-2-butanol for mouse anesthesia, mouse calvaria were implanted with a collagen sheet containing RANKL (5 μg per mouse), *S. aureus* LTA (20, 100, or 500 μg per mouse), Pam2CSK4 (5 μg per mouse), or *S. aureus* LTA (100 μg per mouse) plus Pam2CSK4 (5 μg per mouse). At day 7, the

calvaria were isolated, scanned using the micro-CT, and analyzed by the CT-analyzer program.

11. Measurement of cell viability

BMMs at 1.5×10^5 cells/ml were plated in 200 μl/well on a 96-well culture plate and incubated with 20 ng/ml of M-CSF and 20 ng/ml of RANKL in the presence or absence of *S. aureus* LTA for 2-3 days. The cells were incubated with 0.5 mg/ml of MTT solution at 37°C for 60 min. After removal of the MTT-containing medium, the cells were dissolved in dimethyl sulfoxide (DMSO), and the absorbance at 570 and 650 nm was measured using a microtiter plate reader.

12. Flow cytometric analysis

All cells were pre-incubated with purified rat anti-mouse CD16/CD32 antibody to block Fc receptors for 15 min on ice prior to antibodies staining. Whole BMs were stained with FITC-conjugated anti-mouse CD11b antibody, PE-conjugated anti-mouse CD3ε antibody, and PE-conjugated anti-mouse B220 antibody for 30 min on ice. BMMs or committed osteoclast precursors were stained with FITC-conjugated rat anti-mouse CD14 antibody, PE-conjugated rat anti-mouse TLR2, APC-conjugated anti-mouse c-Fms antibody, PE-conjugated anti-mouse RANK antibody, or anti-TREM2 antibody, followed by Cy3-conjugated anti-goat IgG, for 30 min on ice. The stained cells were washed three times with ice-cold wash buffer (PBS containing 0.1% BSA), harvested, and fixed with 1% paraformaldehyde. The changes in the expression of cell surface molecules were analyzed using FACSCalibur with CellQuest Pro software (BD Biosciences, San Jose, CA, USA). All flow cytometric data were analyzed and plotted with FlowJo software (Tree Star, Ashland, OR, USA).

13. Endocytic activity assay

Cells were incubated with 1 mg/ml of Dextran-FITC (MW 40,000) for 30 min at 37°C or 4°C. The cells were washed with an ice-cold wash buffer (PBS containing 0.1% BSA), harvested, and fixed with 1% paraformaldehyde in PBS. The uptake of FITC-conjugated Dextran was measured using a flow cytometer with CellQuest Pro software. All flow cytometric data were analyzed and plotted with FlowJo software. The actual uptake was determined as the mean fluorescence intensity (MFI) of cells incubated at 37°C minus the MFI of cells incubated at 4°C.

14. Western blotting

To determine phosphorylated and non-phosphorylated form of MAPKs or CREB, BMMs at 5×10^5 cells/ml were plated in 4 ml/dish on a 60 mm culture dish and serum-deprived for 3-4 h. Then the cells were stimulated with 100 ng/ml of RANKL for 0, 5, 15, or 30 min. In a separate experiment, the serum-deprived BMMs were pre-treated with 30 μg/ml of *S. aureus* LTA for 30 min and then stimulated with 200 ng/ml of M-CSF or 200 ng/ml of RANKL for 0, 5, 15, or 30 min. In other experiments, committed osteoclast precursors were serum-deprived for 4 h and then stimulated with 30 μg/ml of *S. aureus* LTA in the presence or absence of 0.1 μg/ml of Pam2CSK4 for 0, 15, 30, or 60 min. To determine c-Fos, NFATc1, or CREB, BMMs at 5×10^5 cells/ml were plated in 4 ml/dish on a 60 mm culture dish and incubated with 20 ng/ml of M-CSF and 100 ng/ml of RANKL for 1 or 2 day(s). The cells were washed with ice-cold PBS and lysed with HEPES lysis buffer (25 mM HEPES, pH 7.5, 150 mM NaCl, 1% Non-Idet P-40, 0.25% sodium deoxycholate, 10% glycerol) or PRO-PREP protein extraction solution containing protease inhibitors (1 μg/ml of aprotinin, 1 μg/ml of leupeptin, 1 mM AEBSF, and 2 mM PMSF) plus phosphatase inhibitors (2 mM Na_3VO_4 and 2 mM NaF). The whole cell lysates were centrifuged at 13,000 × *g* for 30 min at 4°C, and the supernatants were collected. In some experiments, to prepare cytoplasmic extracts and nuclear extracts, the cells were lysed with hypotonic buffer (10 mM HEPES and 1.5 mM $MgCl_2$, pH 7.5) containing protease inhibitors and phosphatase inhibitors at

4°C for 15 min. After centrifugation at 5,000 × *g* for 5 min, and then the supernatants were used as the cytoplasmic extracts. The remained nuclei pellets were washed and lysed using hypertonic buffer (20 mM HEPES, 1.5 mM $MgCl_2$, 500 mM KCl, 0.3 Mm EDTA, 10% glycerol, 0.2 mM DTT, 0.1% Non-Idet P40) containing protease inhibitors and phosphatase inhibitors at 4°C for 40 min with vigorous agitation. Nuclear supernatants were prepared by centrifugation at 14, 500 × *g* for 20 min at 4°C. The protein concentration was determined using a BCA protein assay kit. Cell lysates were separated by 6 to 10% SDS-PAGE and transferred onto PVDF membranes. After blocking with 5% skim milk in Tris-buffered saline (pH 7.4, 0.2 M Tris, 27 mM KCl, and 1.37 M NaCl) containing 0.1% Tween-20, the memranes were probed with specific antibodies and developed for analysis using ECL Plus reagents.

15. Immunoprecipitation

Cells were washed with ice-cold PBS and lysed in HEPES lysis buffer with protease inhibitors and phosphatase inhibitors. Whole cell lysates containing 150 μg of protein were immunoprecipitated with the anti-gelsolin antibody for 12 h followed by further incubation with protein G-agarose beads for 2 h at 4°C with vigorous agitation. After discarding the supernatants, the agarose beads were washed three times with HEPES lysis buffer, and then bead-bound proteins were separated by 8% SDS-PAGE. Gel proteins were transferred onto PVDF membranes. After blocking with 5% skim milk in TBST, the membranes were probed with antibody specific to β-actin and developed for analysis using ECL Plus reagents.

16. Electrophoretic mobility shift assay (EMSA)

BMMs at 5×10^5 cells/ml were plated in 4 ml/dish on a 60 mm culture dish. The BMMs were incubated with 20 ng/ml of M-CSF and 100 ng/ml of RANKL for 1 or 2 day(s). In a separate experiment, The BMMs were serum-starved for 4 h, pre-treated with *S. aureus* LTA at 0, 0.1, 1, or 10 μg/ml for 30 min, and stimulated with

20 ng/ml of M-CSF and 20 ng/ml of RANKL for 90 min. In other experiments, committed osteoclast precursors were stimulated with 30 μg/ml of *S. aureus* LTA and/or 0.1 μg/ml of Pam2CSK4 in the presence of 20 ng/ml of M-CSF for 12 or 24 h. To prepare nuclear extracts, the cells were lysed with hypotonic buffer containing 1 mM PMSF and 1 μg/ml of each aprotinin and leupeptin at 4°C for 15 min. After centrifugation at 5,000 × *g* for 5 min at 4°C, nuclei pellets were lysed using hypertonic buffer containing 1 mM PMSF and 1 μg/ml of each aprotinin and leupeptin at 4°C for 40 min with vigorous agitation. Nuclear supernatants were prepared by centrifugation at 14, 500 × *g* for 30 min at 4°C and the protein concentration was determined using the BCA protein assay kit. A double-stranded deoxyoligonucleotide was prepared by annealing of an oligonucleotide containing consensus recognition sites for activator protein 1 (AP-1) (5'-CGCTTGATGACTCAGCCGGAA-3'), NFAT (5'-CTGTATGAAACAAATTTCCTCTTTGGGC-3'), or NFATc1 (5'-CGCCCAAAGAGGAAAATTTGTTTCATA-3') at 4°C for 40 min, and labeled with a [γ-^{32}P]-dATP at 37°C for 1 h. Seven μg of nuclear extracts were incubated with 1 μg poly (dI-dC) and 1 pmol ^{32}P-labeled DNA probe in binding buffer (20 mM HEPES, 1.5 mM $MgCl_2$, 0.3 mM EDTA, 10% glycerol, 0.2 mM DTT, 0.1% Non-Idet P40) containing 1 mM PMSF and 1 μg/ml of each aprotinin and leupeptin for 15 min on ice. Nuclear protein/DNA binding complexes were separated from free probe using a 5% polyacrylamide gel in Tris-Glycine-EDTA (TGE) buffer (250 mM Tris, 1,920 mM Glycine, and 10 mM EDTA, pH 8.5). To confirm specific binding, one pmole of unlabeled probe was used as a cold competitor. After electrophoresis, the gel was dried and subjected to autoradiography.

17. Immunofluorescence

BMMs at 6 × 10^5 cells/ml were plated in 0.5 ml/well on 12 mm glass coverslips in a 24-well culture plate and incubated with 20 ng/ml of M-CSF and 100 ng/ml of RANKL for 4 days. In a separate experiment, committed osteoclast precursors were incubated with 200 μg/ml of inactivated bacteria, 30 μg/ml of *S. aureus* LTA, and/or

0.1 μg/ml of Pam2CSK4 in the presence of 20 ng/ml of M-CSF for 2 days. The cells were fixed with 4% formaldehyde for 20 min, permeabilized with 0.25% Triton X-100 for 15 min, and then blocked with 1% BSA for 1 h. Actin was stained with Alexa Fluor 488-conjugated phalloidin for 1 h and the nuclei were counterstained with Hoechst 33258 for 2 min. In some experiments, the stained BMMs were further incubated with anti-IRF5 antibody at 4°C for overnight followed by Cy3-conjugated anti-mouse IgG for 1 h. After further washing, the coverslips were mounted and the stained cells were observed by Zeiss LSM 700 confocal fluorescence microscope (Carl Zeiss, Oberkochen, Germany).

18. Enzyme-linked immunosorbent assay (ELISA)

BMMs at 1.25×10^5 cells/ml were plated in 200 μl/well on a 96-well culture plate and stimulated with *S. aureus* LTA in the presence of 20 ng/ml of M-CSF and 20 ng/ml of RANKL for 24 and 48 h. In a separate experiment, macrophages at 5×10^5 cells/ml were plated in 200 μl/well on a 96-well culture plate and stimulated with 0.1 μg/ml of LPS in the presence of 20 ng/ml M-CSF for 24 h. Bone marrow extracellular fluids were obtained by sequentially flushing both tibiae with 500 μl of ice-cold PBS and harvesting supernatant after centrifugation at 13,000 × *g* for 15 min at 4°C. Sera were separated from blood by centrifugation at 13,000 × *g* for 15 min at 4°C. The amounts of adiponectin, TNF-α, IL-6, IL-10, RANKL, or OPG in the culture supernatants, sera, or bone marrow extracellular fluids were determined using commercial ELISA kits according to the manufacturer's instruction.

19. Reverse transcription-polymerase chain reaction (RT-PCR)

Total RNAs were extracted from cells with Trizol reagent, and reversed-transcribed with random hexamers (Promega Corporation, Madison, WI, USA). An equal amount of cDNA was subjected to PCR in 20 μl using EmeraldAmp PCR Master Mix (TaKaRa Bio Inc., Otsu, Shiga, Japan) and 10 pmol of specific primers. For amplification, cDNA was initially denatured at 94°C for 5 min. It was then amplified for 30-35 cycles at 95°C for 40 s, 58-62°C for 40 s, and 72°C for 40 s.

The PCR was completed with a final extension at 72°C for 5 min. An equal volume of PCR products was separated on a 1.5% agarose gel and visualized by ethidium bromide staining with a gel documentation system (Bio-Capt X-press, Vilber-Lourmat, Marne La Vallee, France). Specific primers used in this study were BSP, OCN, ALP, IL-1β, IL-6, CD36, argianse I, and β-actin as follow: BSP: 5'-GTCAAC GGCACCAGCACCAA-3', 5'-GTAGCTGTATTCGTCCTCAT-3'; OCN: 5'-TCTGACAAACCTTCATGTCC-3', 5'-AAATAGTGATACCGTAGATGCG-3'; ALP: 5'-GCCCTCTCCAAGACATATA-3', 5'-CCATGATCACGTCGATATCC-3'; IL-1β: 5'-AAGCTCTCACCTCAATGGA-3', 5'-TGCTTGAGAGGTGCTGATGT-3'; IL-6: 5'-GGAAATTGGGGTAGGAAGGA-3', 5'-CCGGAGAGGAGACTTCACAG-3'; CD36: 5'-TGCTGCACGAGGAGAATGGGC-3', 5'-ACAGTGTGGTCCTCGGGGTCC-3'; arginase 1: 5'-GGCGTGGCCAGAGATGCTTCC-3', 5'-GTCCTGAGTTGCACCGAGCCG-3'; IL-1β: 5'-GTGGGGCGCCCCAGGCACCA-3', 5'-CTCCTTAATGTCACGCACGATTTC-3'.

20. Measurement of intracellular calcium and oscillation

Stroma-free BMs were suspended at 5×10^5 cells/ml, and BMMs at 5×10^5 cells/ml were plated onto a coverslip in a 30 mm culture dish and incubated with 20 ng/ml of M-CSF and 100 ng/ml of RANKL for 2 days. The cells were loaded with 3 μM fluo-4 AM, 0.02% pluronic acid F127, and 1 mM probenecid at 37°C for 30 min, washed three times with HBSS, and then additionally incubated for 30 min at room temperature. The stained stroma-free BMs were plated onto a glass coverslip a 30 mm culture dish at 5×10^5 cells/ml. The coverslip was transferred to a perfusion chamber, and the cells were perfused with HBSS and excited at 488 nm. The emission at 530 nm was detected with an interval of 5 s for 5 min using confocal laser-scanning microscope (Olympus FV-300). The maximum fluorescence intensity of cytosolic calcium was obtained by stimulation with 5 μM ionomycin at the end of each experiment. For quantitative analysis of calcium oscillation, the fluorescence intensity was analyzed in single cell using fluoview (Olympus).

Calcium oscillation was defined when the relative fluorescence was dramatically increased by more than 20% as described previously [82].

21. IRF5 overexpression by transfection

Dr. Tadatsugu Taniguchi (Tokyo University, Tokyo, Japan) kindly provided the murine IRF5 expression plasmid (pCAGGS-HA-IRF5). M2 macrophages were plated on a 30 mm culture dish or a 48-well culture plate at 5×10^5 cells/ml and transfected with the 2 μg/ml of the IRF5 expression plasmid or control plasmid using attractene (Qiagen, Valencia, CA, USA) in the presence of 10 ng/ml of M-CSF for 12 h. After removal of transfection mixture, the cells were further incubated with 20 ng/ml of M-CSF and 100 ng/ml of RANKL for 2-4 days.

22. IRF5 knock-down by transfection with small interfering RNA (siRNA)

M1 macrophages were plated on a 30 mm culture dish or a 48-well culture plate at 5×10^5 cells/ml and transfected with 40 nM IRF5 siRNA or control siRNA (Dharmacon, Lafayette, CO, USA) using DharmaFECT 1 transfection reagent (Dharmacon) in the presence of 5 ng/ml of GM-CSF, according to the manufacturer's instruction. After 24 h, the cells were washed and further incubated with 20 ng/ml of M-CSF and 100 ng/ml of RANKL for 2-5 days.

23. Statistical analysis

All experiments were performed at least two or three times and data were expressed as mean values ± standard deviations of three samples in each experimental group. Statistical significance was examined by two-tailed *t*-test. Differences were considered significant when $P < 0.05$.

Chapter III. Results

1. Role of LTA in osteoclastogenesis

1.1. LTA-deficient *S. aureus* induces massive bone resorption and excessive osteoclast differentiation compared with wild-type *S. aureus*

To investigate the role of LTA on bone metabolism, mice were intraperitoneally administered with ethanol-inactivated *S. aureus* wild-type or LTA-deficient mutant (Δ*ltaS*). Quantitative analysis following micro-CT imaging demonstrated that the Δ*ltaS* strain augmented more massive bone resorption than the wild-type strain (Fig. 3A and B). To examine if LTA-deficient *S. aureus* more induces osteoclast differentiation than wild-type strain, committed osteoclast precursors were stimulated with the ethanol-inactivated *S. aureus* wild-type, Δ*ltaS*, or pS*ltaS* which is the complemented Δ*ltaS* strain. As expected, microscopic analysis following TRAP staining showed that the Δ*ltaS* strain remarkably increased the number of TRAP-positive MNCs compared with the wild-type *S. aureus* while the pS*ltaS* restored the increased number of TRAP-positive MNCs (Fig. 4A). In addition, the Δ*ltaS* strain increased the number of nuclei per MNCs compared with the wild-type strain, and the pS*ltaS* restored such effect as the wild-type did (Fig. 4B). Furthermore, the Δ*ltaS* strain provoked MNCs with a large podosome belt, a typical structure for bone resorption, compared with the pS*ltaS* or the wild-type strain (Fig. 4C). These results suggest that LTA is responsible for inhibition of *S. aureus*-induced bone resorption and osteoclastogenesis.

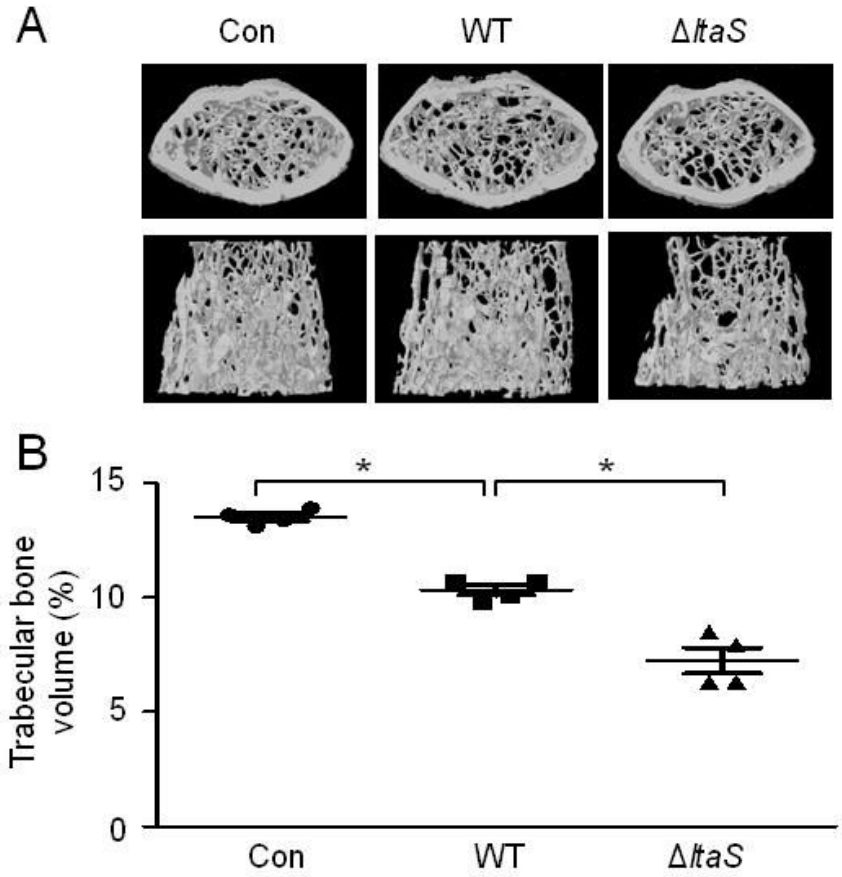

Figure 3. LTA-deficient *S. aureus* induces massive bone resorption compared with wild-type *S. aureus*. Mice (n = 4 per group) were intraperitoneally administered with 4 mg of ethanol-inactivated *S. aureus* wild-type and LTA-deficient mutant (Δ*ltaS*), twice with a 4-day interval. At day 7 after the first administration, the distal femurs were analyzed to obtain (A) micro-CT images and (B) trabecular bone volume. *P < 0.05 when compared with control groups. WT, wild-type. Con, control.

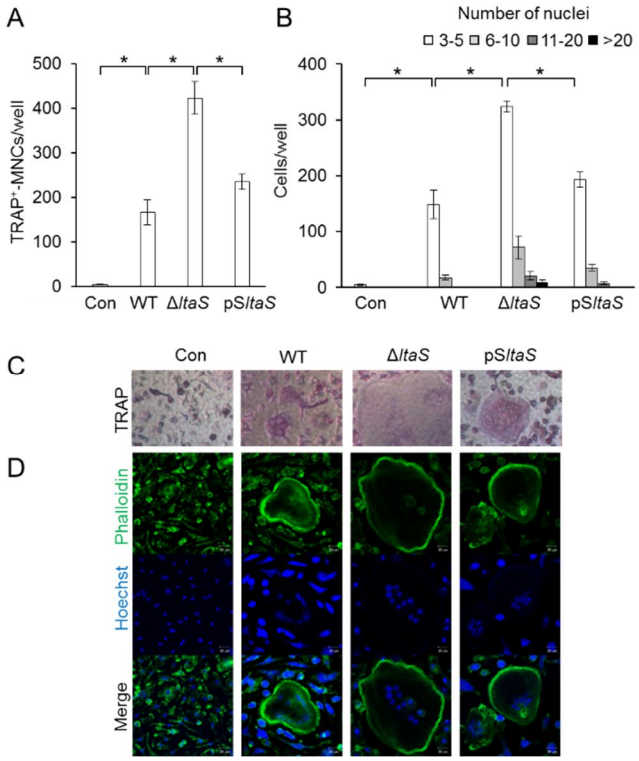

Figure 4. LTA-deficient *S. aureus* excessively augments osteoclast differentiation and activation. BMMs were incubated with M-CSF (20 ng/ml) and RANKL (40 ng/ml) for 36 h to prepare committed osteoclast precursors. The cells were washed and stimulated with ethanol-inactivated *S. aureus* wild-type, Δ*ltaS*, or pS*ltaS* (100 μg/ml) in the presence of M-CSF (20 ng/ml) for 24 h. After TRAP staining, (A) TRAP-positive MNCs or (B) nuclei per TRAP-positive MNCs were enumerated under an inverted phase-contrast microscope. **P* < 0.05. (C) The TRAP-stained cells were photographed under an inverted phase-contrast microscope with magnification at ×40. (D) Committed osteoclast precursors were stimulated with ethanol-inactivated *S. aureus* WT, Δ*ltaS*, or pS*ltaS* (200 μg/ml) in the presence of M-CSF (20 ng/ml) for 48 h. The cells were fixed, stained with FITC-conjugated phalloidin (green), and then analyzed by immunocytochemistry analysis. The nucleus was counterstained with Hoechst 33258 for each sample. Bars, 20 μm. One of three similar results is shown.

1.2. *S. aureus* LTA affects neither osteoclastogenesis nor bone mass

To investigate whether LTA directly affects osteoclastogenesis, committed osteoclast precursors were stimulated with LTA isolated from *S. aureus*. As shown in Fig. 5A, *S. aureus* LTA induced the generation of TRAP-positive MNCs. However, synthetic peptide Pam2CSK4 mimicking Gram-positive bacterial lipoproteins remarkably increased the number of TRAP-positive MNCs. To further examine the bone resorptive capacity, committed osteoclast precursors were prepared on calcium phosphate-coated plates, stimulated with *S. aureus* LTA in the presence of M-CSF, and analyzed for resorption pits. *S. aureus* LTA hardly induced the resorption pits whereas Pam2CSK4 produced resorption pits (Fig. 5B). Furthermore, when collagen sheets soaked in *S. aureus* LTA were implanted in mouse calvaria, bone resorption was not observed in the calvarial bone even at 500 μg of *S. aureus* LTA. However, 5 μg of Pam2CSK4 provoked bone resorption under the same condition (Fig. 5C). Additionally, osteoblast differentiation was examined in the presence of *S. aureus* LTA, but LTA alone did not affect the osteoblast differentiation (data not shown). These findings indicate that *S. aureus* LTA alone affects neither osteoclastogenesis nor bone resorption.

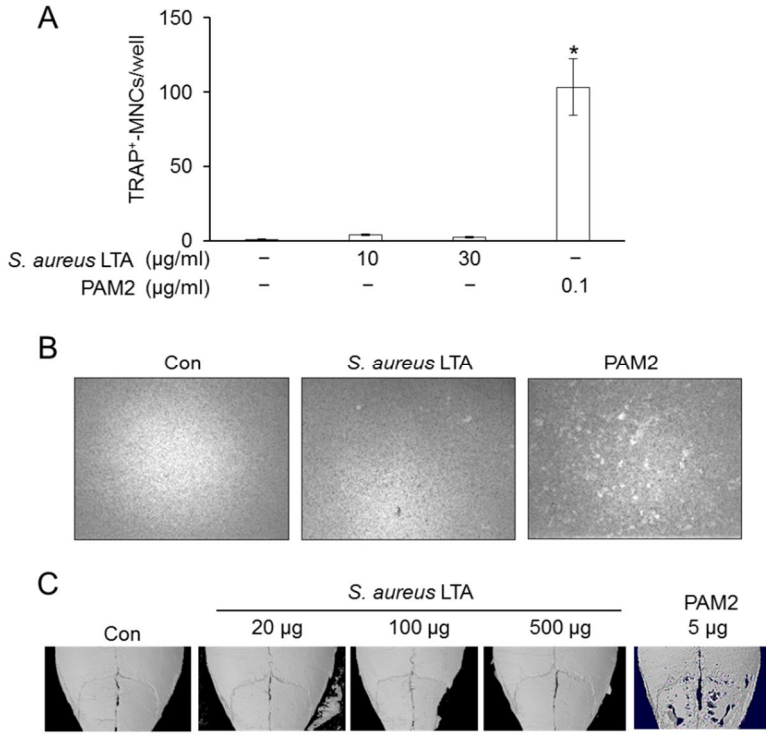

Figure 5. *S. aureus* LTA alone affects neither osteoclastogenesis nor bone mass. (A) Committed osteoclast precursors were stimulated with *S. aureus* LTA (10 or 30 μg/ml) in the presence of M-CSF (20 ng/ml) for 36 h. After TRAP staining, TRAP-positive MNCs were enumerated under an inverted phase-contrast microscope. Pam2CSK4 (0.1 μg/ml) was used as a positive control. **P* < 0.05 when compared with untreated cells. (B) Committed osteoclast precursors plated on calcium phosphate-coated plates were stimulated with *S. aureus* LTA (30 μg/ml) or Pam2CSK4 (0.1 μg/ml) in the presence of M-CSF (20 ng/ml) for 4 days. The resorbed areas were photographed under an inverted phase-contrast microscope with magnification at ×40. (C) Mouse calvaria (*n* = 3 per group) were implanted with collagen sponges soaked with *S. aureus* LTA (20, 100, or 500 μg) or Pam2CSK4 (5 μg). After 7 days, the calvaria were analyzed to obtain micro-CT images. The micro-CT image of the calvaria shown is one of three similar results. PAM2, Pam2CSK4.

1.3. *S. aureus* LTA inhibits M-CSF/RANKL-induced osteoclastogenesis from macrophages

1.3.1. *S. aureus* LTA inhibits M-CSF/RANKL-induced osteoclast differentiation from macrophages

To determine if *S. aureus* LTA plays an inhibitory role in osteoclastogenic conditions, BMMs as osteoclast precursors were incubated with M-CSF and RANKL in the presence or absence of *S. aureus* LTA for 2 days. RANKL facilitated the generation of TRAP-positive MNCs, but *S. aureus* LTA inhibited the number of TRAP-positive MNCs in a dose-dependent manner (Fig. 6A and B). All treatment groups showed no change in cell viability, which indicates that the inhibitory effect of LTA on M-CSF/RANKL-induced osteoclastogenesis is not associated with cell death (Fig. 6C). To further examine whether LTAs from other gram-positive bacteria also suppress M-CSF/RANKL-induced osteoclast differentiation from macrophage, LTAs isolated from *B. subtilis* and *L. plantarum* were treated to BMMs with M-CSF/RANKL for 48 h. As expected, LTAs isolated from *B. subtilis* or *L. plantarum* significantly inhibited the generation of TRAP-positive MNCs (Fig. 6D and E), implying that LTA possesses the ability to inhibit osteoclast differentiation. To examine bone resorptive capacity, BMMs were prepared on calcium phosphate-coated plates, incubated with *S. aureus* LTA in the presence of M-CSF and RANKL, and analyzed for resorption pits. As shown in Fig. 7, M-CSF and RANKL produced the resorption pits with various areas, but *S. aureus* LTA decreased the resorption pits under the same condition. These results suggest that LTA inhibits M-CSF/RANKL-induced osteoclastogenesis from macrophages.

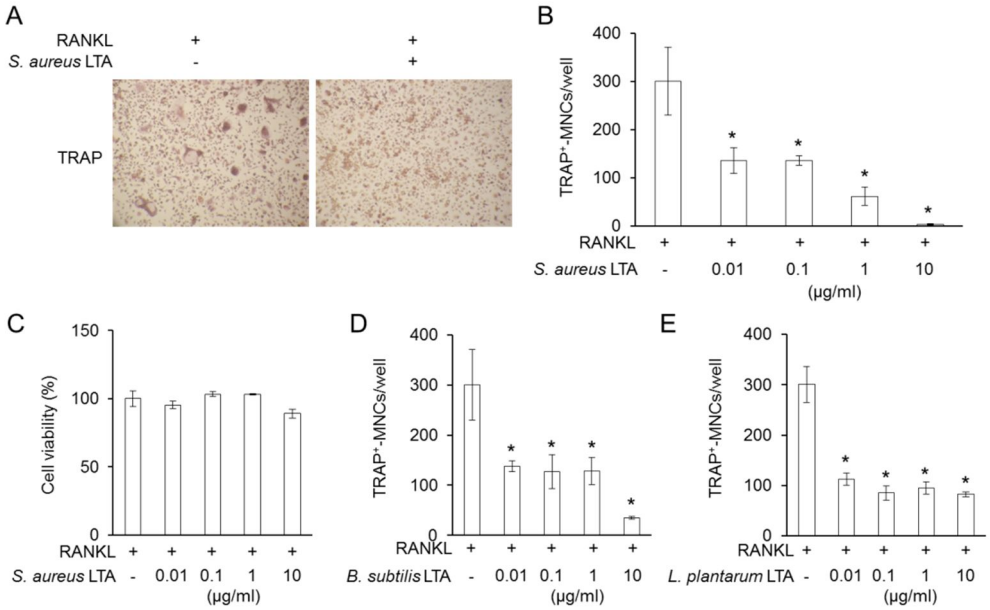

Figure 6. LTA inhibits M-CSF/RANKL-induced osteoclast differentiation from macrophages. BMMs were incubated with M-CSF (20 ng/ml) and RANKL (20 ng/ml) in the presence or absence of *S. aureus* LTA (0.01, 0.1, 1, and 10 μg/ml) for 2 days. After TRAP staining, (A) the cells were photographed under an inverted-phase-contrast microscope with magnification at ×40 and (B) TRAP-positive MNCs were enumerated. (C) Cell viability was determined by MTT-based cytotoxicity assay. BMMs were incubated with M-CSF (20 ng/ml) and RANKL (20 ng/ml) in the presence or absence of (D) *B. subtilis* LTA or (E) *L. plantarum* LTA (0.01, 0.1, 1, and 10 μg/ml) for 2 days. After TRAP staining, TRAP-positive MNCs were enumerated under an inverted-phase-contrast microscope. **P* < 0.05 when compared with untreated cells. One of three similar results is shown.

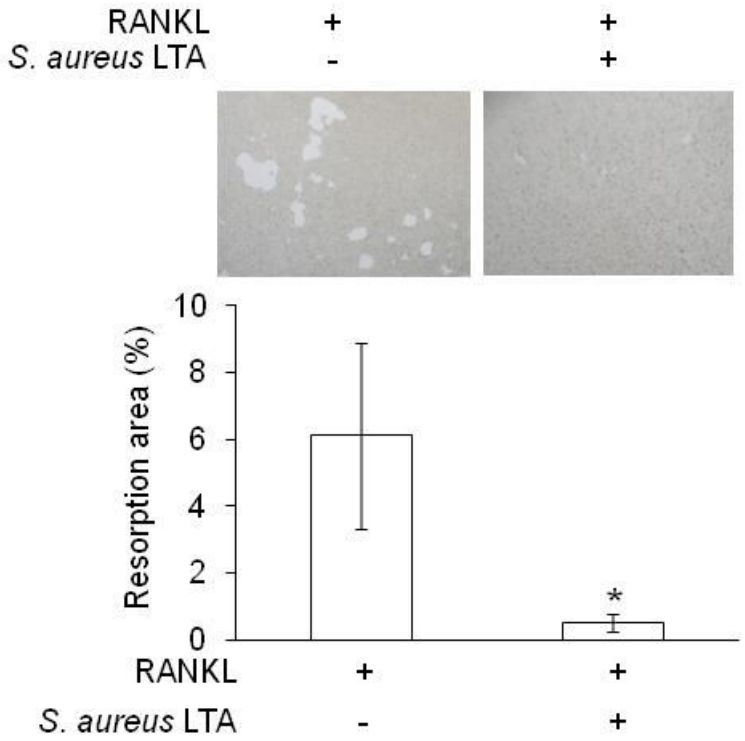

Figure 7. *S. aureus* LTA attenuates M-CSF/RANKL-induced bone resorption capacity in macrophages. Stroma-free BMs were plated onto a 96-well calcium phosphate-coated plate and differentiated into BMMs by incubation with M-CSF (20 ng/ml) for 3 days. The BMMs were further incubated with *S. aureus* LTA (10 μg/ml) in the presence of M-CSF (20 ng/ml) and RANKL (20 ng/ml) for 3 days. The resorbed areas were photographed under an inverted phase-contrast microscope with magnification at ×40. The total resorption area per well was measured with Scion image software. *$P < 0.05$ when compared with untreated cells. One of the three similar results is shown.

1.3.2. *S. aureus* LTA enhances both endocytic capacity and TNF-α production in macrophages

Macrophages play a pivotal role in the innate immune responses with phagocytosis and production of inflammatory cytokines [14]. As macrophages are differentiated into osteoclast, the endocytic and inflammatory abilities gradually decrease in the macrophages [30]. Thus, the effect of LTA on endocytic capacity was determined during M-CSF/RANKL-induced osteoclastogenesis by measuring uptake of Dextran-FITC in BMMs. As shown in Fig. 8A, the endocytic capacity gradually decreased during osteoclastogenesis (MFIs at day 0, 1, and 2 were 128, 48, and 37, respectively). Treatment with *S. aureus* LTA, however, significantly enhanced endocytic capacity. In addition, *S. aureus* LTA dose dependently increased TNF-α production during osteoclastogenesis (Fig. 8B). These results imply that LTA makes macrophages keep the phagocytic and inflammatory abilities by inhibiting the osteoclastogenesis.

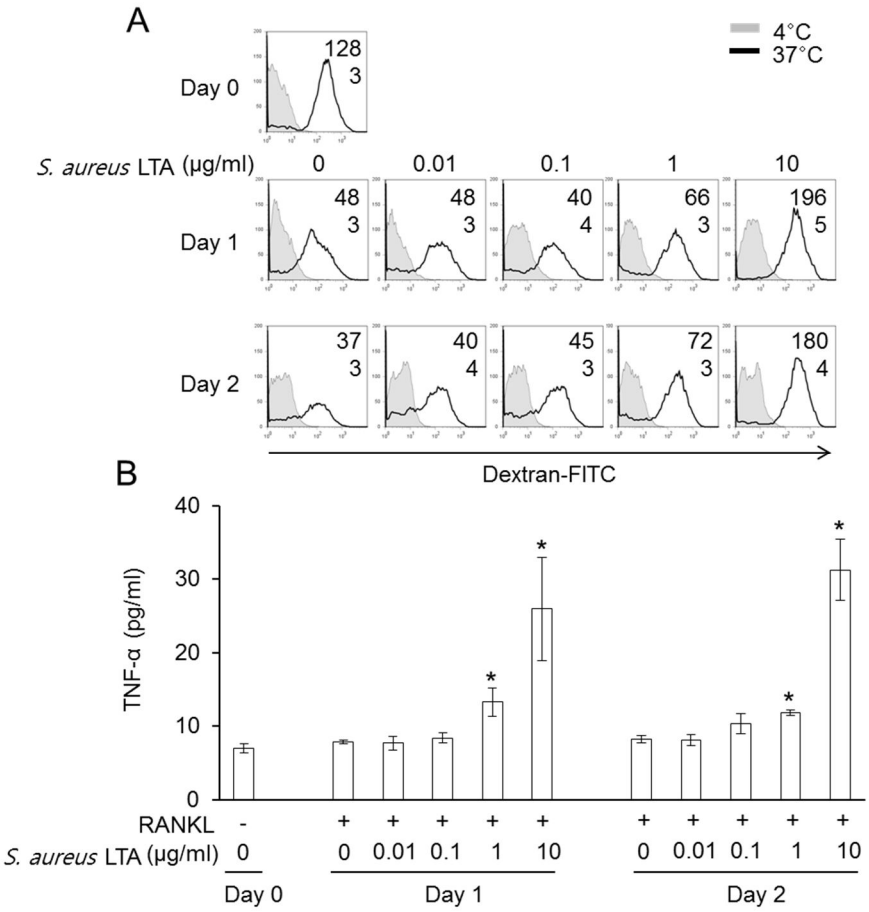

Figure 8. *S. aureus* LTA enhances endocytic capacity and TNF-α production of BMMs during osteoclastogenesis. BMMs were incubated with *S. aureus* LTA (0.01, 0.1, 1, and 10 μg/ml) in the presence of M-CSF (20 ng/ml) and RANKL (20 ng/ml) for 1 or 2 day(s). (A) The cells were incubated with Dextran-FITC (1 mg/ml) for 30 min at 4°C (*shaded area*) or 37°C (*open area*). Dextran-FITC uptake at 37°C was analyzed by flow cytometry and compared with that at 4°C. Mean fluorescence intensity (MFI) is shown in the upper right in each histogram (the number in the upper row: MFI at 37°C; lower row: MFI at 4°C). (B) The amounts of TNF-α were determined in the culture supernatants by ELISA. *$P < 0.05$ when compared with untreated cells. One of the three similar results is shown.

1.3.3. Inhibitory effect of *S. aureus* LTA on osteoclastogenesis is mediated through TLR2 but partial involvement of MyD88

Since signaling by CD14 and TLR2 is reported to mediate the activities of LTA [83], the surface expression of these receptors on osteoclast precursors was analyzed in the presence or absence of *S. aureus* LTA during osteoclastogenesis. Flow cytometry demonstrated that the BMMs expressed both CD14 and TLR2 on their surfaces (Fig. 9). During RANKL/M-CSF-induced osteoclastogenesis, the expression of and CD14 and TLR2 was gradually decreased on the osteoclast precursors, but *S. aureus* LTA maintained the surface expression of TLR2 (Fig. 9A) but not CD14 (Fig. 9B). LTA signaling has been reported to invoke MyD88-dependent pathway via TLR2 [83-85]. To examine whether TLR2 and MyD88 are required for the inhibitory effect of LTA on M-CSF/RANKL-induced osteoclastogenesis from macrophages, BMMs were prepared from TLR2-deficient or MyD88-deficient mice and then stimulated with *S. aureus* LTA in the presence of M-CSF and RANKL. In the TLR2-deficient macrophages, *S. aureus* LTA hardly inhibited osteoclast differentiation even at 10 μg/ml where almost complete attenuation of osteoclastogenesis was observed in the wild-type macrophages (Fig. 10A). Unexpectedly, *S. aureus* LTA still inhibited the osteoclastogenesis from MyD88-deficient macrophages in a dose-dependent manner, although the inhibitory effect of *S. aureus* LTA was less effective in the MyD88-deficient macrophages than in the wild-type cells (Fig. 10B). These findings indicate that *S. aureus* LTA inhibits M-CSF/RANKL-induced osteoclastogenesis through TLR2-dependent but with partial MyD88-dependent pathway.

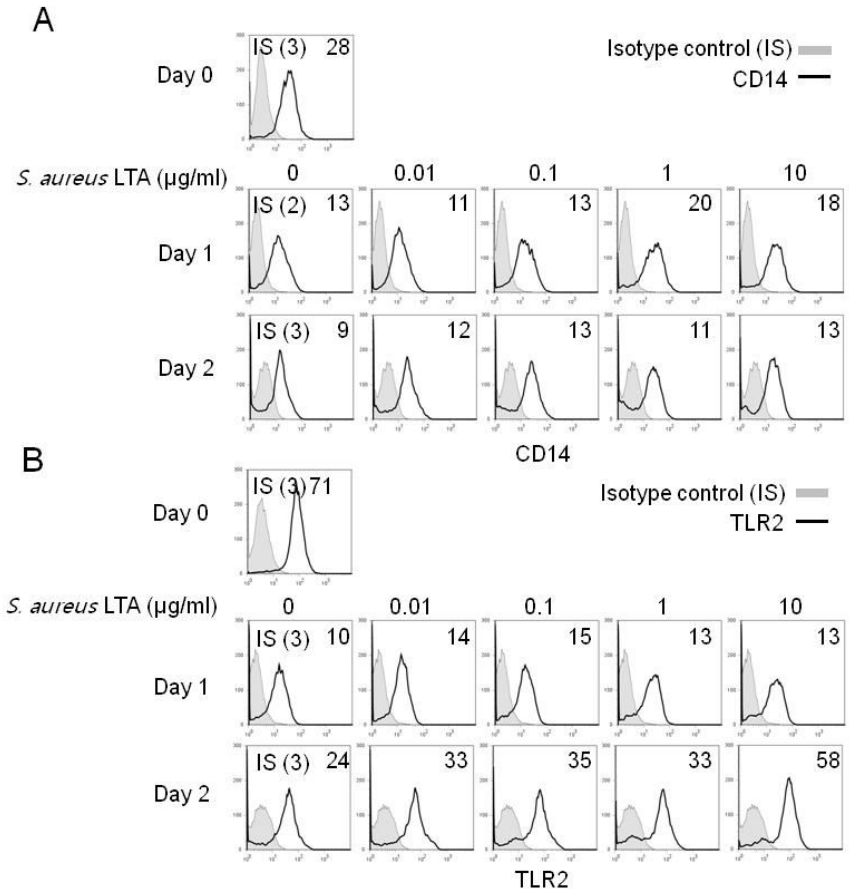

Figure 9. *S. aureus* LTA induces TLR2 expression on osteoclast precursors. BMMs were incubated with M-CSF (20 ng/ml) and RANKL (20 ng/ml) in the presence or absence of *S. aureus* LTA (0, 0.01, 0.1, 1, and 10 μg/ml) for additional 1 or 2 day(s). The cells were analyzed by flow cytometry after staining with fluorescent dye-conjugated specific antibodies to (A) CD14 and (B) TLR2. Shaded and open areas indicate isotype control and cell surface expression, respectively. MFI is shown in the upper right in each histogram. IS, isotype control. One of five similar results is shown.

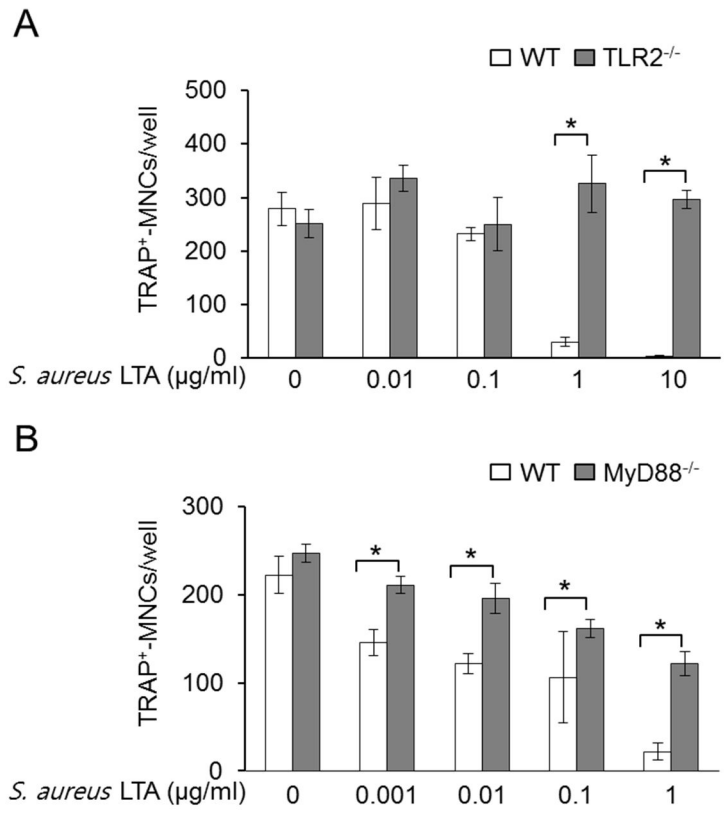

Figure 10. *S. aureus* LTA suppresses M-CSF/RANKL-induced osteoclast differentiation through TLR2-dependent and partial MyD88-dependent pathway. Stroma-free BMs were obtained from (A and B) wild-type mice, (A) TLR2-deficient mice, or (B) MyD88-deficient mice, and differentiated into BMMs by incubation with M-CSF (20 ng/ml) for 3 days. The BMMs were further incubated with *S. aureus* LTA (0.001-10 μg/ml) in the presence of M-CSF (20 ng/ml) and RANKL (20 ng/ml) for 2 days. After TRAP staining, TRAP-positive MNCs were enumerated under an inverted phase-contrast microscope with magnification at ×40. *$P < 0.05$ when compared with wild-type cells. WT, wild-type. $TLR2^{-/-}$, TLR2-deficient. $MyD88^{-/-}$, MyD88-deficient. One of the three similar results is shown.

1.3.4. *S. aureus* LTA inhibits both M-CSF and RANKL signaling and reduces DNA-binding activity of AP-1

Since M-CSF and RANKL activate MAPKs to induce osteoclastogenesis [33], MAPK phosphorylation was examined in M-CSF- or RANKL-stimulated BMMs. Phosphorylation of extracellular signal-regulated kinase (ERK) and c-Jun N-terminal kinase 1 (JNK1), but not p38 kinase, increased substantially at 5 minute in the presence of M-SCF or RANKL. However, LTA suppressed the increased phosphorylation of ERK and JNK1, while LTA hardly affected the p38 kinase phosphorylation (Fig. 11A and B). To examine the effect of LTA on activation of AP-1 and NFAT for LTA-inhibited osteoclastogenesis, the DNA-binding activities of AP-1 and NFAT were observed using EMSA. As shown in Fig. 11C, M-CSF and RANKL markedly increased the DNA-binding activity of AP-1 and NFAT in the BMMs. However, LTA inhibited the DNA-binding activity of AP-1, but not NFAT. These results indicate that LTA-inhibited osteoclastogenesis might be caused by the decreased activation of ERK and JNK and the reduced DNA-binding activity of AP-1.

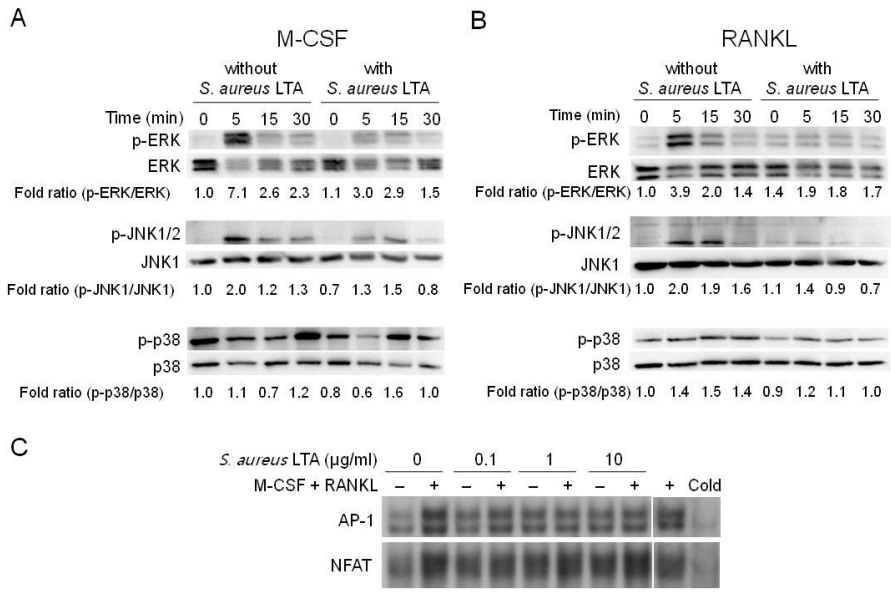

Figure 11. *S. aureus* LTA inhibits M-CSF- and RANKL-induced signaling. (A and B) BMMs were serum-deprived for 4 h, pre-treated with *S. aureus* LTA (10 μg/ml) for 30 min, and then stimulated with (A) M-CSF (200 ng/ml) or (B) RANKL (200 ng/ml) for 5, 15, or 30 min. Cell lysates were prepared and subjected to Western blot analysis to determine phosphorylated or non-phosphorylated forms of MAPKs, including ERK, JNK, and p38 kinase. The relative values of phosphorylated forms to non-phosphorylated forms were determined by densitometry. (C) BMMs were simulated with *S. aureus* LTA (0, 0.1, 1, and 10 μg/ml) for 30 min, followed by M-CSF (20 ng/ml) and RANKL (20 ng/ml) for 90 min. Nuclear extracts were incubated with ^{32}P-labeled oligonucleotides containing binding sites for AP-1 and NFAT. Protein-DNA binding complexes were electrophoresed and subjected to autoradiography. One picomole of each unlabeled probe was used as a control and marked "Cold". One of the three similar results is shown.

1.4. *S. aureus* LTA inhibits osteoclast differentiation triggered from committed osteoclast precursors

1.4.1. *S. aureus* LTA inhibits *S. aureus*- and Pam2CSK4-induced osteoclast differentiation from committed osteoclast precursors

LTA-deficient *S. aureus* remarkably induced the bone resorption and osteoclastogenesis (Fig. 2), suggesting that *S. aureus* LTA may inhibit *S. aureus*-induced osteoclast differentiation of committed osteoclast precursors. *S. aureus* augmented the number of TRAP-positive MNCs, but *S. aureus* LTA significantly decreased the number of TRAP-positive MNCs (Fig. 12A). Bacterial lipoproteins were reported to be augment excessive generation of osteoclastogenesis, contributing to bone resorption occurring by bacterial infection [42]. To investigate whether *S. aureus* LTA inhibits lipoprotein-induced osteoclastogenesis, committed osteoclast precursors were stimulated with *S. aureus* LTA and/or Pam2CSK4 mimicking Gram-positive bacterial lipoprotein. *S. aureus* LTA significantly inhibited Pam2CSK4-induced TRAP-positive MNCs in a dose-dependent manner (Fig. 12B). In addition, LTA from *B. subtilis* or *L. plantarum* also suppressed Pam2CSK4-induced osteoclast differentiation (Fig. 13). These findings suggest that LTA generally inhibits *S. aureus*- and Pam2CSK4-induced osteoclast differentiation of committed osteoclast precursors.

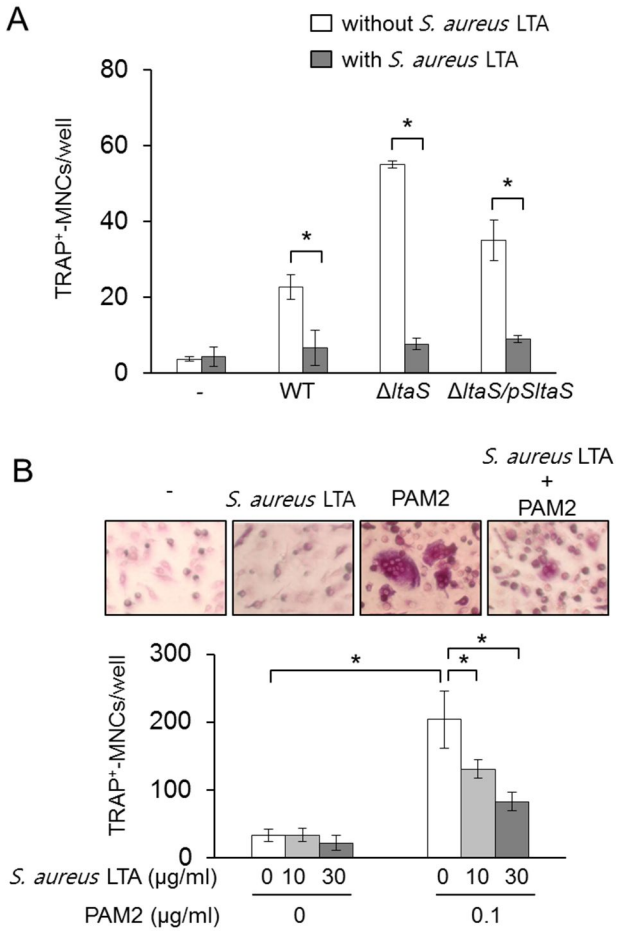

Figure 12. *S. aureus* LTA inhibits *S. aureus*- or Pam2CSK4-induced osteoclast differentiation from committed osteoclast precursors. (A) Committed osteoclast precursors were stimulated with *S. aureus* LTA (30 μg/ml), along with ethanol-inactivated *S. aureus* wild-type, LTA-deficient mutant (Δ*ltaS*), or its complementary stain (p*SltaS*) (100 μg/ml) in the presence of M-CSF (20 ng/ml) for 24 h. (B) Committed osteoclast precursors were stimulated with *S. aureus* LTA (10 or 30 μg/ml) and/or Pam2CSK4 (0.1 μg/ml) in the presence of M-CSF (20 ng/ml) for 24 h. After TRAP staining, the stained cells were photographed and TRAP-positive MNCs were enumerated. **P* < 0.05 when compared with untreated cells. One of three similar results is shown.

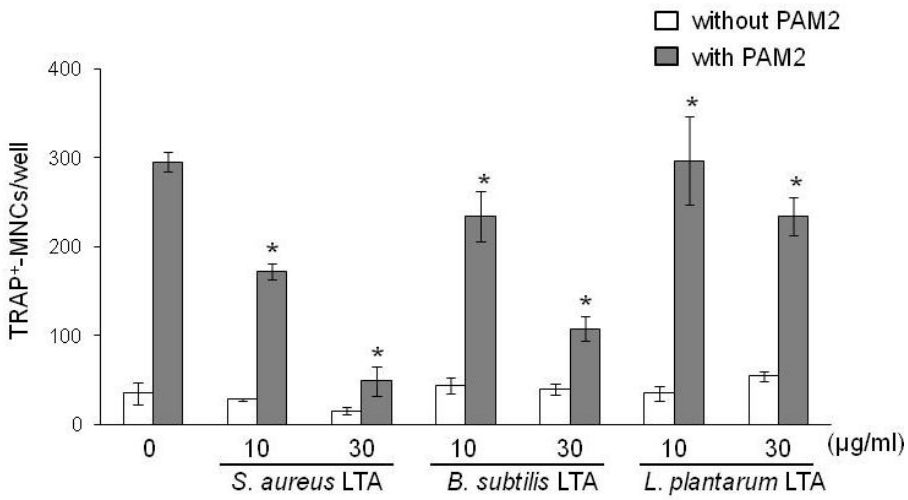

Figure 13. LTA isolated from *B. subtilis* or *L. plantarum* inhibits PAM2CSK4-induced osteoclast differentiation from committed osteoclast precursors. Committed osteoclast precursors were stimulated with Pam2CSK4 (0.1 μg/ml) and/or LTAs (30 μg/ml) isolated from *S. aureus*, *B. subtilis*, and *L. plantarum* in the presence of M-CSF (20 ng/ml) for 24 h. After TRAP staining, TRAP-positive MNCs were enumerated. **P* < 0.05 when compared with Pam2CSK4-untreated cells. One of three similar results is shown.

1.4.2. *S. aureus* LTA inhibits Pam2CSK4-induced osteoclast activation and bone resorption

To ascertain whether *S. aureus* LTA influences osteoclast activation, committed osteoclast precursors were incubated with *S. aureus* LTA in the presence or absence of Pam2CSK4 for 48 h and the formation of podosome belt in osteoclasts was analyzed. As shown in Fig. 14A, Pam2CSK4 induced the MNCs with large podosome belt, but such effect was reduced by the co-treatment with *S. aureus* LTA and Pam2CSK4. To further examine the inhibitory effect of *S. aureus* LTA on the bone resorption capacity of osteoclasts, committed osteoclast precursors seeded on calcium phosphate coated-plates were incubated with *S. aureus* LTA and/or Pam2CSK4. As expected, the large areas of resorption pits were observed in the presence of Pam2CSK, but *S. aureus* LTA decreased Pam2CSK4-induced the bone resorption pits (Fig. 14B). Moreover, *S. aureus* LTA inhibited Pam2CSK4-induced the massive bone resorption (Fig. 14C). These findings indicate that *S. aureus* LTA inhibits bacterial lipoproteins-induced osteoclastogenesis of committed osteoclast precursors and bone resorption.

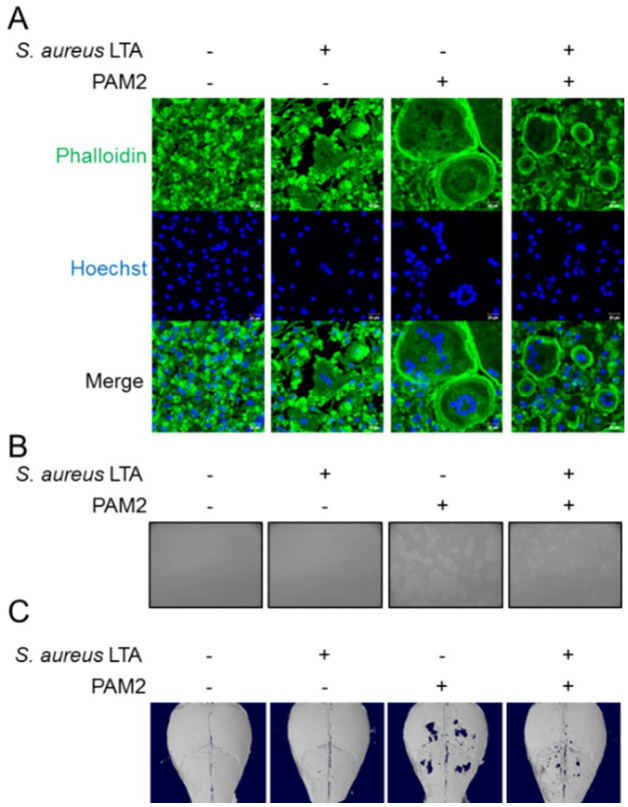

Figure 14. *S. aureus* LTA suppresses Pam2CSK4-induced osteoclast activation and bone resorption. (A) Committed osteoclast precursors were stimulated with *S. aureus* LTA (30 μg/ml) and/or Pam2CSK4 (0.1 μg/ml) in the presence of M-CSF (20 ng/ml) for 48 h. After fixation, the cells were stained with FITC-conjugated phalloidin (green) to determine actin expression using immunocytochemistry analysis. The nucleus was counterstained with Hoechst 33258. Bars, 20 μm. (B) Committed osteoclast precursors, plated on 96-well calcium phosphate-coated plates, were stimulated with LTA (30 μg/ml) and/or Pam2CSK4 (0.1 μg/ml) in the presence of M-CSF (20 ng/ml) for 48 h. The resorbed areas were photographed under an inverted phase-contrast microscope with magnification at ×40. (C) A collagen sheet soaked with 100 μg of LTA and/or 5 μg of Pam2CSK4 was implanted on mouse calvaria. After 7 days, micro-CT image of the calvaria was obtained.

1.4.3. *S. aureus* LTA inhibits differentiation of committed osteoclast precursors into osteoclasts in response to LPS, TNF-α, or RANKL

Osteoclastogenesis occurs in committed osteoclast precursors by various osteoclast-inducing factors such as LPS, TNF-α, and RANKL [20, 28, 42]. To examine whether *S. aureus* LTA inhibits LPS-induced osteoclast differentiation, committed osteoclast precursors were stimulated with *S. aureus* LTA and/or LPS. As shown in Fig. 15A, LPS augmented the number of TRAP-positive MNCs, but *S. aureus* LTA remarkably inhibited the osteoclast differentiation. In addition, TNF-α robustly increased the number of TRAP-positive MNCs, but *S. aureus* LTA decreased the number of TRAP-positive MNCs (Fig. 15B). Furthermore, *S. aureus* LTA inhibited the generation of RANKL-induced TRAP-positive (Fig. 15C). These results indicate that *S. aureus* LTA may act negatively act in osteoclastogenesis.

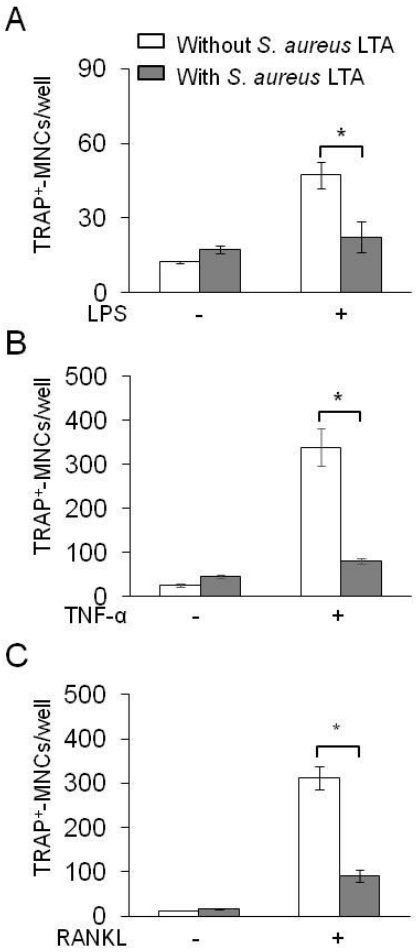

Figure 15. *S. aureus* LTA inhibits differentiation of committed osteoclast precursors into osteoclasts in response to LPS, TNF-α, or RANKL. Committed osteoclast precursors were stimulated with *S. aureus* LTA (30 μg/ml) in the presence or absence of (A) LPS (1 μg/ml), (B) TNF-α (0.2 μg/ml), or (C) RANKL (0.1 μg/ml) with M-CSF (20 ng/ml) for 24 h. Then, the cells were stained for TRAP and TRAP-positive MNCs were enumerated. **P* < 0.05. One of three similar results is shown.

1.4.4. TLR2 signaling is not necessary for LTA-mediated inhibition of osteoclast differentiation

Since *S. aureus* LTA is mostly recognized by TLR2 triggering immune responses [83], committed osteoclast precursors were prepared from stroma-free BMs of wild-type or TLR2-deficient mice, and osteoclast differentiation was examined in the presence of *S. aureus* LTA. TNF-α remarkably augmented the number of TRAP-positive MNCs in wild-type and TLR2-deficient committed osteoclast precursors. In addition, *S. aureus* LTA inhibited the increased number of TRAP-positive MNCs (Fig. 16A). RANKL remarkably increased the number of TRAP-positive MNCs of TLR2-deficient committed osteoclast precursors compared with the wild-type precursors, but *S. aureus* LTA significantly decreased the number of TRAP-positive MNCs (Fig. 16B). These findings suggest that TLR2 signaling is not necessary for *S. aureus* LTA-mediated inhibition of osteoclast differentiation.

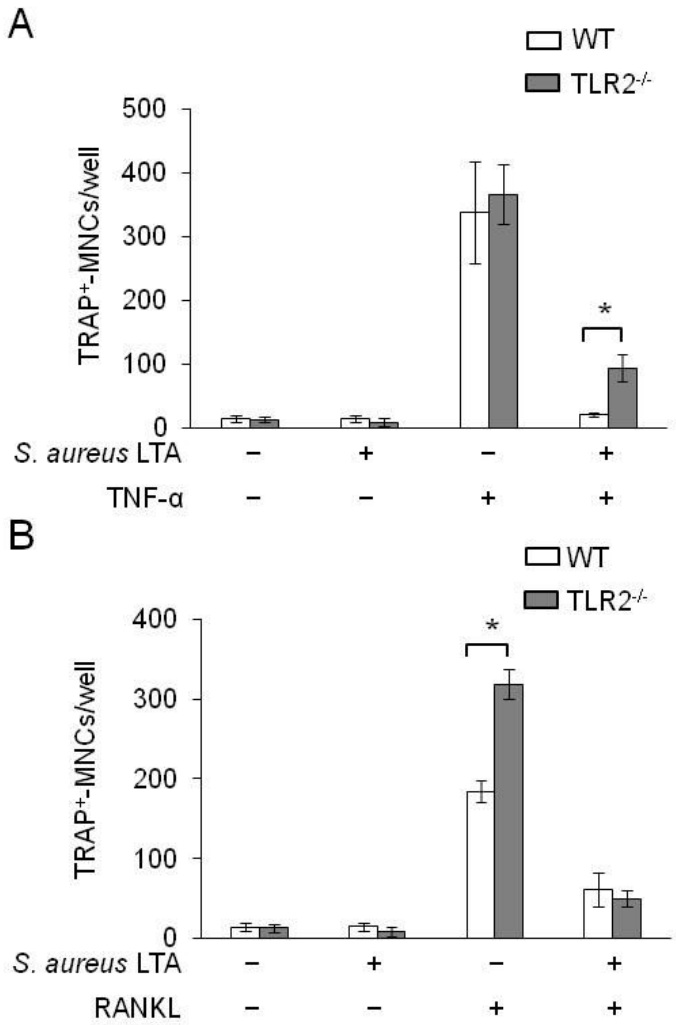

Figure 16. TLR2 signaling is not necessary for *S. aureus* LTA-mediated inhibition of osteoclast differentiation from committed osteoclast precursors. Committed osteoclast precursors were prepared from wild-type and TLR2-deficient mice. The cells were stimulated with *S. aureus* LTA (30 μg/ml) in the presence or absence of (A) TNF-α (0.2 μg/ml) or (B) RANKL (0.1 μg/ml) for 24 h. After TRAP staining, TRAP-positive MNCs were enumerated. **P* < 0.05 when compared with wild-type cells. One of three similar results is shown.

1.4.5. LTA inhibits Pam2CSK4-induced MAPK activation and DNA-binding activity of NFATc1

Since MAPKs are essential for Pam2CSK4-induced osteoclastogenesis of committed osteoclast precursors [42], MAPK phosphorylation induced by Pam2CSK4 was examined in the presence of *S. aureus* LTA in committed osteoclast precursors. Phosphorylation of MAPKs such as ERK, JNK, and p38 kinase was robustly induced in Pam2CSK4-treated cells. However, the phosphorylation of MAPKs was remarkably inhibited in the presence of *S. aureus* LTA (Fig. 17A). Next, the expression of c-Fos and NFATc1 was examined in committed osteoclast precursors stimulated with Pam2CSK4 and/or *S. aureus* LTA. Although *S. aureus* LTA did not inhibit the expression of c-Fos and NFATc1 in the cytosol of the Pam2CSK4-treated cells, it remarkably inhibited the expression of c-Fos and NFATc1 in the nucleus of the Pam2CSK4-treated cells (Fig. 17B and C). Concordantly, DNA-binding activity of NFATc1 was remarkably increased in the Pam2CSK4-treated cells, but *S. aureus* LTA inhibited the DNA-binding activity of NFATc1 (Fig. 17D). These results imply that *S. aureus* LTA attenuates intracellular signaling involved in Pam2CSK4-induced osteoclastogenesis.

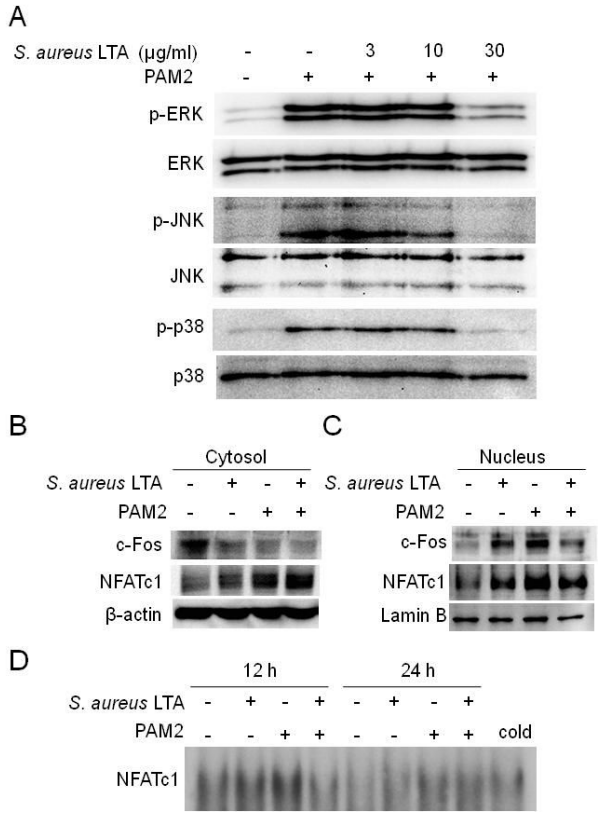

Figure 17. *S. aureus* LTA inhibits Pam2CSK4-induced MAPK activation and DNA-binding activity of NFATc1. (A) Committed osteoclast precursors were serum-deprived for 4 h followed by stimulation with Pam2CSK4 (0.1 μg/ml) and/or *S. aureus* LTA (3, 10, or 30 μg/ml) for 20 min. Cell lysates were prepared and subjected to Western blot analysis to determine phosphorylated or non-phosphorylated forms of ERK, JNK, and p38 kinase. (B to D) Committed osteoclast precursors were stimulated with Pam2CSK4 (0.1 μg/ml) and/or *S. aureus* LTA (30 μg/ml) for 12 h. (B) Cytosolic extracts or (C) nuclear extracts were prepared and subjected to Western blot analysis to determine expression of c-Fos and NFATc1. (D) Nuclear extracts were incubated with ^{32}P-labeled oligonucleotides containing binding site for NFATc1. Protein-DNA binding complex were electrophoresed and subjected to autoradiography. Unlabeled probe was used as a control and marked as ″cold″. One of two similar results is shown.

1.4.6. LTA inhibits dissociation of gelsolin-actin complex induced by Pam2CSK4 or RANKL

The increased actin polymerization by dissociation of gelsolin from actin leads to osteoclast differentiation and activation [86]. However, *S. aureus* LTA directly binds to the active site of gelsolin, resulting in the impairment of gelsolin and actin dissociation [87]. To investigate if *S. aureus* LTA directly inhibits the gelsolin and actin dissociation, the interaction of gelsolin with actin was investigated in committed osteoclast precursors treated with *S. aureus* LTA in the presence or absence of Pam2CSK4 and RANKL. Pam2CSK4 or RANKL remarkably induced the dissociation of gelsolin from actin, but *S. aureus* LTA partially inhibited the dissociation of gelsolin from actin (Fig. 18). These results suggest that *S. aureus* LTA inhibits Pam2CSK4- or RANKL-induced actin polymerization by inhibiting gelsolin-actin dissociation.

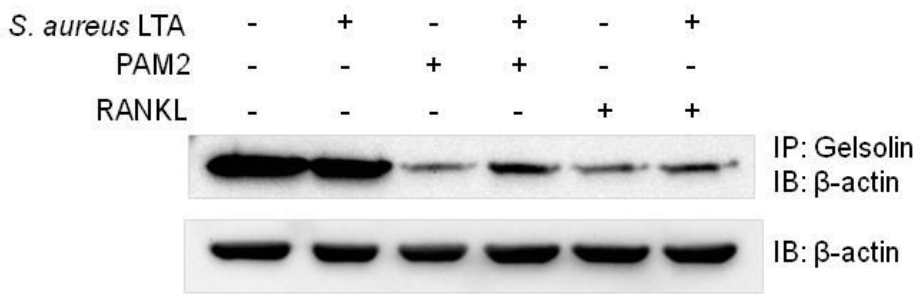

Figure 18. *S. aureus* LTA inhibits dissociation of gelsolin-actin induced by Pam2CSK4 or RANKL. Committed osteoclast precursors were stimulated with *S. aureus* LTA (30 μg/ml) in the presence or absence of Pam2CSK4 (0.1 μg/ml) or RANKL (0.1 μg/ml), with M-CSF (20 ng/ml) for 12 h. Cell lysates at 150 μg were incubated with antibody specific to gelsolin for 12 h followed by further incubation with protein G-agarose beads for 2 h. After discarding the supernatant, the agarose beads were washed and bead-bound proteins were subjected to Western blot analysis using anti-β-actin antibody. One of two similar results is shown.

2. Role of adiponectin in osteoclastogenesis

2.1. Adiponectin-deficient mice exhibit decreased bone mass but increased bone marrow adiposity

To investigate whether adiponectin deficiency affects bone metabolism, the femurs isolated from wild-type and adiponectin-deficient mice were scanned with micro-CT. Trabecular bone volume and trabecular number were 2-fold lower in the femurs of adiponectin-deficient mice than in those of wild-type mice. Concomitantly, trabecular separation was increased and trabecular thickness was similar in the femurs of adiponectin-deficient mice compared with those of wild-type mice (Fig. 19A and B). To determine whether the decreased bone mass in adiponectin deficiency is due to excessive bone resorption and/or attenuated bone formation, bone histomorphometric parameters were analyzed in the femurs of wild-type and adiponectin-deficient mice. As expected, TRAP staining of the femur section showed that both osteoclast number and osteoclast surface were 2.4-fold higher in adiponectin-deficient mice than in wild-type mice (Fig. 20A and B). In contrast, both osteoblast number and osteoblast surface were 3.2-fold lower in the femur section of adiponectin-deficient mice than in that of wild-type mice (Fig. 20C). Moreover, the femur section demonstrated an increase of bone marrow adiposity in the adiponectin-deficient mice compared with the wild-type mice. Both adipocyte number and adipocyte area were also 6.9-fold higher in the femur section of adiponectin-deficient mice than in that of wild-type mice (Fig. 20D). These results indicate that adiponectin deficiency decreases bone mass by enhancing bone resorption and attenuating bone formation but, instead, increases bone marrow adiposity by enhancing adipocyte formation.

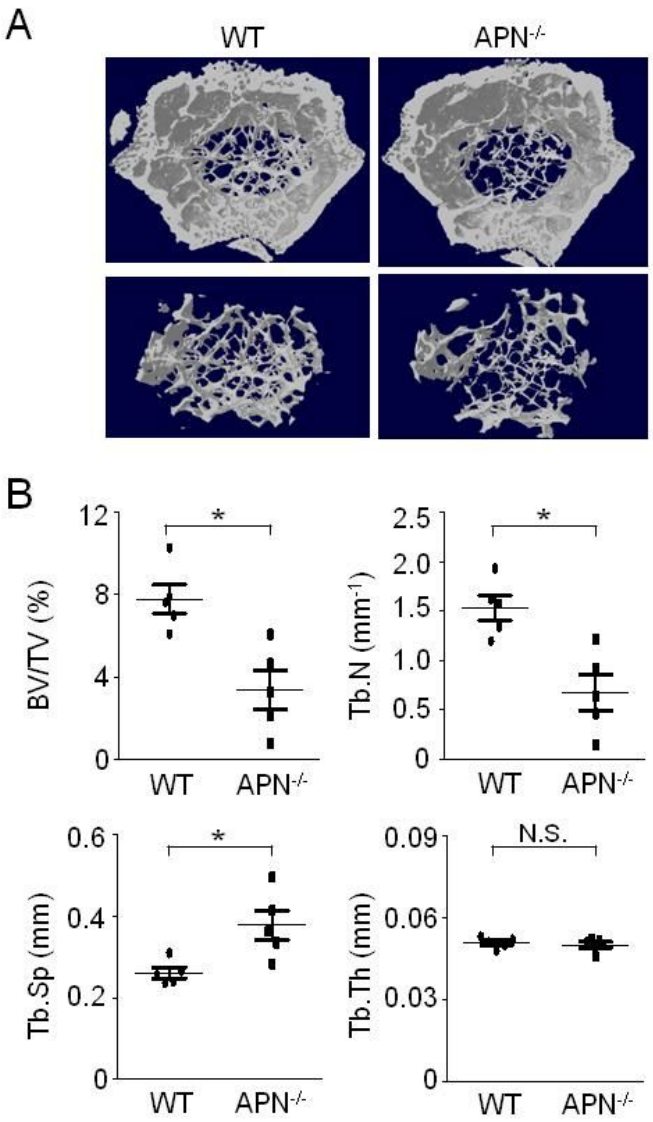

Figure 19. Adiponectin-deficient mice exhibit decreased bone mass. The femurs were obtained from wild-type and adiponectin-deficient mice (n = 5 per group), and subjected to micro-CT analysis to (A) obtain three dimensional images or (B) trabecular bone parameters. BV/TV, trabecular bone volume. Tb.N, trabecular number. Tb.Sp, trabecular separation. Tb.Th, trabecular thickness. N.S., not significant. APN$^{-/-}$, adiponectin-deficient. *P < 0.05 when compared with wild-type mice.

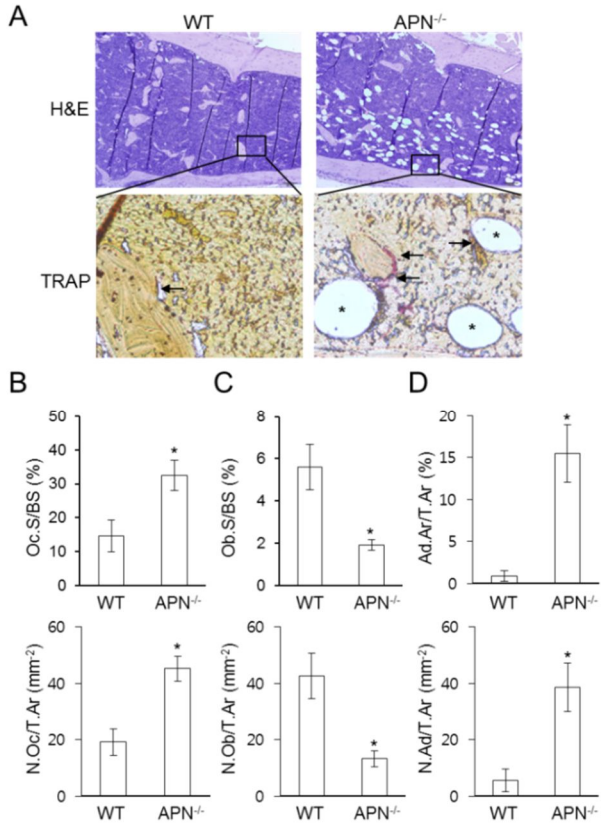

Figure 20. The femurs of adiponectin-deficient mice display increased bone resorption, decreased bone formation, and increased adiposity. The femurs (n = 3 per group) were formalin-fixed, embedded, and sectioned. (A) After H&E or TRAP staining, the sections were subjected to microscopic analysis under an inverted phase-contrast microscope with magnification at ×100 (*upper*) and ×1600 (*lower*). Arrow and asterisk indicate TRAP-positive osteoclasts and adipocytes, respectively. Histomorphometric analysis was performed for static indices related with (B) bone resorption, (C) bone formation, and (D) adiposity formation using osteomeasure software. Oc.S/BS, osteoclast surface per bone surface. N.Oc/T.Ar, osteoclast number per tissue area. Ob.S/BS, osteoblast surface per bone surface. N.Ob/ T.Ar, osteoblast number per tissue area. N.Ad/T.Ar, adipocyte number per tissue area. Ad.Ar/T.Ar, adiposity area per tissue area. *P < 0.05 when compared with wild-type mice.

2.2. Adiponectin-deficient osteoblast precursors preferentially differentiate into adipocytes rather than osteoblasts

Since osteoblasts and adipocytes are known to be exclusively differentiated from common bone marrow mesenchymal cell lineages in bone microenvironment [9], it was examined if adiponectin deficiency shifts differentiation of mesenchymal cell lineages toward adipocytes rather than osteoblasts. When osteoblast differentiation was induced from calvarial osteoblast precursors by incubating ascorbic acid and β-glycerophosphate, adiponectin-deficient cells were weakly differentiated into ALP- and Alizarin Red S-positive cells compared with the wild-type cells (Fig. 21A and B). Consistently, quantitative measurements of Alizarin Red S absorbance showed that the adiponectin-deficient cells showed attenuation of the deposition of calcified matrix (Fig. 21C). Moreover, the mRNA levels of the osteogenic marker genes including ALP, BSP, and OCN were attenuated in the adiponectin-deficient cells (Fig. 21D), indicating that adiponectin-deficient osteoblast precursors have weak osteoblastogenic potential. Next, when adipocyte differentiation was induced from calvarial osteoblast precursors by incubating with dexamethasone, insulin, and IBMX, Oil Red O staining demonstrated that adiponectin-deficient cells produced an increase of lipid droplets compared with wild-type cells (Fig. 22A and B). The mRNA level of PPARγ, a major transcription factor for adipogenesis, was also increased in the adiponectin-deficient cells compared with the wild-type cells (Fig. 22C). Taken together, these results suggest that adiponectin deficiency skews differentiation of osteoblast precursors toward adipocytes rather than osteoblasts.

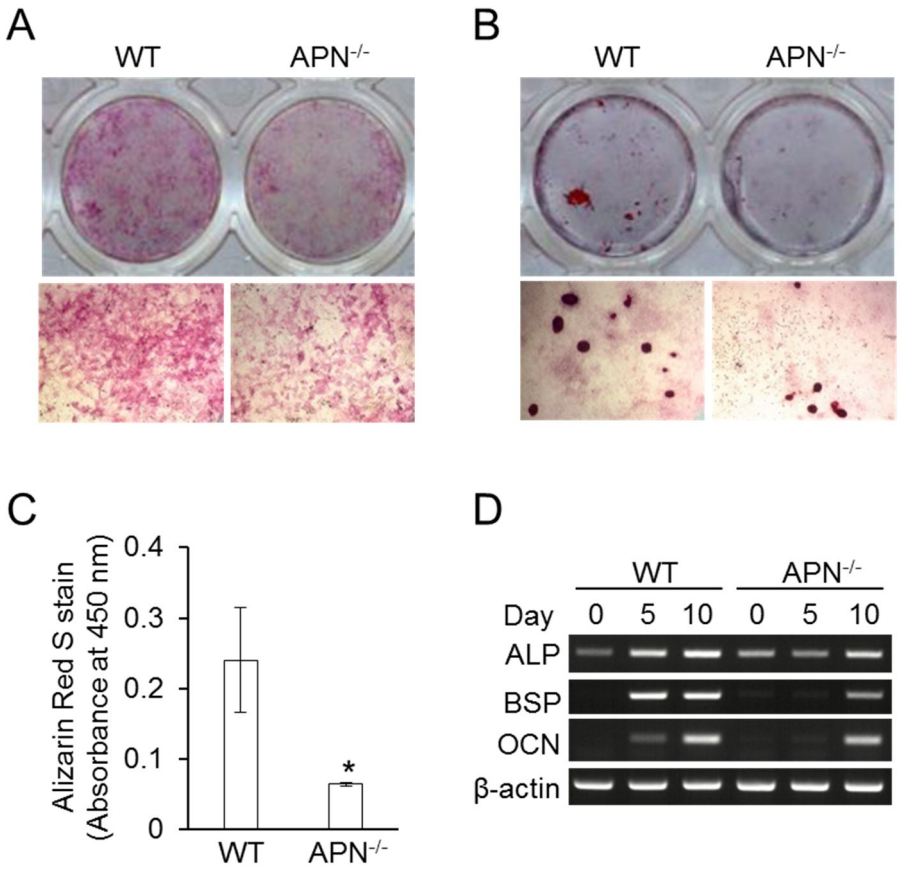

Figure 21. Adiponectin-deficient calvarial cells hardly differentiate into osteoblasts. Calvarial cells were grown until fully confluent and then incubated with β-glycerophosphate (10 mM) and ascorbic acid (50 μM). At day 7 or 21 after the initial incubation, the cells were stained with (A) ALP or (B) Alizarin Red S, respectively. The cells were photographed (*upper*) or observed under an inverted phase-contrast microscope with magnification at ×20 (*lower*). (C) After Alizarin Red S staining, the cells were dissolved and the absorbance at 450 nm was measured. *$P < 0.05$ when compared with wild-type cells. (D) Total RNAs were isolated, reversed-transcribed, and subjected to PCR.

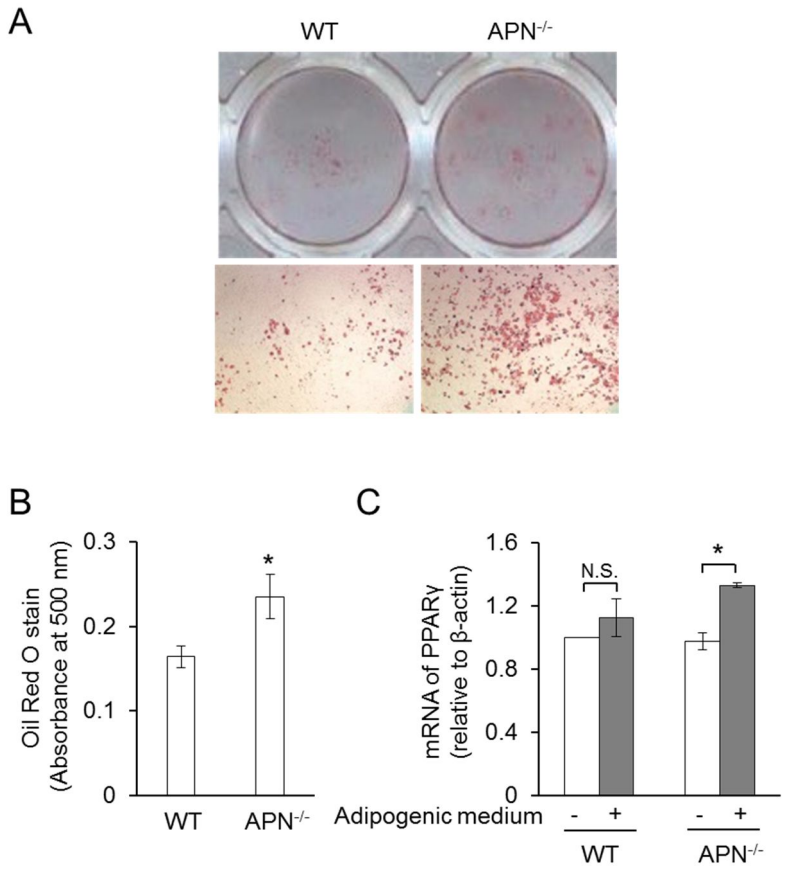

Figure 22. Adiponectin-deficient calvarial cells preferentially differentiate into adipocytes. For adipocyte differentiation, calvarial cells were grown until fully confluent and then incubated with dexamethasone (1 μM), insulin (5 μg/ml), and IBMX (0.5 mM) for 21 days. (D) After Oil Red O staining, the cells were photographed (*upper*) or observed under an inverted phase-contrast microscope with magnification at ×20 (*lower*). (E) The cells were dissolved and the absorbance at 500 nm was measured. (F) At day 5, the mRNA level of PPARγ was determined by RT-PCR. The cDNA copy number was normalized to that of β-actin, and relative expression was calculated by comparing the ratio of samples to that of wild-type control using densitometric analysis. **P* < 0.05 when compared with non-treated cells. N.S., not significant.

2.3. Adiponectin-deficient macrophages have weak osteoclastogenic potential

2.3.1. Adiponectin-deficient BMMs scarcely differentiate into osteoclasts

Based on excessive bone resorption in the femur of the adiponectin-deficient mice (Fig. 20B), this study hypothesized that adiponectin-deficient osteoclast precursors may efficiently differentiate into osteoclasts. Thus, osteoclast differentiation from BMMs was induced by M-CSF and RANKL. Unexpectedly, the number of TRAP-positive MNCs was attenuated in the BMMs from adiponectin-deficient mice than in those from wild-type mice (Fig. 23A). In addition, when BMMs were plated onto calcium phosphate-coated culture plates and then incubated with M-CSF and RANKL, resorption pit area was also 3.3-fold lower in the BMMs from adiponectin-deficient cells than those from wild-type mice (Fig. 23B). These results indicate that adiponectin-deficient BMMs possess weak osteoclastogenic potential.

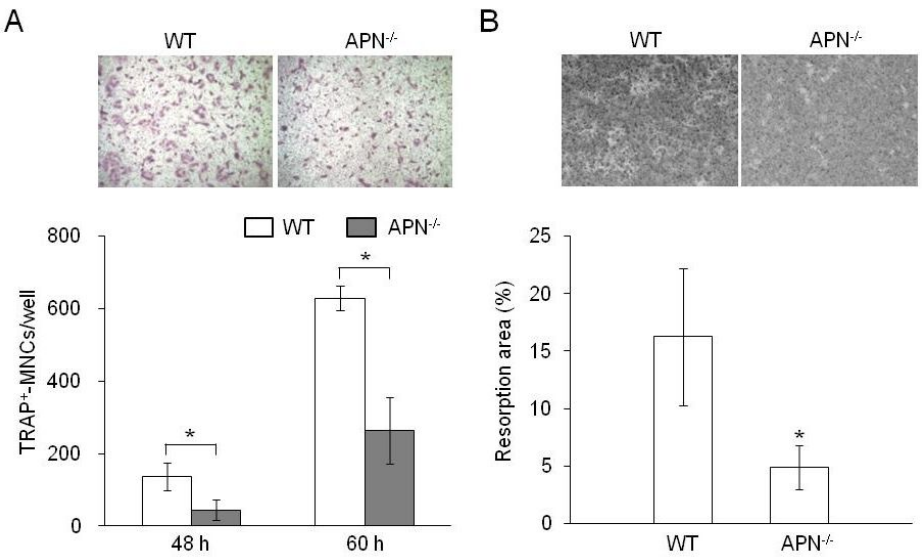

Figure 23. Adiponectin-deficient BMMs scarcely differentiate into osteoclasts. (A) BMMs were incubated with M-CSF (20 ng/ml) and RANKL (40 ng/ml) for 48 h or 60 h. After TRAP staining, the stained cells were photographed under an inverted phase-contrast microscope with magnification at ×40 and TRAP-positive multinucleated cells were enumerated. (B) BMMs were plated onto calcium phosphate-coated plates and then incubated with M-CSF (20 ng/ml) and RANKL (40 ng/ml) for 5 days. Resorbed pits were photographed under an inverted phase-contrast microscope with magnification at ×40 and total resorption area per well was measured by ImageJ software. WT, wild-type. $APN^{-/-}$, adiponectin-deficient. **P* < 0.05 when compared with wild-type cells. One of three similar results is shown.

2.3.2. Osteoclast progenitors in whole BMs are similar between wild-type and adiponectin-deficient mice

Osteoclast progenitors in BMs are classified into two types with different osteoclastogenic potential [88]. $CD11b^{low}B220^{-}CD3\varepsilon^{-}$ cells are composed of about 10% of whole BMs and have potent osteoclastogenic potential, whereas $CD11b^{high}B220^{-}CD3\varepsilon^{-}$ cells are composed of about 60% of whole BMs and have inefficient osteoclastogenic potential [88]. To investigate whether the attenuated osteoclast differentiation of adiponectin-deficient BMMs is related to a decrease of osteoclast progenitors in BMs, osteoclast progenitors were analyzed by flow cytometry. As shown in Fig. 24, the percentages of the cells were similar between wild-type and adiponectin-deficient cells. These results indicate that the decreased osteoclastogenesis of adiponectin-deficient BMMs is not associated with the number of osteoclast progenitors in BMs.

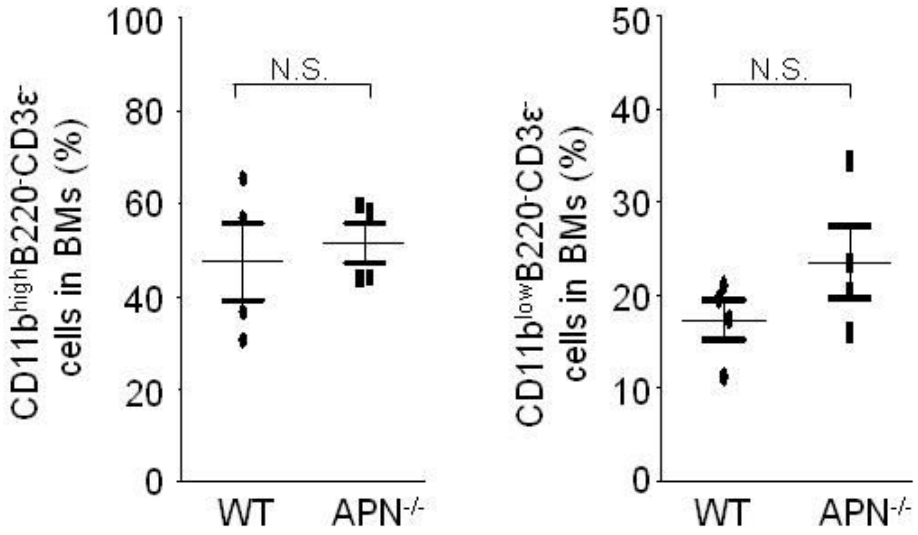

Figure 24. No difference of osteoclast progenitors in BMs from wild-type and adiponectin-deficient mice. Whole BMs were isolated from wild-type and adiponectin-deficient mice. After blocking Fc receptors, the BMs were stained with fluorescent dye-conjugated antibodies specific for CD11b, B220, and CD3ε. The percentage of $CD11b^{high}B220^{-}CD3\varepsilon^{-}$ cells and $CD11b^{low}B220^{-}CD3\varepsilon^{-}$ cells was analyzed by flow cytometry. $*P < 0.05$ when compared with wild-type cells. N.S., not significant.

2.3.3. Adiponectin-deficient BMMs show reduced DNA-binding activities of AP-1 and NFATc1 by decreasing activation of p38 kinase and CREB in response to RANKL

Next, activation of MAPKs and CREB in BMMs was determined in response to RANKL, because MAPKs and CREB are closely associated with RANKL-induced osteoclastogenesis [18, 89]. Western blot analysis demonstrated that phosphorylation of p38 kinase, ERK, and CREB was slightly induced in BMMs from adiponectin-deficient mice compared with those from wild-type mice at 15 min without change of JNK (Fig. 25A). Expression of c-Fos and NFATc1 was further determined by Western blot analysis because c-Fos and NFATc1 are essential transcription factors for RANKL-induced osteoclastogenesis. The expression of c-Fos and NFATc1 was scarcely induced in the BMMs from adiponectin-deficient mice in response to RANKL and M-CSF (Fig. 25B). Indeed, DNA-binding activities of AP-1 and NFATc1 were also attenuated in the BMMs from adiponectin-deficient mice compared with those from wild-type mice under the same conditions (Fig. 25C). These results indicate that adiponectin-deficient BMMs have weak osteoclastogenic potential through decreased activation of p38 kinase, ERK, and CREB followed by reduced DNA-binding activities of AP-1 and NFATc1.

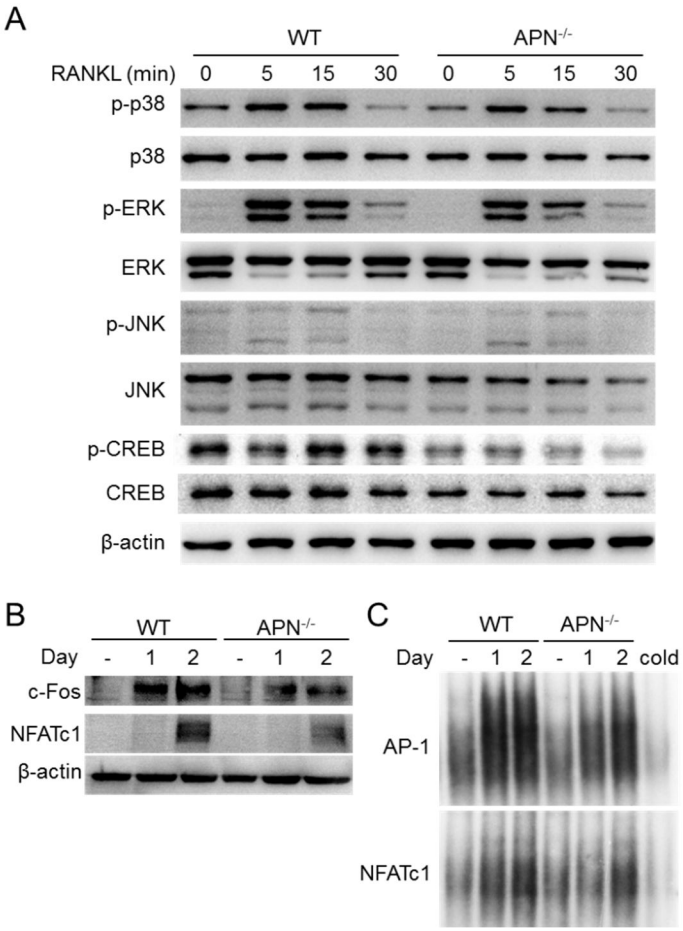

Figure 25. Adiponectin-deficient BMMs slightly induce RANKL-induced signaling. (A) BMMs were serum-starved for 3 h and stimulated with RANKL (100 ng/ml) for 0, 5, 15, and 30 min. Then, the cells were lysed and subjected to Western blot analysis using antibodies specific to phosphorylated or nonphosphorylated p38 kinase, ERK, JNK, and CREB. (B) BMMs were incubated with M-CSF (20 ng/ml) and RANKL (100 ng/ml) for 1 or 2 day(s). Expression of c-Fos and NFATc1 was determined by Western blot analysis. (C) Nuclear extracts were incubated with ^{32}P-labeled oligonucleotides containing binding sites for AP-1 and NFATc1. Protein-DNA binding complexes were electrophoresed and subjected to autoradiography. Unlabeled probe was used as a control and marked as ″cold″.

2.3.4. Weak osteoclastogenic potential of adiponectin-deficient macrophages is associated with properties of M1 macrophages

Osteoclast precursors, macrophages, can be polarized toward inflammatory M1 or anti-inflammatory M2 macrophages [26], and previous reports have shown that adiponectin deficiency induces M1 macrophages [90, 91]. Thus, this study investigated whether the weak osteoclastogenic potential of adiponectin-deficient BMMs is associated with properties of M1 macrophages. As shown in Fig. 26A, adiponectin-deficient BMMs highly expressed mRNA levels of not only M1 markers such as IL-6 and IL-1β but also M2 markers such as CD36 and arginase I. However, the adiponectin-deficient BMMs more expressed protein level of IRF5, a major transcription factor for M1 macrophages, than the wild-type cells (Fig. 26B). In addition, the adiponectin-deficient BMMs induced up-regulated IL-6 and down-regulated IL-10 production upon exposure to LPS, indicating that adiponectin-deficient BMMs are M1 macrophages (Fig. 26C).

Next, this study further examined whether resident peritoneal macrophages from adiponectin-deficient mice have weak osteoclastogenic potential as well as properties of M1 macrophages. To exclude contamination of monocytes during isolation of peritoneal macrophages, expression of F4/80 and C62L was analyzed as F4/80-positive and CD62L-negative cells are known to be macrophages [92]. Flow cytometry demonstrated that the isolated cells were F4/80-positive and CD62L-negative cells (Fig. 26D), indicating that peritoneal macrophages were not contaminated with monocytes. Consistent with the results using BMMs, when the peritoneal macrophages were incubated with M-CSF and RANKL, the number of TRAP-positive MNCs was 2.7-fold lower in adiponectin-deficient peritoneal macrophages than in the wild-type cells (Fig. 26E). In addition, up-regulated IL-6 and down-regulated IL-10 productions were observed in the adiponectin-deficient

cells compared with the wild-type cells upon exposure to LPS (Fig. 26F), implying that macrophages in adiponectin deficiency have weak osteoclastogenic potential as well as M1 polarizing potential.

In contrast, treatment with adiponectin increased the number of TRAP-positive MNCs (Fig. 27A). In addition, the adiponectin-treated cells induced down-regulated IL-6 and up-regulated IL-10 production, which is a typical feature of M2 macrophages (Fig. 27B). These findings suggest that weak osteoclastogenic potential of adiponectin-deficient macrophages is associated with properties of M1 macrophages.

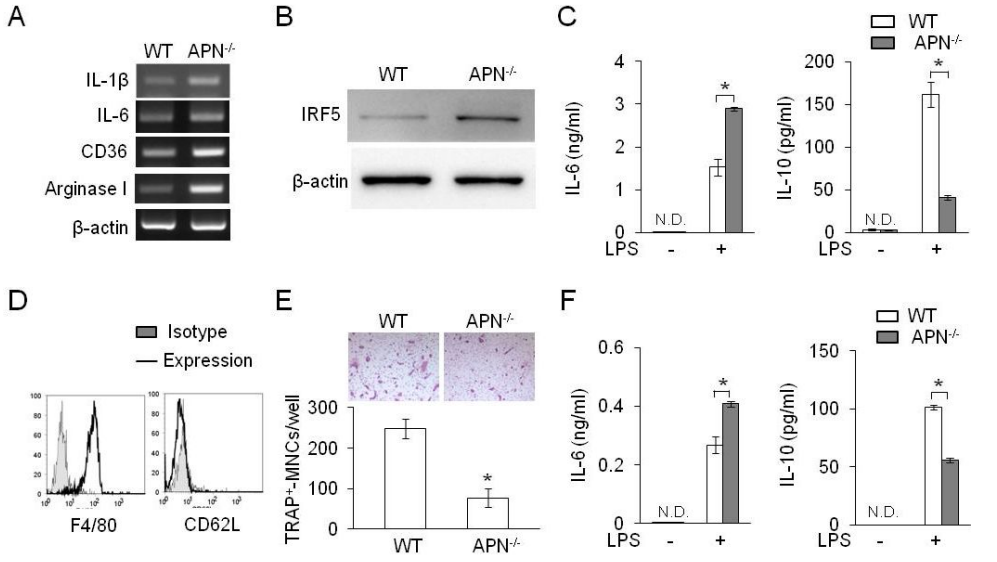

Figure 26. Adiponectin-deficient macrophages possess both weak osteoclastogenic potential and characteristics of M1 macrophages. (A) Total RNAs were isolated from BMMs, reversed-transcribed, and subjected to PCR. (B) Lysates were prepared from BMMs and subjected to Western blot analysis using anti-IRF5 antibody. (C) BMMs were stimulated with LPS (0.1 μg/ml) for 24 h. The culture supernatants were analyzed to determine the amounts of IL-6 and IL-10 by ELISA. (D) Peritoneal macrophages were isolated, blocked Fc receptors, and then stained with fluorescent dye-conjugated antibodies specific for F4/80 and CD62L. The cells were analyzed by flow cytometry. (E) Peritoneal macrophages were incubated with M-CSF (20 ng/ml) and RANKL (40 ng/ml) for 4 days. After TRAP staining, the cells were photographed were photographed under an inverted phase-contrast microscope with magnification at ×40 and $TRAP^+$-MNCs were enumerated. (F) Peritoneal macrophages were stimulated with LPS (0.1 μg/ml) for 24 h. Production of IL-6 and IL-10 was determined in the culture supernatants by ELISA. *$P < 0.05$ when compared with wild-type cells. N.D., not detected. One of three similar results is shown.

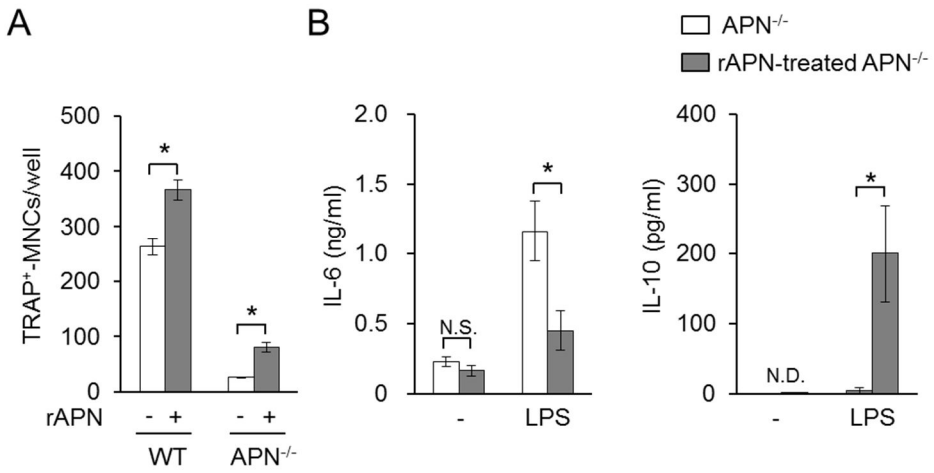

Figure 27. Adiponectin-treated cells have potent osteoclastogenic potential and anti-inflammatory properties of M2 macrophages. BMs were incubated with adiponectin (2 μg/ml) for 24 h and the stroma-free BMs were harvested. (A) The cells were incubated with M-CSF (20 ng/ml) and RANKL (40 ng/ml) for 3 days. After TRAP staining, $TRAP^+$-MNCs were enumerated. (B) The cells were incubated with M-CSF (20 ng/ml) for 5 days followed by stimulation with LPS (0.1 μg/ml) for 24 h. The culture supernatants were analyzed to determine the amounts of IL-6 and IL-10 by ELISA. *$P < 0.05$ when compared with non-treated cells. N.D., not detected. N.S., not significant. rAPN, recombinant adiponectin. One of three similar results is shown.

2.3.5. M1 macrophages have weak osteoclastogenic potential

2.3.5.1. M1 macrophages scarcely differentiate into osteoclasts

Next, this study further investigated the different osteoclastogenic potential between M1 and M2 macrophages. Macrophages derived from monocytes by GM–CSF and M-CSF have been commonly used as M1 and M2 macrophages, respectively [26, 93]. Thus, stroma-free BMs were incubated with either GM-CSF for M1 macrophages or M-CSF for M2 macrophages, and the BMMs were differentiated to osteoclasts by RANKL and M-CSF. Microscopic analysis following TRAP staining showed that RANKL dose-dependently increased the number of TRAP-positive MNCs from M2 macrophages but not M1 macrophages (Fig. 28A). To clarify whether the attenuated osteoclast differentiation is a general feature of the M1 macrophages, osteoclast differentiation was further examined using M1 macrophages induced by LPS plus interferon-γ (IFN-γ) or M2 macrophages induced by IL-4 or IL-10. As expected, the number of TRAP-positive MNCs was remarkably increased in the M2 macrophages compared with the M1 macrophages (Fig. 28B). These results indicate that M1 macrophages have weak osteoclastogenic potential compared with M2 macrophages.

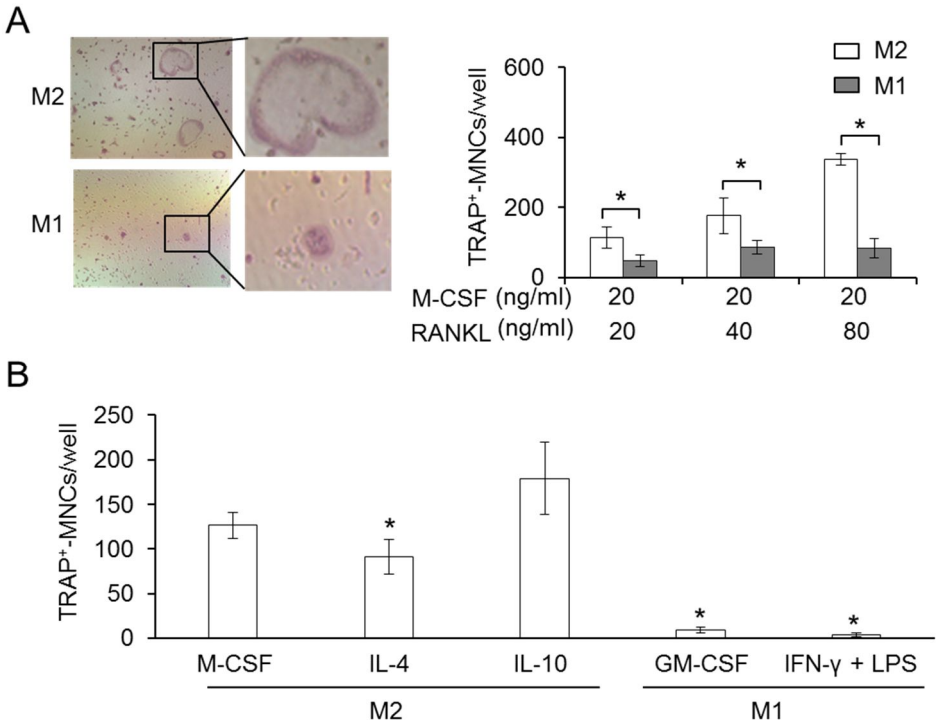

Figure 28. M1 macrophages scarcely differentiate to osteoclasts in response to RANKL and M-CSF. (A) M1 and M2 macrophages were prepared from stroma-free BMs by incubation with GM-CSF (10 ng/ml) and M-CSF (20 ng/ml) for 5 days, respectively. (A) Macrophages were further incubated with M-CSF (20 ng/ml) and RANKL (20, 40, or 80 ng/ml) for 3 days. After TRAP staining, the cells were photographed under an inverted phase-contrast microscope with magnification at ×40 (*left*) or ×400 (*right*), and $TRAP^+$-MNCs were enumerated. M-CSF-induced BMMs were further incubated with IL-4 (50 ng/ml), IL-10 (20 ng/ml), GM-CSF (20 ng/ml), and LPS (100 ng/ml) along with IFN-γ (20 ng/ml) in the presence of M-CSF (20 ng/ml) for 24 h. Then, the cells were incubated with M-CSF (20 ng/ml) and RANKL (40 ng/ml) for 3 days. After TRAP staining, $TRAP^+$-MNCs were enumerated. *$P < 0.05$ when compared with M2 macrophages. One of three similar results was shown.

2.3.5.2. M1 macrophages have reduced bone resorptive capacity

Next, osteoclast functions, such as bone-resorption capacity and podosome belt formation, in M1 and M2 macrophages were further investigated in the presence of M-CSF and RANKL. When BMMs were plated on calcium phosphate-coated plates and differentiated to osteoclasts by M-CSF and RANKL, large areas of resorption pits were observed in M2 macrophages compared with M1 macrophages (Fig. 29A). Immunofluorescence confocal microscopic analysis also showed that the size of podosome belt at the cell periphery was larger in M2 macrophages than in M1 macrophages in response to M-CSF and RANKL (Fig. 29B). These results indicate that M1 macrophages are weak osteoclast precursors whereas M2 macrophages are potent osteoclast precursors.

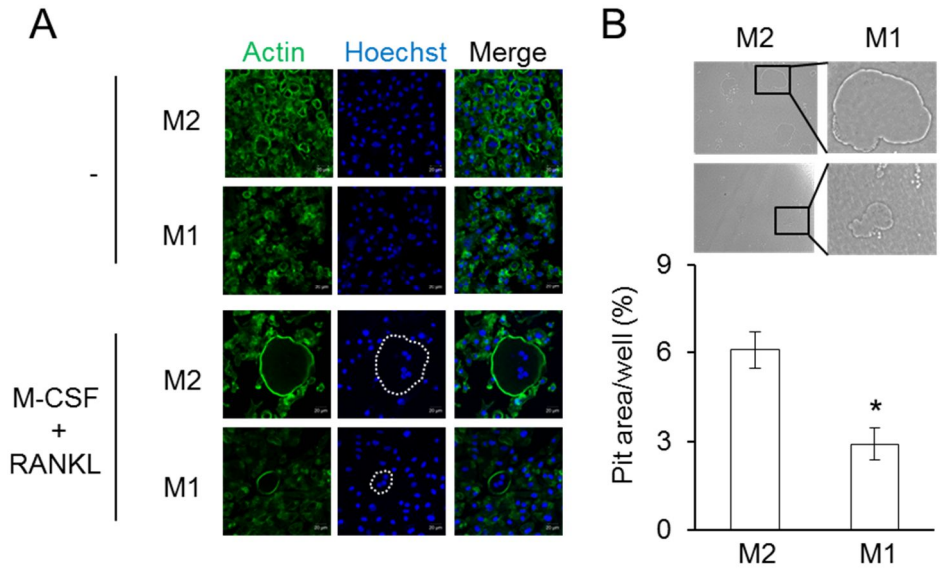

Figure 29. Osteoclast activation is attenuated in M1 macrophages compared with M2 macrophages. (A) Macrophages were plated on coverslips in 24-well culture plates and incubated with M-CSF (20 ng/ml) and RANKL (100 ng/ml) for 4 days. The cells were fixed, permeabilized, and stained for F-actin (green). Then, the stained cells were examined by immunocytochemistry analysis. The nucleus was counterstained with Hoechst for each sample. Bars, 20 μm. (B) Macrophages were plated onto calcium phosphate-coated plates and incubated with M-CSF (20 ng/ml) and RANKL (50 ng/ml) for 4 days. The resorbed area were photographed under an inverted phase-contrast microscope with magnification at ×40 (*left*) or ×400 (*right*), and total resorption area per well was measured with ImageJ software. **P* < 0.05 when compared with M2 macrophages. One of three similar results was shown

2.3.5.3. Efficient osteoclastogenic potential of M2 macrophages is not associated with expression of osteoclastogenesis-associated receptors

Osteoclastogenesis-associated receptors such as c-Fms, RANK, and TREM2 are important for initiation of osteoclast differentiation [94]. To investigate whether M2 macrophages have efficient osteoclastogenic potential by upregulating c-Fms, RANK, and TREM2 expression, their expression was determined in M1 and M2 macrophages. Flow cytometry demonstrated that M2 macrophages highly expressed c-Fms compared with M1 macrophages. The up-regulated expression of c-Fms was also observed in M2 macrophages treated with M-CSF alone or together with RANKL (Fig. 30A). RANK and TREM2 were barely expressed in M2 and M1 macrophages. Upon exposure to M-CSF with or without RANKL, the expression of RANK and TREM2 was similarly increased in both M2 and M1 macrophages (Fig. 3B and C). These results indicate that expression of osteoclastogenesis-associated receptors is not associated with efficient different osteoclastogenic potential between macrophage subtypes.

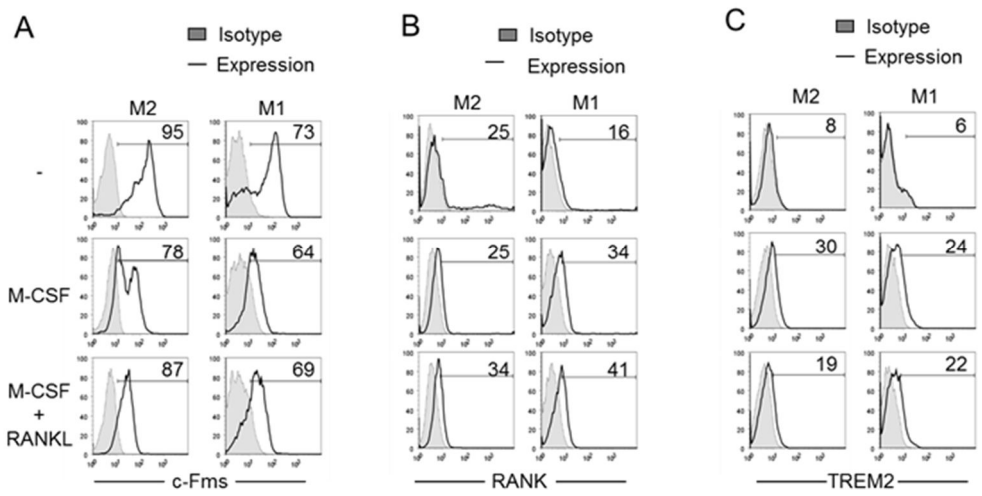

Figure 30. Expression of c-Fms, RANK, and TREM2 on M1 and M2 macrophages. M1 and M2 macrophages were incubated with M-CSF (20 ng/ml) and RANKL (100 ng/ml) for 2 days. After blocking Fc receptors, the cells were stained with fluorescent dye-conjugated antibodies specific to (A) c-Fms, (B) RANK, and (C) TREM2. The stained cells were analyzed by flow cytometry. Number in each histogram indicates the percentage of positive cells. One of three similar results is shown.

2.3.5.4. M2 macrophages remarkably activate AP-1 and NFATc1 through up-regulation of calcium oscillation followed by CREB activation

MAPKs and CREB are closely associated with RANKL-induced early signaling pathways for osteoclast differentiation. Therefore, the activation of MAPKs and CREB was analyzed to determine if effective osteoclastogenic potential of M2 macrophages is due to increased RANK-mediated activation of MAPKs and CREB. Western blot analysis showed that M2 macrophages highly induced phosphorylation of MAPKs, such as p38 kinase, ERK, and JNK, and CREB in response to RANKL compared with M1 macrophages (Fig. 31A), indicating that RANKL-induced early signaling pathways are slightly involved in the efficient osteoclastogenic potential of M2 macrophages. To determine whether RANKL-induced late signaling pathways are involved in the efficient osteoclastogenic potential of M2 macrophages, calcium oscillation was determined in M1 and M2 macrophages. Stroma-free BMs showed spontaneous calcium oscillations. Similar to previous reports [18], M2 macrophage barely generated calcium oscillations but had upregulation of that upon exposure to M-CSF and RANKL. In contrast, M1 macrophages remarkably generated calcium oscillations but showed an attenuation of that by M-CSF and RANKL (Fig. 32A and B). Since calcium oscillation is required for efficient expression and activation of crucial transcription factors such as c-Fos and NFATc1 by sustaining CREB activation [18], phosphorylation of CREB was determined in macrophages treated with M-CSF and RANKL for 2 days. As expected, M2 macrophages showed sustained phosphorylation of CREB and increased expression of CREB compared with M1 macrophages. Concordantly, expression and DNA-binding activities of c-Fos and NFATc1 were also remarkably increased in M2 macrophages compared with M1 macrophages under the same conditions (Fig. 33 A and B). These results suggest that M2 macrophages act as potent osteoclast precursors by enhancing activation of AP-1 and NFATc1 through CREB activation.

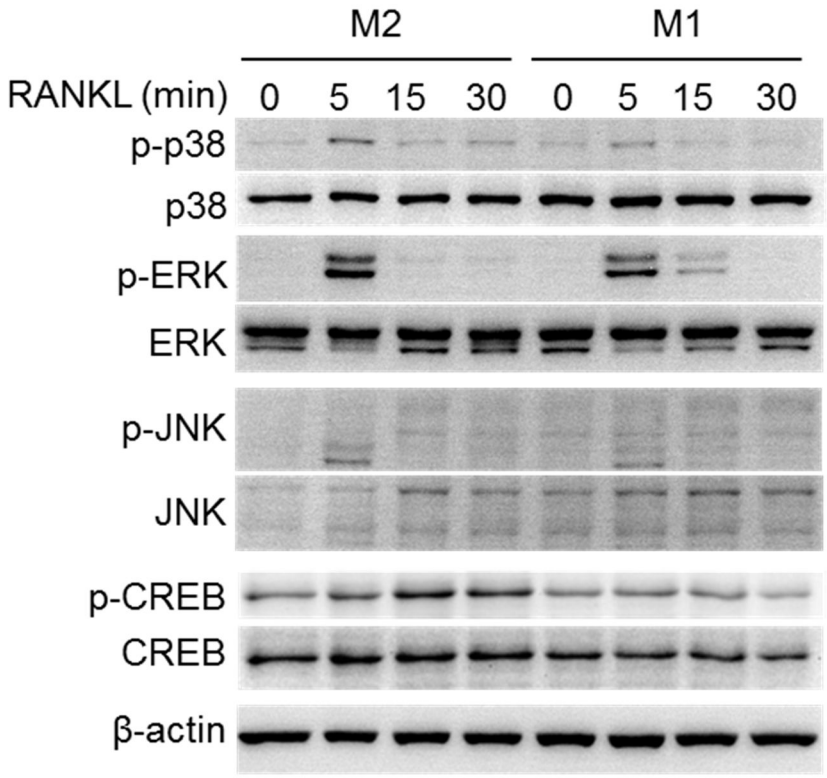

Figure 31. RANKL-mediated activation of MAPKs and CREB is attenuated in M1 macrophages. M1 and M2 macrophages were serum-deprived for 3 h and incubated with 100 ng/ml of RANKL for 0, 5, 15, and 30 min. Cell lysates were prepared and subjected to Western blot analysis to determine phosphorylated and non-phosphorylated forms of MAPKs and CREB. One of three similar results is shown.

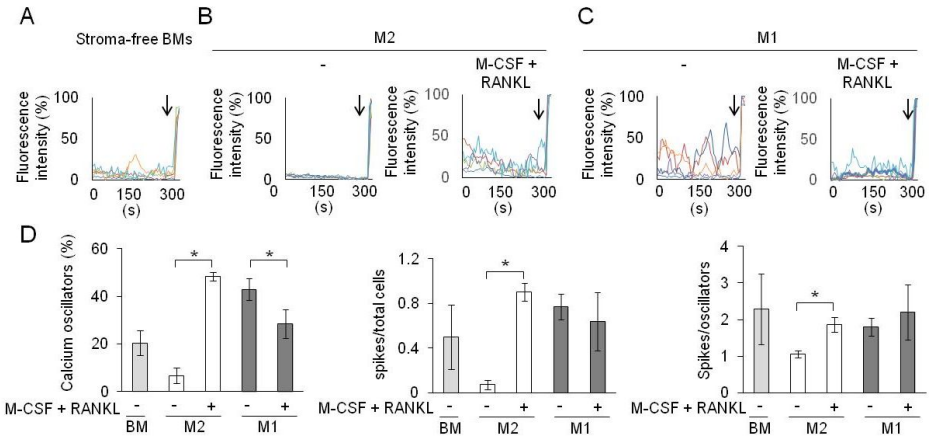

Figure 32. Calcium oscillation is barely induced in M1 macrophages during osteoclast differentiation. (A) Stroma-free BMs were loaded with fluo-4/AM (3 μM), pluronic F-127 (0.02%), and probenecid (1 mM) for 30 min at 37°C. The cells were washed with calcium-free HBSS three times and plated onto coverslips for 30 min at RT. (B and C) Macrophages were plated onto coverslips in 24-well culture plates and incubated with M-CSF (20 ng/ml) and RANKL (100 ng/ml) for 2 days. The cells were loaded and washed as above mentioned. Calcium oscillatory change was measured with an interval 5 sec using a confocal-laser scanning microscope. Each color indicates a different cell in the same field. An arrow indicates treatment with ionomycin (10 μM) at the end of each experiment. (D) Calcium oscillation frequency (the percentage of oscillators) and the number of calcium oscillation spikes (spikes per oscillators or spikes per total cells) were analyzed by a relative fluorescence intensity change in each single cell. $*P < 0.05$. One of three similar results is shown.

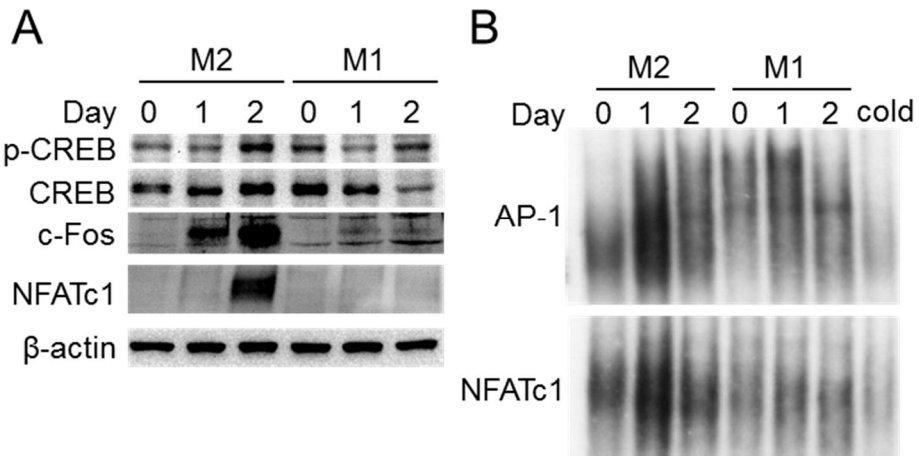

Figure 33. M1 macrophages show reduced DNA-binding activities of AP-1 and NFATc1 through down-regulation of CREB activation. BMMs were incubated with M-CSF (20 ng/ml) and RANKL (100 ng/ml) for 1 and 2 day(s). (A) Total cell lysates were isolated and subjected to Western blot analysis to determine expression of phospho-CREB, CREB, c-Fos, and NFATc1. (B) Nuclear extract were incubated with ^{32}P-labeled oligonucleotides containing binding sites for NFATc1 and AP-1. Protein-DNA binding complex were electrophoresed and subjected to autoradiography. Unlabeled probe was used as a control and marked as "cold". One of three similar results was shown.

2.3.5.5. Osteoclastogenic potential of macrophage is reversible by converting macrophage subtypes

Macrophages can convert from M1 to M2 or from M2 to M1 macrophages [22]. Therefore, osteoclastogenic potential may change depending on conversion of macrophage subtypes. When M2 macrophages were incubated with GM-CSF to convert to M1 macrophages and then differentiated to osteoclasts by M-CSF and RANKL, the number of TRAP-positive MNCs was remarkably decreased in the GM-CSF-treated M2 macrophages compared with the M2 macrophages. In contrast, M-CSF-treated M1 macrophages were rapidly differentiated into TRAP-positive MNCs than untreated M1 macrophages (Fig. 34), implying that osteoclastogenic potential of macrophage is reversible by converting macrophage subtypes.

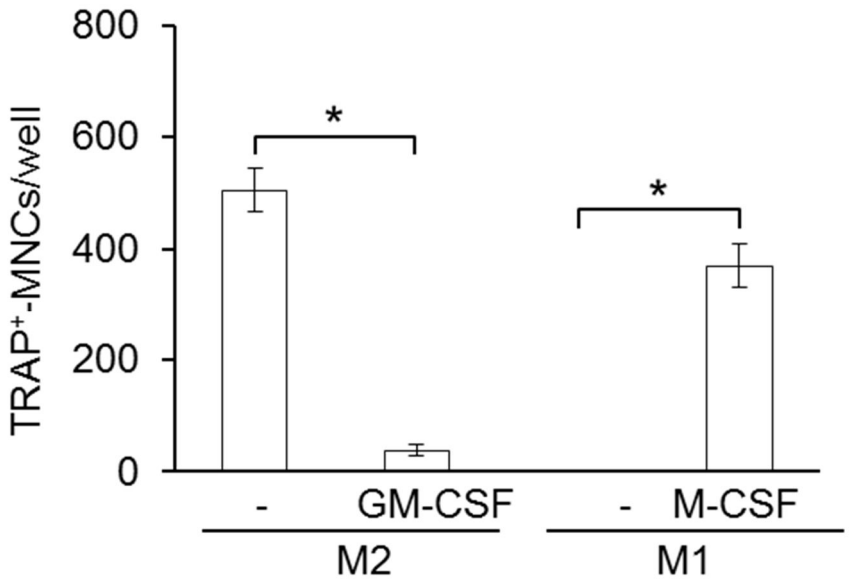

Figure 34. Osteoclastogenic potential of macrophage is reversible by converting macrophage subtypes. M2 and M1 macrophages were incubated with GM-CSF (10 ng/ml) and M-CSF (20 ng/ml) for 24 h, respectively. After washing, the cells were incubated with M-CSF (20 ng/ml) and RANKL (100 ng/ml) for 3 additional days. After TRAP staining, TRAP-positive MNCs were enumerated. *$P < 0.05$ when compared with untreated cells. One of three similar results is shown.

2.3.5.6. Expression of IRF5 modulates osteoclast differentiation

Osteoclastogenic potential was reversible depending on macrophage subtypes, suggesting that factors responsible for macrophage polarization may influence osteoclastogenic potential. Among the factors, IRF5 may be crucial for regulation of osteoclastogenic potential in macrophage subtypes, because IRF5 is a well-known factor capable of inducing M1 macrophages and attenuating M2 macrophages by increasing IRF5 expression [26]. Therefore, based on the results showing that IRF5 was scarcely observed in osteoclasts (Fig. 29A), the effect of IRF5 on osteoclast differentiation was examined using overexpression or silencing of IRF5. When M2 macrophages were transfected with IRF5 overexpression vector and then incubated with RANKL and M-CSF, the cells showed decreased phosphorylation of CREB and reduced expression of NFATc1 compared to the control vector-transfected cells (Fig. 34A). Consistently, the number of TRAP-positive MNCs was also decreased in the cells transfected with IRF5 overexpression vector (Fig. 34B). In contrast, when M1 macrophages were transfected with siRNA targeting IRF5 and then incubated with M-CSF and RANKL, the cells robustly induced phosphorylation of CREB and increased expression of NFATc1 (Fig. 35A). Concordantly, the number of TRAP-positive MNCs was also increased in the IRF5-silenced cells (Fig. 35B). These results indicate that IRF5 may be a crucial factor responsible for the change of osteoclastogenic potential by conversion of macrophage subtypes.

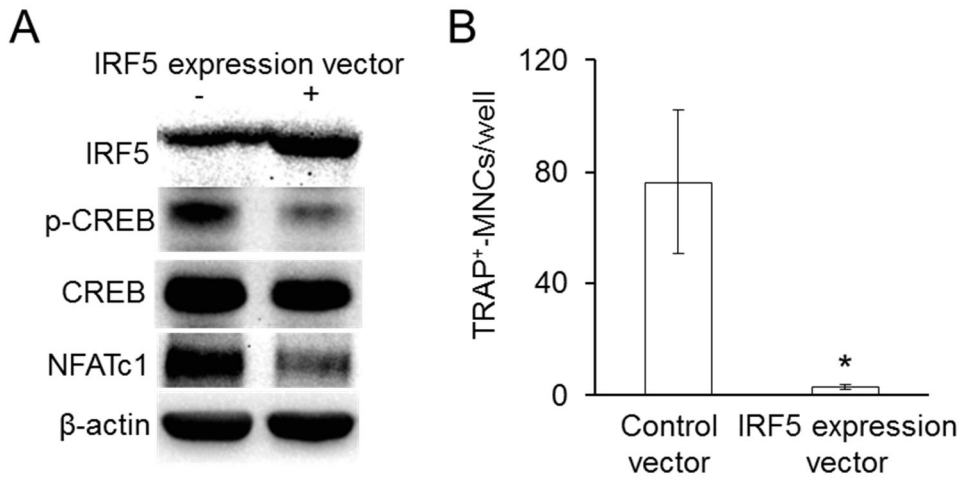

Figure 35. Overexpression of IRF5 inhibits osteoclast differentiation by attenuating CREB phosphorylation and NFATc1 expression in the M2 macrophages. M2 macrophages were transfected with pCGAGS-HA-murine IRF5 (2 μg/ml) or control vector (2 μg/ml) in the presence of M-CSF (10 ng/ml) for 12 h, washed, and further incubated with M-CSF (20 ng/ml) and RANKL (100 ng/ml). (A) After 2 days, the cell lysates were prepared and subjected to Western blot analysis. (B) After 4 days, the cells were stained for TRAP and the number of TRAP-positive MNCs was counted. *$P < 0.05$ when compared with control vector-transfected cells. One of two similar results is shown.

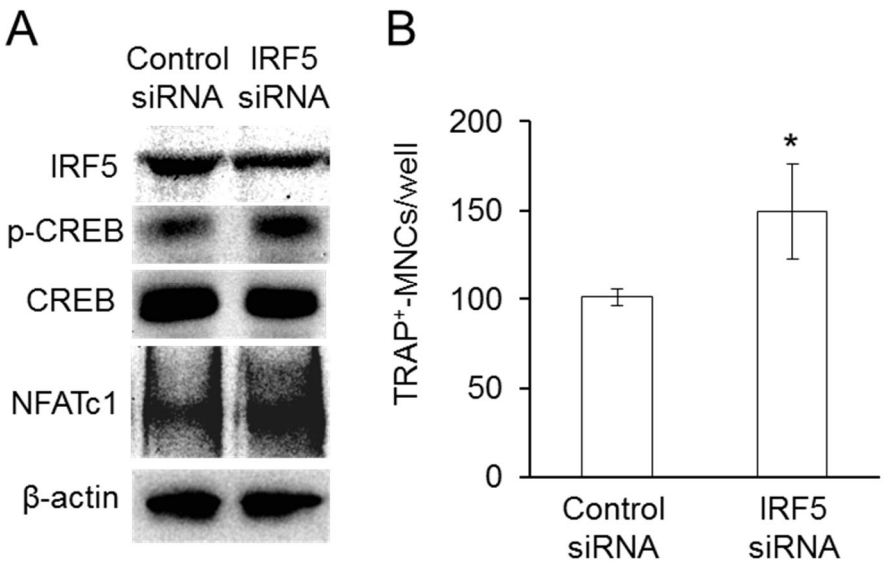

Figure 36. Knockdown of IRF5 enhanced osteoclast differentiation by inducing CREB phosphorylation and NFATc1 expression in the M1 macrophages. M1 macrophages were transfected with IRF5 siRNA (20 nM) or control siRNA (20 nM) in the presence of GM-CSF (5 ng/ml) for 24 h, washed, and further incubated with M-CSF (20 ng/ml) and RANKL (100 ng/ml) (A) After 2 days, the cell lysates were prepared and subjected to Western blot analysis. (B) After 4 days, the cells were stained for TRAP and TRAP-positive MNCs were enumerated. *$P < 0.05$ when compared with control siRNA-transfected cells. One of two similar results is shown.

2.4. Up-regulated RANKL/OPG ratio enhances osteoclast differentiation in adiponectin deficiency

2.4.1. Adiponectin-deficient osteoblast precursors have up-regulated RANKL/OPG ratio

Contrary to the enhanced bone resorption shown in the femur of adiponectin-deficient mice, adiponectin-deficient macrophages had weak osteoclastogenic potential. Thus, this study hypothesized that osteoclast differentiation is indirectly modulated by other cells or their soluble factors in the bone. Since RANKL/OPG ratio is known to be crucial for osteoclast differentiation [16], expression of RANKL and OPG was determined in calvarial osteoblast precursors. The expression of OPG was 2.2-fold lower in the adiponectin-deficient osteoblast precursors than in the wild-type mice (Fig. 37A). The expression of RANKL was slightly decreased under the same condition (Fig. 37B). The RANKL/OPG ratio, an index of osteoclast activation, was 2-fold higher in the calvarial osteoblast precursors obtained from adiponectin-deficient mice than in those obtained from wild-type mice (Fig. 37C). These results suggest that adiponectin-deficient osteoblast precursors up-regulate RANKL/OPG ratio by decreasing OPG expression.

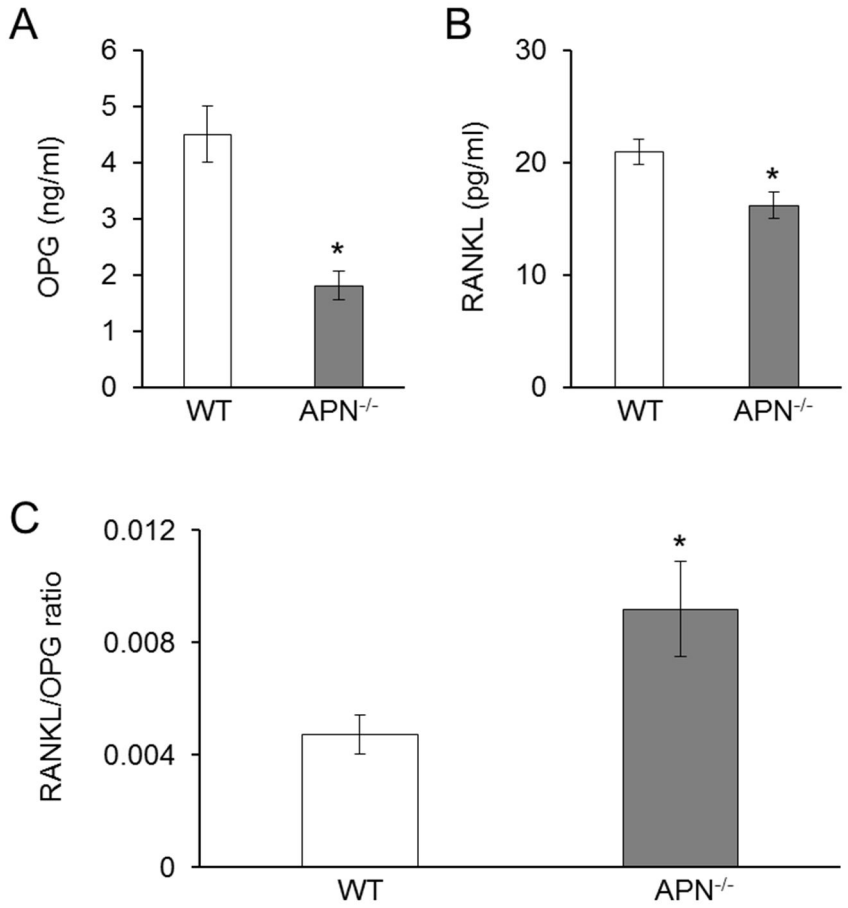

Figure 37. Adiponectin-deficient osteoblast precursors have up-regulated RANKL/OPG ratio by decreasing OPG expression. Calvarial cells were incubated with 1α,25-dihydroxyvitamin D_3 (50 nM) for 3 days. The amounts of (A) OPG and (B) RANKL in the culture supernatants were determined by ELISA. (C) A RANKL/OPG ratio was calculated from protein amounts of RANKL and OPG. *$P < 0.05$ when compared with wild-type cells. WT, wild-type. $APN^{-/-}$, adiponectin-deficient. One of three similar results is shown.

2.4.2. Osteoclast differentiation is enhanced by osteoblast from adiponectin-deficient mice through up-regulation of RANKL/OPG ratio

To determine whether osteoclast differentiation is enhanced by up-regulated RANKL/OPG ratio of adiponectin-deficient osteoblast precursors, co-culture of osteoblast precursors with osteoclast precursors was examined because the co-culture system has been used as a representative *in vitro* model to demonstrate dynamic interaction of osteoblast precursor and osteoclast precursor in the bone [43]. The expression of OPG was 2.8-fold lower but RANKL expression was 2-fold higher in the co-culture of adiponectin-deficient cells than in that of wild-type cells (Fig. 38A and B). Notably, RANKL/OPG ratio was 1.4-fold higher in the co-culture of adiponectin-deficient cells than in that of wild-type cells (Fig. 38C). As expected, the number of TRAP-positive MNCs was 4-fold higher under the same condition (Fig. 38D), implying that osteoclast differentiation is indirectly ameliorated by up-regulating RANKL/OPG ratio of adiponectin-deficient osteoblast precursors. To investigate whether adiponectin inhibits osteoclast differentiation by down-regulating RANKL/OPG ratio, adiponectin was treated in the co-culture condition. As shown in Fig. 39A, the expression of OPG was robustly increased in the osteoblast precursors from both mice. The level of RANKL was not detected under the same condition (Fig. 39B). In addition, adiponectin inhibited the generation of TRAP-positive MNCs in all co-culture groups (Fig. 39C). These findings indicate that adiponectin deficiency indirectly induces osteoclast differentiation by up-regulating RANKL/OPG ratio of osteoblast precursors.

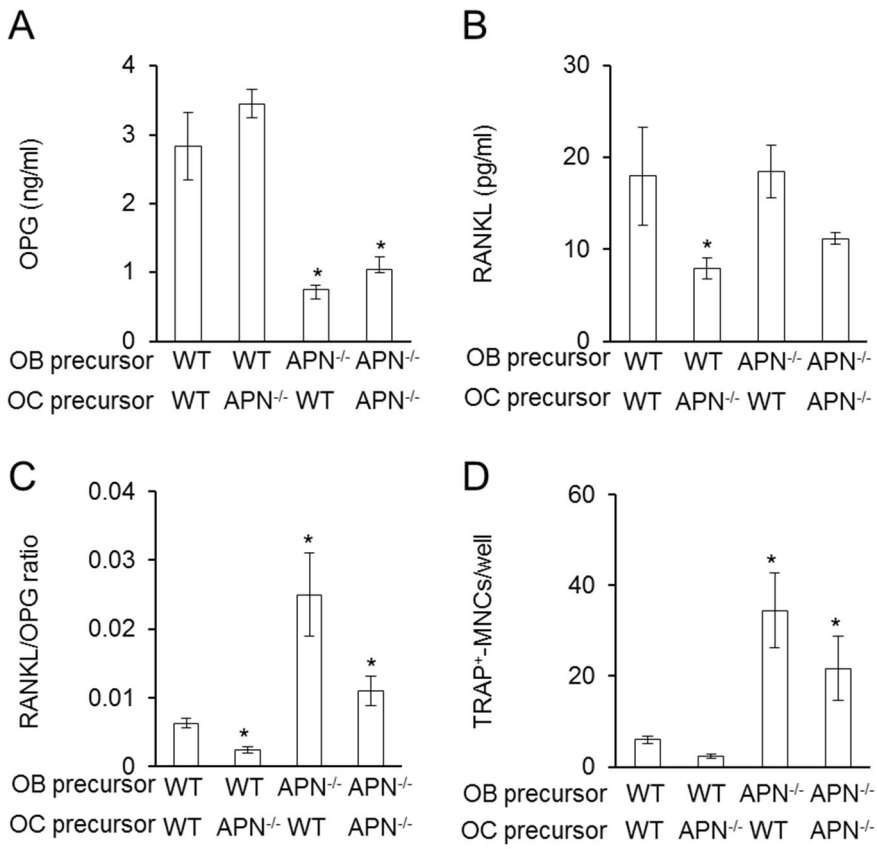

Figure 38. Up-regulation of RANKL/OPG ratio in adiponectin deficiency contributes to the increased osteoclast differentiation. Calvarial cells were seeded in 48-well plates for 6 h and then added BMMs in the presence of 1α,25-dihydroxyvitamin D_3 (50 nM). At day 3, the culture supernatants were analyzed to determine the amounts of (A) OPG and (B) RANKL by ELISA. (C) The RANKL/OPG ratio was calculated from the amounts of RANKL and OPG. (D) At day 7, the cells were stained for TRAP and $TRAP^+$-MNCs was enumerated. *$P <$ 0.05 when compared with co-culture of wild-type osteoblast precursors with wild-type BMMs. One of three similar results is shown. OB precursor, calvarial osteoblast precursor. OC precursor, BMM.

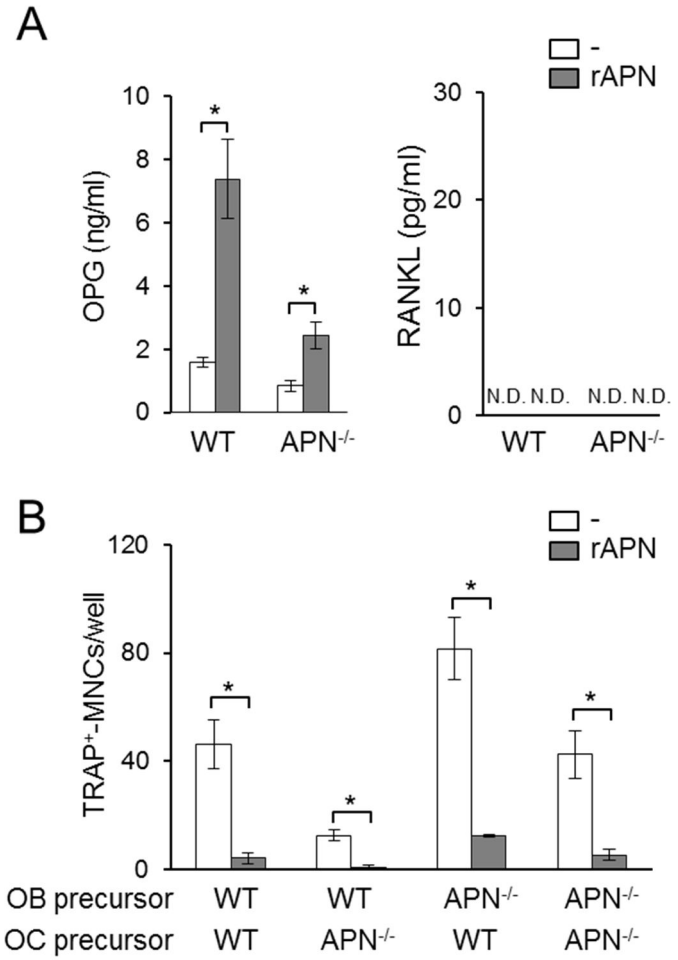

Figure 39. Adiponectin inhibits osteoclast differentiation by up-regulating OPG expression. Calvarial cells were incubated with adiponectin (2 μg/ml) for 3 days. The amounts of (A) OPG and RANKL were determined in the culture supernatant by ELISA. (B) Calvarial cells were co-cultured with BMMs in the presence of 1α,25-dihydroxyvitamin D_3 (50 nM) and/or adiponectin (2 μg/ml) for 7 days. After TRAP staining, the number of $TRAP^+$-MNCs was counted. *$P < 0.05$ when compared with non-treated cells. One of three similar results is shown. rAPN, recombinant adiponectin. OB precursor, calvarial osteoblast precursor. OC precursor, BMM.

2.4.3. RANKL/OPG ratio is increased in the bone marrow of adiponectin-deficient mice

To further investigate whether RANKL/OPG ratio is increased in adiponectin-deficient mice, expression of OPG and RANKL was analyzed in bone marrow extracellular fluids and serum from wild-type and adiponectin-deficient mice. The expression of OPG and RANKL was significantly increased in both the bone marrow and the serum from adiponectin-deficient mice compared with those from wild-type mice. However, RANKL/OPG ratio was 1.7-fold higher in the bone marrow of adiponectin-deficient mice than in that of wild-type mice (Fig. 40A), while serum RANKL/OPG ratio was similar to both wild-type and adiponectin-deficient mice (Fig. 40B). These findings indicate that up-regulated RANKL/OPG ratio influences decreased bone mass of adiponectin-deficient mice.

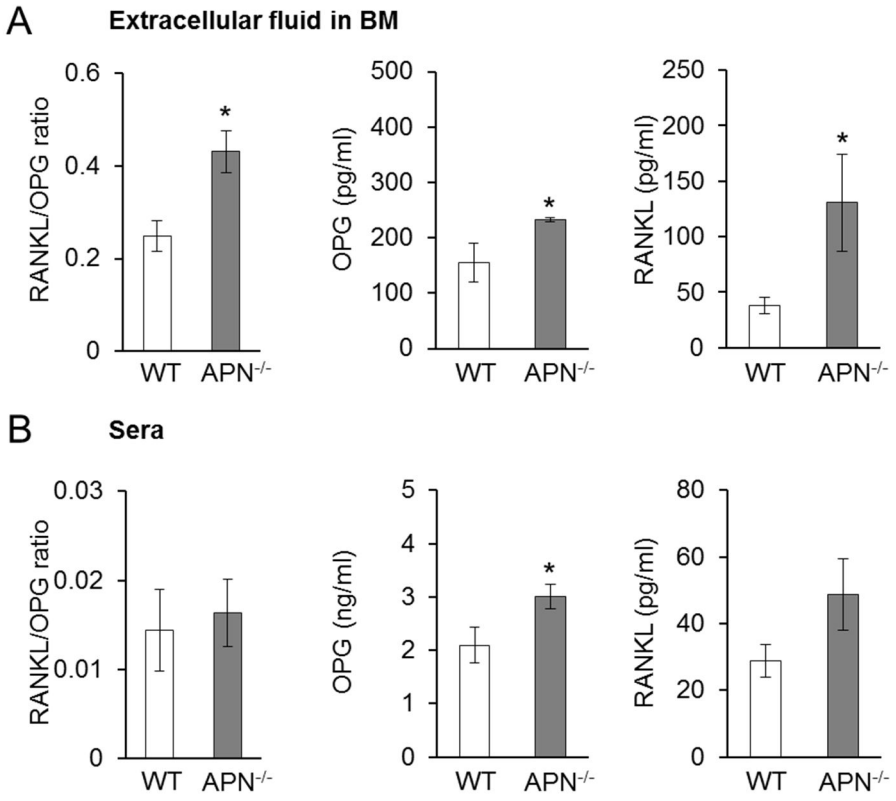

Figure 40. Increased RANKL/OPG ratio is observed in the bone marrow but not the serum of adiponectin-deficient mice. (A) The bone marrow extracellular fluids were obtained by flushing two tibias with 500 μl of pre-chilled PBS. (B) The serum was separated from blood of mice (n = 3 per group). The amounts of OPG and RANKL in the bone marrow and the serum were determined by ELISA. A ratio of RANKL/OPG was calculated from the amounts of RANKL and OPG. *$P < 0.05$ when compared with wild-type mice.

2.5. Adiponectin deficiency facilitates RANKL-induced bone resorption

Finally, to investigate if adiponectin deficiency facilitates bone resorption, mice were intraperitoneally administrated with 200 μg per mouse of RANKL. Micro-CT analysis demonstrated that both trabecular bone volume and trabecular number in the femur of adiponectin-deficient mice were reduced as those in the femur of RANKL-treated wild-type mice. In addition, administration with RANKL significantly decreased trabecular number and increased trabecular separation in adiponectin-deficient mice but not the wild-type mice. Notably, the lowest bone volume was found in the femur of RANKL-treated adiponectin-deficient mice (Fig. 41A and B), indicating that adiponectin deficiency could induce a condition favoring bone destruction. To further confirm in different skeletal sites of adiponectin-deficient mice, mouse calvaria were implanted with collagen sheets soaked in 5 μg per mouse of RANKL. Consistent with results of trabecular bone, calvarial bone volume of adiponectin-deficient mice was decreased as that of RANKL-treated wild-type mice. In addition, RANKL-induced bone resorption was also higher in the adiponectin-deficient mice than in the wild-type mice (the difference of resorbed calvarial volume between wild-type and adiponectin-deficient mice: 0.35 ± 0.09 mm^3, $p = 0.0190$ *vs.* 0.38 ± 0.11 mm^3, $p = 0.0002$). Moreover, the lowest bone volume was also observed in the RANKL-implanted calvarial bone of adiponectin-deficient mice (Fig. 41C and D). Taken together, these findings suggest that adiponectin deficiency facilitates bone resorption.

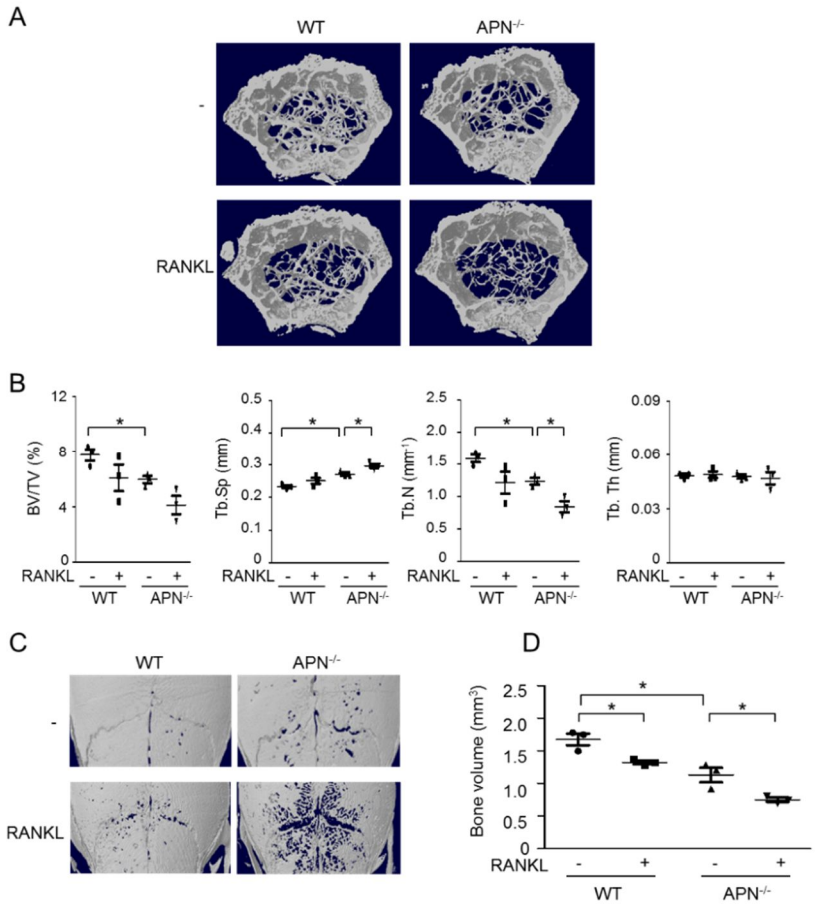

Figure 41. Adiponectin deficiency facilitates RANKL-induced bone resorption. (A and B) Mice (n = 3 per group) were intraperitoneally administered with 200 μg of RANKL twice with a 4-day interval. (A) At day 7 after the administration, the distal femurs were scanned to obtain three dimensional micro-CT images. N.S., not significant. (B) The femurs were analyzed to measure the trabecular bone parameters. (C and D) Collagen sheets soaked with 5 μg of GST-RANKL were implanted on mouse calvaria (n = 3 per group). After 7 days, the calvaria were subjected to micro-CT analysis. *$P < 0.05$ when compared with non-treated groups.

Chapter IV. Discussion

Controlling the osteoclastogenesis is important for an efficient treatment or prevention of bone diseases accompanying excessive osteoclastogenesis, such as bacteria-induced bone diseases and osteoporosis. Therefore, it is important to identify the molecular targets controlling osteoclastogenesis and to characterize their regulatory mechanisms. This study demonstrated that LTA and adiponectin inhibit osteoclastogenesis through distinct molecular mechanisms.

1. Inhibitory role of LTA in osteoclastogenesis

Bacterial infection could not only induce an immune response but also interfere with bone homeostasis by shifting the balance of osteoclasts and osteoblasts in the skeletal system. The prominent role of Gram-positive bacteria in chronic inflammatory bone diseases has received attention to the cell-signaling molecules such as MAMPs, and the responses of osteoclasts and osteoblasts in particular. Here, this study demonstrated that inactivated LTA-deficient *S. aureus* excessively induced bone destruction and enhanced osteoclastogenesis compared with wild-type *S. aureus*. Furthermore, the results showed that the LTA purified from *S. aureus* inhibited the generation of osteoclasts derived from both macrophages and committed osteoclast precursors, although *S. aureus* LTA alone affected neither bone destruction nor osteoclastogenesis. This study further identified action mechanisms for the *S. aureus* LTA-mediated inhibition of both osteoclast differentiation and bone resorption via (i) suppression of ERK, JNK, and AP-1 activation through TLR2 with partial involvement with MyD88 pathway in the macrophages and (ii) suppression of MAPKs activation and actin polymerization

through TLR2-independent pathway in the committed osteoclast precursors, as summarized in Fig. 42.

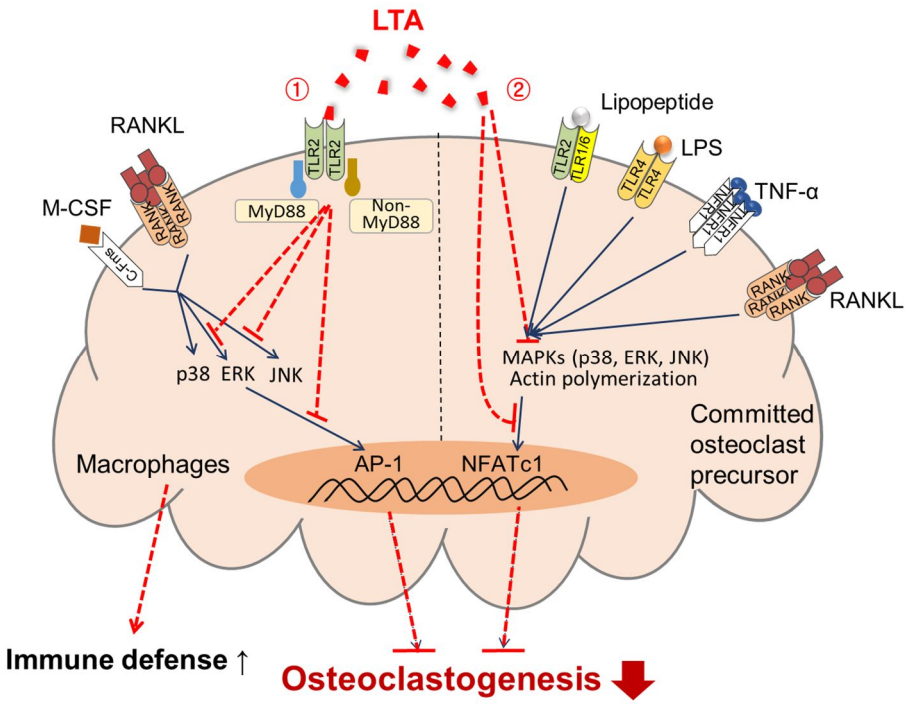

Figure 42. Schematic illustration of the proposed action mechanism of LTA on osteoclastogenesis. LTA inhibits osteoclast differentiation and bone resorption. LTA suppresses the activation of ERK, JNK, and AP-1 though TLR2 with partial involvement of MyD88 in macrophages. In addition, LTA inhibits the activation of MAP kinases, actin polymerization, and NFATc1 through TLR2-independent pathway in committed osteoclast precursors.

The study observed that LTA-deficient *S. aureus* augmented massive bone destruction and excessive osteoclastogenesis compared with wild-type *S. aureus*, indicating the possibility that LTA may inhibit osteoclastogenesis. Previous reports showed that LTA-deficient *S. aureus* possesses more potent pathogenic ability than the wild-type strain [95]. Administration with LTA-deficient *S. aureus* induced higher mortality rate in mouse than that of wild-type *S. aureus* [95]. In addition, LTA-deficient *S. aureus* was reported to be barely recognized in splenic macrophages and to be escaped from phagocytosis in drosophila hemocytes, leading to continuous activation of host immune cells followed by excessive inflammation [96]. Therefore, LTA-deficient *S. aureus* might continuously activate osteoclast precursors to differentiate osteoclasts leading to massive bone resorption

LTA stimulating TLR2 inhibited the differentiation of macrophages to osteoclasts. However, this phenomenon is not restricted to LTA. Previous reports have demonstrated that TLR ligands originated from both bacteria and the host have also such effect [30, 41]. For example, LPS is reported to inhibit RANKL-induced osteoclast differentiation and activation through TLR4 [30]. *P. gingivalis* and bacterial lipoproteins are also reported to inhibit RANKL-induced osteoclastogenesis from macrophages through TLR2 [97]. Notably, previous reports showed that hyaluronan as an extracellular matrix component inhibits RANKL-induced osteoclastogenesis through TLR4 [98].

LTA inhibited M-CSF/RANKL-induced osteoclast differentiation from macrophages in this study. The inhibitory effect of LTA apparently required TLR2, but signaling through MyD88-dependent pathway was partially involved in this phenomenon. Almost all TLRs except TLR3 trigger MyD88-dependent signaling pathways [39]. Previous reports also showed that TLR2 and MyD88 are required for LTA-induced heme oxygenage-1 expression in human tracheal smooth muscle cells [85]. However, MyD88-independent pathway may also participate in TLR2 signaling. For instance, acute ischemic renal injury was dependent on TLR2

signaling in conjunction with MyD88-independent and MyD88-dependent pathways [99]. Indeed, LTA inhibited LPS or TNF-α-induced neutrophil recruitment through TLR2-dependent and MyD88-independent pathway [100]. Thus, MyD88-independent pathway may be also important for LTA-mediated inhibition of osteoclastogenesis.

This study also demonstrated that LTA inhibited osteoclast differentiation from committed osteoclast precursors. Notably, LTA attenuated osteoclast differentiation triggered by *S. aureus*, virulence factors such as LPS and bacterial lipoproteins, TNF-α, and RANKL. Notably, the inhibitory effect of LTA stands in contrast finding in bacterial bone diseases such as bacterial arthritis, osteomyelitis, and periodontitis, which causes excessive osteoclastogenesis leading to massive bone resorption. Some possible hypotheses regarding this discrepancy can be made. First, LTA may have distinct properties unlike other MAMPs such as LPS and bacterial lipopeptides. LTA is less potent to trigger immune response than LPS or bacterial lipoproteins, and instead can negatively control immune response [86, 95]. Second, LTA would be recognized by various binding receptors expressed on committed osteoclast precursors. Several reports have suggested that LTA can inhibit robust immune response through binding to gelsolin or paired immunoglobulin-like receptor B (PIR-B) [86, 95]. Thus, LTA may inhibit osteoclastogenesis, unlike other MAMPs such as LPS and lipoproteins through unique mechanisms.

The inhibitory effect of LTA on osteoclast differentiation from committed osteoclasts was mediated by attenuating MAPKs activation and actin polymerization via TLR2-independent pathway. This study could not fully resolve the TLR-independent pathway in the LTA-suppressed osteoclastogenesis, but could offer the possible mechanism conferred by LTA-binding proteins. Several reports have demonstrated that LTA-binding proteins such as gelsolin, CD14, and mannose-binding protein (MBP) are able to either facilitate LTA-mediated immune responses or inhibit the LTA-induced immune responses [86, 95, 101, 102]. Among the LTA-

binding proteins, gelsolin is a well-known actin binding protein responsible for actin filament assembly to regulate actin cytoskeleton [87]. A previous report showed that LTA directly binds to the active site of gelsolin, resulting in the impairment of gelsolin and actin dissociation [86]. Thus, the interaction of LTA with gelsolin might be an important mechanism for LTA-mediated inhibition of osteoclast differentiation contributing to suppression of severe bone resorption.

Conclusively, the present study suggests that LTA might be an important factor capable of inhibiting osteoclastogenesis. LTA contributes to suppression of osteoclastogenesis through inhibition of intracellular signals required for osteoclastogenesis in committed osteoclast precursors as well as macrophages. These findings call for further research to develop effective therapeutics using LTA for the prevention and treatment of bone diseases.

2. Inhibitory role of adiponectin in osteoclastogenesis

Osteoporosis is a representative bone disease that has distinct characteristics of both decreased bone mass and increased bone marrow adiposity. Excessive generation of adipocytes could lead to a decrease of adiponectin production in bone marrow, which affects differentiation of both osteoclasts and osteoblasts. Nevertheless, the effect of adiponectin on bone metabolism has not been sufficiently investigated. Here, this study demonstrated that adiponectin-deficient mice showed decreased bone mass by both enhancing bone resorption and suppressing bone formation instead of increasing bone marrow adiposity by enhancing adipocyte formation. This study further identified three mechanisms for the decreased bone mass under the adiponectin deficiency via (i) skewed differentiation potential toward adipocytes of osteoblast precursors, (ii) up-regulation of RANKL/OPG ratio in osteoblast precursors, and (iii) degenerated differentiation of both osteoclasts and osteoblasts from their precursors, as summarized in Fig. 43.

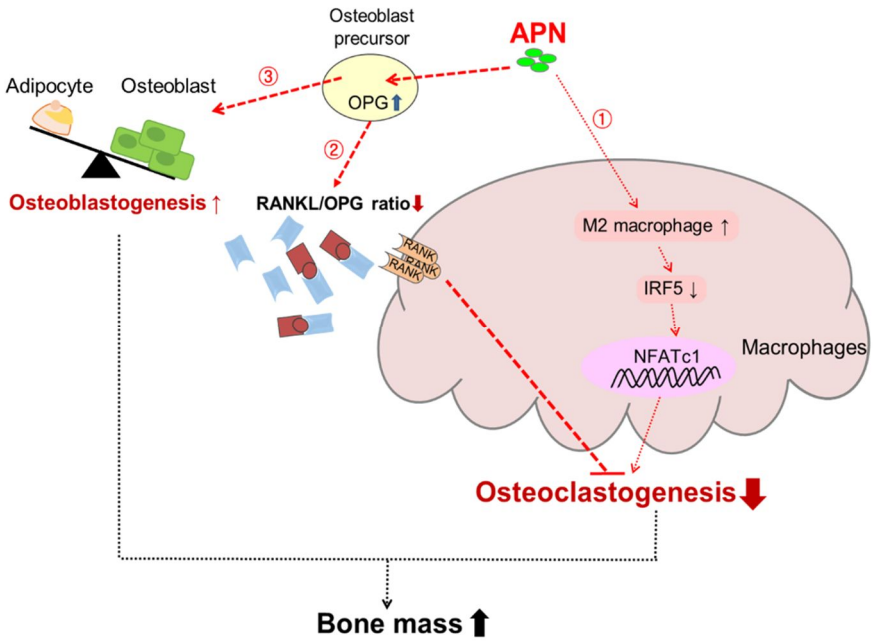

Figure 43. Schematic illustration of the proposed action mechanism of adiponectin on osteoclastogenesis. Adiponectin directly induces osteoclast differentiation via inhibition of NFATc1 activation and IRF5 expression through polarization toward M2 macrophages with enhanced osteoclastogenic potential. In bone microenvironment, however, adiponectin inhibits osteoclast differentiation via down-regulation of RANKL/OPG ratio through induction of OPG production in osteoblast precursors. In addition, adiponectin induces differentiation of osteoblast precursors into osteoblasts rather than adipocytes contributing to an increase of bone mass. APN, adiponectin

Our findings that adiponectin deficiency decreased bone mass are in agreement with previous reports. Transgenic mice overexpressing adiponectin and adiponectin-administered mice, both exhibited an increase of bone mass [70, 78, 103]. However, opposite results were also reported. Some reports showed that adiponectin-deficient mice exhibited normal bone mass [71, 72], increased bone mass below fourteen-week-old mice [72, 73], or decreased bone mass by aging [73]. One possible explanation of this discrepancy is a difference in the genetic background of animals used in those studies. Consistent with the results observed in this study, Wu et al. also observed that adiponectin-deficient mice, considered congenic following ten generations of backcrossing into C57BL/6 mice, exhibited decreased bone mass but increased bone marrow adiposity [74]. However, such effects were not shown in adiponectin-deficient mice obtained before backcrossing ten generations [72, 73]. The other possible explanation is a difference of housing conditions. Bone metabolism is known to be affected by environmental factors such as chow materials, lighting, and the number of mice per cage [104-106]. Nevertheless, further study is needed to comprehensively address this question on the discrepancy.

This study showed that adiponectin-deficient osteoblast precursors had weak osteoblastogenic potential but, instead, efficient adipogenic potential. Adiponectin has been reported to induce osteoblast differentiation and to inhibit adipocyte differentiation [77, 107]. Because osteoblasts and adipocytes differentiate from common mesenchymal cell lineage, attenuation of osteoblast or adipocyte differentiation can result in enhancement of adipocyte or osteoblast differentiation, respectively [8]. Adipokines have been reported to modulate differentiation of osteoblasts and adipocytes. For instance, leptin promoted osteoblast differentiation but inhibited adipocyte differentiation [59]. In contrast, chemerin attenuated osteoblast differentiation but increased adipocyte differentiation [64]. Notably, clinical studies also showed that plasma adiponectin levels are decreased in patients with type 2 diabetes mellitus accompanying decreased bone mineral density and increased bone marrow adiposity [108]. Therefore, adiponectin deficiency might skew differentiation of the mesenchymal cell lineages toward adipocytes rather than

osteoblasts, thereby contributing to decreased bone mass and increased bone marrow adiposity.

Our results demonstrated that adiponectin deficiency increased RANKL/OPG ratio in both calvarial osteoblast precursor culture and bone marrow, resulting in enhancement of osteoclast differentiation. In contrast, treatment with adiponectin suppressed osteoclast differentiation by inducing OPG production, indicating that adiponectin can induce down-regulation of RANKL/OPG ratio. RANKL promotes osteoclast differentiation through recognition of RANK expression on osteoclast precursors, while OPG suppresses osteoclast differentiation through inhibition of RANKL-RANK interaction by sequestering RANKL [109]. Accordingly, up-regulation of RANKL/OPG ratio can trigger excessive bone resorption leading to a decrease of bone mass, whereas down-regulation of that can attenuate bone resorption contributing to an increase of bone mass [109]. Previous reports have also shown that the RANKL/OPG ratio is up-regulated in the culture supernatants of mesenchymal stem cells obtained from patients with osteoporosis [110] and the bone of age-related osteoporosis mouse model [111]. Therefore, adiponectin deficiency might be one of important factors capable of up-regulating RANKL/OPG ratio, thereby leading to a decrease of bone mass.

This study observed an increase of bone resorption in the femur of adiponectin-deficient mice, implying that adiponectin-deficient osteoclast precursors would efficiently differentiate into osteoclasts. However, adiponectin-deficient macrophages were barely differentiated into osteoclasts even in the co-culture of wild-type osteoblast precursors. Some possible explanations regarding this discrepancy can be suggested. First, adiponectin-deficient macrophages had immunological features of M1 macrophages as well as weak osteoclastogenic potential in this study. Macrophages are classified into inflammatory M1 and anti-inflammatory M2 macrophages [21]. Adiponectin induced M2 macrophages, but its deficiency promoted M1 macrophages [91, 112]. Several reports have suggested that M1 polarizing factors such as IRF5 and STAT1 inhibit osteoclast

differentiation [113, 114], whereas M2 polarizing factors such as IRF4 and PPARγ promote osteoclast differentiation [115, 116]. Notably, this study revealed that IRF5, a major transcription factor for macrophage plasticity, was important for determining osteoclastogenic potential depending on macrophage subtypes. Thus, weak osteoclastogenic potential of adiponectin-deficient macrophages is due to a feature of M1 macrophages. Second, the features of macrophages were analyzed in the absence of other cell types, such as osteoblasts, stromal cells, and immune cell. Osteoclast differentiation is controlled by interaction with other cell types as well as by osteoclastogenic potential of macrophages [20]. Importantly, osteoclast differentiation was enhanced in the co-culture with adiponectin-deficient osteoblast precursors in this study. Therefore, the interaction between osteoclasts and osteoblasts is crucial for elucidating the *in vivo* phenomenon.

Adiponectin deficiency attenuated differentiation of both osteoclasts and osteoblasts in our study. Because appropriate bone turnover is required for maintaining normal bone mass through the balance between osteoclasts and osteoblasts [1], impaired differentiation of osteoclasts and osteoblasts can ultimately result in low bone turnover leading to various bone diseases, in particular age-related osteoporosis [117] and chronic glucocorticoid-induced osteoporosis [118]. Notably, low bone turnover is observed in obese or type 2 diabetic patients with decreased levels of serum adiponectin [119, 120], suggesting that a decrease of adiponectin production may influence occurrence of bone diseases mediated by low bone turnover. Therefore, adiponectin deficiency might induce low bone turnover leading to the decrease of bone mass.

Conclusively, *in vivo* and *in vitro* results in this study suggested that adiponectin deficiency might be an important factor for decreasing bone mass but, instead, for increasing bone marrow adiposity. Adiponectin could develop as an efficient target molecule for a treatment or prevention of bone diseases characterized by decreased bone mass with increased bone marrow adiposity.

Chapter V. References

1. Sims, N. A. and Vrahnas, C. (2014) **Regulation of cortical and trabecular bone mass by communication between osteoblasts, osteocytes and osteoclasts**. *Arch Biochem Biophys*. 561:22-8.
2. Raggatt, L. J. and Partridge, N. C. (2010) **Cellular and molecular mechanisms of bone remodeling**. *J Biol Chem.* 285:25103-8.
3. Teitelbaum, S. L. (2000) **Bone resorption by osteoclasts**. *Science* 289:1504-8.
4. Teitelbaum, S. L. (1993) **Bone remodeling and the osteoclast**. *J Bone Miner Res.* 8 Suppl 2:S523-5.
5. Centrella, M., McCarthy, T. L., Canalis, E. (1991) **Transforming growth factor-beta and remodeling of bone**. *J Bone Joint Surg Am.* 73:1418-28.
6. Hayden, J. M., Mohan, S., Baylink, D. J. (1995) **The insulin-like growth factor system and the coupling of formation to resorption**. *Bone* 17:93S-98S.
7. Garnero, P., Sornay-Rendu, E., Chapuy, M. C., Delmas, P. D. (1996) **Increased bone turnover in late postmenopausal women is a major determinant of osteoporosis**. *J Bone Miner Res.* 11:337-49.
8. Rosen, C. J. and Bouxsein, M. L. (2006) **Mechanisms of disease: is osteoporosis the obesity of bone?** *Nat Clin Pract Rheumatol.* 2:35-43.
9. Abdallah, B. M., Haack-Sorensen, M., Fink, T., Kassem, M. (2006) **Inhibition of osteoblast differentiation but not adipocyte differentiation of mesenchymal stem cells by sera obtained from aged females**. *Bone* 39:181-8.
10. Redlich, K. and Smolen, J. S. (2012) **Inflammatory bone loss: pathogenesis and therapeutic intervention**. *Nat Rev Drug Discov.* 11:234-50.
11. Henderson, B. and Nair, S. P. (2003) **Hard labour: bacterial infection of the skeleton**. *Trends Microbiol.* 11:570-7.
12. Lew, D. P. and Waldvogel, F. A. (1997) **Osteomyelitis**. *N Engl J Med.* 336:999-1007.
13. Shank, C. F. and Feibel, J. B. (2006) **Osteomyelitis in the diabetic foot: diagnosis and management**. *Foot Ankle Clin.* 11:775-89.
14. Udagawa, N., Takahashi, N., Akatsu, T., Tanaka, H., Sasaki, T., Nishihara, T., Koga, T., Martin, T. J., Suda, T. (1990) **Origin of osteoclasts: mature monocytes and macrophages are capable of differentiating into osteoclasts under a suitable microenvironment prepared by bone marrow-derived stromal cells**. *Proc Natl Acad Sci U S A* 87:7260-4.

15. Lacey, D. L., Timms, E., Tan, H. L., Kelley, M. J., Dunstan, C. R., Burgess, T., Elliott, R., Colombero, A., Elliott, G., Scully, S., Hsu, H., Sullivan, J., Hawkins, N., Davy, E., Capparelli, C., Eli, A., Qian, Y. X., Kaufman, S., Sarosi, I., Shalhoub, V., Senaldi, G., Guo, J., Delaney, J., Boyle, W. J. (1998) **Osteoprotegerin ligand is a cytokine that regulates osteoclast differentiation and activation**. *Cell* 93:165-76.
16. Fakhry, M., Hamade, E., Badran, B., Buchet, R., Magne, D. (2013) **Molecular mechanisms of mesenchymal stem cell differentiation towards osteoblasts**. *World J Stem Cells* 5:136-48.
17. Takayanagi, H. (2009) **Osteoimmunology and the effects of the immune system on bone**. *Nat Rev Rheumatol.* 5:667-76.
18. Sato, K., Suematsu, A., Nakashima, T., Takemoto-Kimura, S., Aoki, K., Morishita, Y., Asahara, H., Ohya, K., Yamaguchi, A., Takai, T., Kodama, T., Chatila, T. A., Bito, H., Takayanagi, H. (2006) **Regulation of osteoclast differentiation and function by the CaMK-CREB pathway**. *Nat Med.* 12:1410-6.
19. Takayanagi, H., Kim, S., Koga, T., Nishina, H., Isshiki, M., Yoshida, H., Saiura, A., Isobe, M., Yokochi, T., Inoue, J., Wagner, E. F., Mak, T. W., Kodama, T., Taniguchi, T. (2002) **Induction and activation of the transcription factor NFATc1 (NFAT2) integrate RANKL signaling in terminal differentiation of osteoclasts**. *Dev Cell* 3:889-901.
20. Wada, T., Nakashima, T., Hiroshi, N., Penninger, J. M. (2006) **RANKL-RANK signaling in osteoclastogenesis and bone disease**. *Trends Mol Med.* 12:17-25.
21. Lawrence, T. and Natoli, G. (2011) **Transcriptional regulation of macrophage polarization: enabling diversity with identity**. *Nat Rev Immunol.* 11:750-61.
22. Sica, A. and Mantovani, A. (2012) **Macrophage plasticity and polarization: in vivo veritas**. *J Clin Invest.* 122:787-95.
23. Hamilton, J. A. (2008) **Colony-stimulating factors in inflammation and autoimmunity**. *Nat Rev Immunol.* 8:533-44.
24. Satoh, T., Kidoya, H., Naito, H., Yamamoto, M., Takemura, N., Nakagawa, K., Yoshioka, Y., Morii, E., Takakura, N., Takeuchi, O., Akira, S. (2013) **Critical role of Trib1 in differentiation of tissue-resident M2-like macrophages**. *Nature* 495:524-8.
25. Mosser, D. M. and Edwards, J. P. (2008) **Exploring the full spectrum of macrophage activation**. *Nat Rev Immunol.* 8:958-69.

26. Krausgruber, T., Blazek, K., Smallie, T., Alzabin, S., Lockstone, H., Sahgal, N., Hussell, T., Feldmann, M., Udalova, I. A. (2011) **IRF5 promotes inflammatory macrophage polarization and TH1-TH17 responses**. *Nat Immunol.* 12:231-8.
27. Kodama, H., Nose, M., Niida, S., Yamasaki, A. (1991) **Essential role of macrophage colony-stimulating factor in the osteoclast differentiation supported by stromal cells**. *J Exp Med.* 173:1291-4.
28. Souza, P. P. and Lerner, U. H. (2013) **The role of cytokines in inflammatory bone loss**. *Immunol Invest.* 42:555-622.
29. Takeshita, S., Kaji, K., Kudo, A. (2000) **Identification and characterization of the new osteoclast progenitor with macrophage phenotypes being able to differentiate into mature osteoclasts**. *J Bone Miner Res.* 15:1477-88.
30. Takami, M., Kim, N., Rho, J., Choi, Y. (2002) **Stimulation by toll-like receptors inhibits osteoclast differentiation**. *J Immunol.* 169:1516-23.
31. Liu, J., Wang, S., Zhang, P., Said-Al-Naief, N., Michalek, S. M., Feng, X. (2009) **Molecular mechanism of the bifunctional role of lipopolysaccharide in osteoclastogenesis**. *J Biol Chem.* 284:12512-23.
32. Maruyama, K., Takada, Y., Ray, N., Kishimoto, Y., Penninger, J. M., Yasuda, H., Matsuo, K. (2006) **Receptor activator of NF-kappa B ligand and osteoprotegerin regulate proinflammatory cytokine production in mice**. *J Immunol.* 177:3799-805.
33. Asagiri, M. and Takayanagi, H. (2007) **The molecular understanding of osteoclast differentiation**. *Bone* 40:251-64.
34. Park-Min, K. H., Ji, J. D., Antoniv, T., Reid, A. C., Silver, R. B., Humphrey, M. B., Nakamura, M., Ivashkiv, L. B. (2009) **IL-10 suppresses calcium-mediated costimulation of receptor activator NF-kappa B signaling during human osteoclast differentiation by inhibiting TREM-2 expression**. *J Immunol.* 183:2444-55.
35. Guarner, F. and Malagelada, J. R. (2003) **Gut flora in health and disease**. *Lancet.* 361:512-9.
36. O'Hara, A. M. and Shanahan, F. (2006) **The gut flora as a forgotten organ**. *EMBO Rep.* 7:688-93.
37. Kayaoglu, G. and Orstavik, D. (2004) **Virulence factors of Enterococcus faecalis: relationship to endodontic disease**. *Crit Rev Oral Biol Med.* 15:308-20.
38. Bar-Shavit, Z. (2008) **Taking a toll on the bones: regulation of bone metabolism by innate immune regulators**. *Autoimmunity* 41:195-203.

39. West, A. P., Koblansky, A. A., Ghosh, S. (2006) **Recognition and signaling by toll-like receptors**. *Annu Rev Cell Dev Biol.* 22:409-37.
40. O'Neill, L. A., Golenbock, D., Bowie, A. G. (2013) **The history of Toll-like receptors - redefining innate immunity**. *Nat Rev Immunol.* 13:453-60.
41. Zou, W., Schwartz, H., Endres, S., Hartmann, G., Bar-Shavit, Z. (2002) **CpG oligonucleotides: novel regulators of osteoclast differentiation**. *FASEB J.* 16:274-82.
42. Kim, J., Yang, J., Park, O. J., Kang, S. S., Kim, W. S., Kurokawa, K., Yun, C. H., Kim, H. H., Lee, B. L., Han, S. H. (2013) **Lipoproteins are an important bacterial component responsible for bone destruction through the induction of osteoclast differentiation and activation**. *J Bone Miner Res.* 28:2381-91.
43. Suda, T., Jimi, E., Nakamura, I., Takahashi, N. (1997) **Role of 1 alpha,25-dihydroxyvitamin D3 in osteoclast differentiation and function**. *Methods Enzymol.* 282:223-35.
44. Amcheslavsky, A., Hemmi, H., Akira, S., Bar-Shavit, Z. (2005) **Differential contribution of osteoclast- and osteoblast-lineage cells to CpG-oligodeoxynucleotide (CpG-ODN) modulation of osteoclastogenesis**. *J Bone Miner Res.* 20:1692-9.
45. Ha, H., Lee, J. H., Kim, H. N., Kwak, H. B., Kim, H. M., Lee, S. E., Rhee, J. H., Kim, H. H., Lee, Z. H. (2008) **Stimulation by TLR5 modulates osteoclast differentiation through STAT1/IFN-beta**. *J Immunol.* 180:1382-9.
46. Hussain Mian, A., Saito, H., Alles, N., Shimokawa, H., Aoki, K., Ohya, K. (2008) **Lipopolysaccharide-induced bone resorption is increased in TNF type 2 receptor-deficient mice in vivo**. *J Bone Miner Metab.* 26:469-77.
47. Yang, J., Ryu, Y. H., Yun, C. H., Han, S. H. (2009) **Impaired osteoclastogenesis by staphylococcal lipoteichoic acid through Toll-like receptor 2 with partial involvement of MyD88**. *J Leukoc Biol.* 86:823-31.
48. Sato, N., Takahashi, N., Suda, K., Nakamura, M., Yamaki, M., Ninomiya, T., Kobayashi, Y., Takada, H., Shibata, K., Yamamoto, M., Takeda, K., Akira, S., Noguchi, T., Udagawa, N. (2004) **MyD88 but not TRIF is essential for osteoclastogenesis induced by lipopolysaccharide, diacyl lipopeptide, and IL-1alpha**. *J Exp Med.* 200:601-11.
49. Jiang, J., Zuo, J., Hurst, I. R., Holliday, L. S. (2003) **The synergistic effect of peptidoglycan and lipopolysaccaride on osteoclast formation**. *Oral Surg Oral Med Oral Pathol Oral Radiol Endod.* 96:738-43.

50. Miyamoto, A., Takami, M., Matsumoto, A., Mochizuki, A., Yamada, T., Tachi, K., Shibuya, I., Nakamachi, T., Shioda, S., Baba, K., Inoue, T., Miyamoto, Y., Yim, M., Kamijo, R. (2012) **R848, a toll-like receptor 7 agonist, inhibits osteoclast differentiation but not survival or bone-resorbing function of mature osteoclasts**. *Cytotechnology* 64:331-9.
51. Morath, S., Geyer, A., Hartung, T. (2001) **Structure-function relationship of cytokine induction by lipoteichoic acid from Staphylococcus aureus**. *J Exp Med.* 193:393-7.
52. Wicken, A. J. and Knox, K. W. (1975) **Lipoteichoic acids: a new class of bacterial antigen**. *Science* 187:1161-7.
53. Thiemermann, C. (2002) **Interactions between lipoteichoic acid and peptidoglycan from Staphylococcus aureus: a structural and functional analysis**. *Microbes Infect.* 4:927-35.
54. Gao, J. J., Xue, Q., Zuvanich, E. G., Haghi, K. R., Morrison, D. C. (2001) **Commercial preparations of lipoteichoic acid contain endotoxin that contributes to activation of mouse macrophages in vitro**. *Infect Immun.* 69:751-7.
55. Ouchi, N., Parker, J. L., Lugus, J. J., Walsh, K. (2011) **Adipokines in inflammation and metabolic disease**. *Nat Rev Immunol.* 11:85-97.
56. Lago, F., Gomez, R., Gomez-Reino, J. J., Dieguez, C., Gualillo, O. (2009) **Adipokines as novel modulators of lipid metabolism**. *Trends Biochem Sci.* 34:500-10.
57. Fantuzzi, G. (2005) **Adipose tissue, adipokines, and inflammation**. *J Allergy Clin Immunol.* 115:911-9; quiz 920.
58. Gong, H., Ni, Y., Guo, X., Fei, L., Pan, X., Guo, M., Chen, R. (2004) **Resistin promotes 3T3-L1 preadipocyte differentiation**. *Eur J Endocrinol.* 150:885-92.
59. Thomas, T., Gori, F., Khosla, S., Jensen, M. D., Burguera, B., Riggs, B. L. (1999) **Leptin acts on human marrow stromal cells to enhance differentiation to osteoblasts and to inhibit differentiation to adipocytes**. *Endocrinology* 140:1630-8.
60. Liu, Y., Song, C. Y., Wu, S. S., Liang, Q. H., Yuan, L. Q., Liao, E. Y. (2013) **Novel adipokines and bone metabolism**. *Int J Endocrinol.* 2013:895045.
61. Holloway, W. R., Collier, F. M., Aitken, C. J., Myers, D. E., Hodge, J. M., Malakellis, M., Gough, T. J., Collier, G. R., Nicholson, G. C. (2002) **Leptin inhibits osteoclast generation**. *J Bone Miner Res.* 17:200-9.

62. Lamghari, M., Tavares, L., Camboa, N., Barbosa, M. A. (2006) **Leptin effect on RANKL and OPG expression in MC3T3-E1 osteoblasts**. *J Cell Biochem.* 98:1123-9.
63. Gordeladze, J. O., Drevon, C. A., Syversen, U., Reseland, J. E. (2002) **Leptin stimulates human osteoblastic cell proliferation, de novo collagen synthesis, and mineralization: Impact on differentiation markers, apoptosis, and osteoclastic signaling**. *J Cell Biochem.* 85:825-36.
64. Muruganandan, S., Roman, A. A., Sinal, C. J. (2010) **Role of chemerin/CMKLR1 signaling in adipogenesis and osteoblastogenesis of bone marrow stem cells**. *J Bone Miner Res.* 25:222-34.
65. Muruganandan, S., Dranse, H. J., Rourke, J. L., McMullen, N. M., Sinal, C. J. (2013) **Chemerin neutralization blocks hematopoietic stem cell osteoclastogenesis**. *Stem Cells* 31:2172-82.
66. Xie, H., Xie, P. L., Luo, X. H., Wu, X. P., Zhou, H. D., Tang, S. Y., Liao, E. Y. (2012) **Omentin-1 exerts bone-sparing effect in ovariectomized mice**. *Osteoporos Int.* 23:1425-36.
67. Cornish, J., Callon, K. E., Bava, U., Lin, C., Naot, D., Hill, B. L., Grey, A. B., Broom, N., Myers, D. E., Nicholson, G. C., Reid, I. R. (2002) **Leptin directly regulates bone cell function in vitro and reduces bone fragility in vivo**. *J Endocrinol.* 175:405-15.
68. Thommesen, L., Stunes, A. K., Monjo, M., Grosvik, K., Tamburstuen, M. V., Kjobli, E., Lyngstadaas, S. P., Reseland, J. E., Syversen, U. (2006) **Expression and regulation of resistin in osteoblasts and osteoclasts indicate a role in bone metabolism**. *J Cell Biochem.* 99:824-34.
69. Berner, H. S., Lyngstadaas, S. P., Spahr, A., Monjo, M., Thommesen, L., Drevon, C. A., Syversen, U., Reseland, J. E. (2004) **Adiponectin and its receptors are expressed in bone-forming cells**. *Bone* 35:842-9.
70. Oshima, K., Nampei, A., Matsuda, M., Iwaki, M., Fukuhara, A., Hashimoto, J., Yoshikawa, H., Shimomura, I. (2005) **Adiponectin increases bone mass by suppressing osteoclast and activating osteoblast**. *Biochem Biophys Res Commun.* 331:520-6.
71. Shinoda, Y., Yamaguchi, M., Ogata, N., Akune, T., Kubota, N., Yamauchi, T., Terauchi, Y., Kadowaki, T., Takeuchi, Y., Fukumoto, S., Ikeda, T., Hoshi, K., Chung, U. I., Nakamura, K., Kawaguchi, H. (2006) **Regulation of bone formation by adiponectin through autocrine/paracrine and endocrine pathways**. *J Cell Biochem.* 99:196-208.
72. Williams, G. A., Wang, Y., Callon, K. E., Watson, M., Lin, J. M., Lam, J. B., Costa, J. L., Orpe, A., Broom, N., Naot, D., Reid, I. R., Cornish, J. (2009) **In**

vitro and in vivo effects of adiponectin on bone. *Endocrinology* 150:3603-10.

73. Kajimura, D., Lee, H. W., Riley, K. J., Arteaga-Solis, E., Ferron, M., Zhou, B., Clarke, C. J., Hannun, Y. A., DePinho, R. A., Guo, X. E., Mann, J. J., Karsenty, G. (2013) **Adiponectin regulates bone mass via opposite central and peripheral mechanisms through FoxO1**. *Cell Metab.* 17:901-15.
74. Wu, Y., Tu, Q., Valverde, P., Zhang, J., Murray, D., Dong, L. Q., Cheng, J., Jiang, H., Rios, M., Morgan, E., Tang, Z., Chen, J. (2014) **Central adiponectin administration reveals new regulatory mechanisms of bone metabolism in mice**. *Am J Physiol Endocrinol Metab.* 306:E1418-30.
75. Mohammadzadeh, G. and Zarghami, N. (2011) **Hypoadiponectinemia in obese subjects with type II diabetes: A close association with central obesity indices**. *J Res Med Sci.* 16:713-23.
76. Tu, Q., Zhang, J., Dong, L. Q., Saunders, E., Luo, E., Tang, J., Chen, J. (2011) **Adiponectin inhibits osteoclastogenesis and bone resorption via APPL1-mediated suppression of Akt1**. *J Biol Chem.* 286:12542-53.
77. Lee, H. W., Kim, S. Y., Kim, A. Y., Lee, E. J., Choi, J. Y., Kim, J. B. (2009) **Adiponectin stimulates osteoblast differentiation through induction of COX2 in mesenchymal progenitor cells**. *Stem Cells* 27:2254-62.
78. Zhang, L., Meng, S., Tu, Q., Yu, L., Tang, Y., Dard, M. M., Kim, S. H., Valverde, P., Zhou, X., Chen, J. (2014) **Adiponectin ameliorates experimental periodontitis in diet-induced obesity mice**. *PLoS One* 9:e97824.
79. Oku, Y., Kurokawa, K., Matsuo, M., Yamada, S., Lee, B. L., Sekimizu, K. (2009) **Pleiotropic roles of polyglycerolphosphate synthase of lipoteichoic acid in growth of Staphylococcus aureus cells**. *J Bacteriol.* 191:141-51.
80. Han, S. H., Kim, J. H., Seo, H. S., Martin, M. H., Chung, G. H., Michalek, S. M., Nahm, M. H. (2006) **Lipoteichoic acid-induced nitric oxide production depends on the activation of platelet-activating factor receptor and Jak2**. *J Immunol.* 176:573-9.
81. Takahashi, N., Yamana, H., Yoshiki, S., Roodman, G. D., Mundy, G. R., Jones, S. J., Boyde, A., Suda, T. (1988) **Osteoclast-like cell formation and its regulation by osteotropic hormones in mouse bone marrow cultures**. *Endocrinology* 122:1373-82.
82. Zhu, S. Q., Qi, L., Rui, Y. F., Li, R. X., He, X. P., Xie, Z. P. (2008) **Astragaloside IV inhibits spontaneous synaptic transmission and synchronized Ca2+ oscillations on hippocampal neurons**. *Acta Pharmacol Sin.* 29:57-64.

83. Ellingsen, E., Morath, S., Flo, T., Schromm, A., Hartung, T., Thiemermann, C., Espevik, T., Golenbock, D., Foster, D., Solberg, R., Aasen, A., Wang, J. (2002) **Induction of cytokine production in human T cells and monocytes by highly purified lipoteichoic acid: involvement of Toll-like receptors and CD14**. *Med Sci Monit.* 8:BR149-56.
84. Velayudham, A., Hritz, I., Dolganiuc, A., Mandrekar, P., Kurt-Jones, E., Szabo, G. (2006) **Critical role of toll-like receptors and the common TLR adaptor, MyD88, in induction of granulomas and liver injury**. *J Hepatol.* 45:813-24.
85. Lee, I. T., Wang, S. W., Lee, C. W., Chang, C. C., Lin, C. C., Luo, S. F., Yang, C. M. (2008) **Lipoteichoic acid induces HO-1 expression via the TLR2/MyD88/c-Src/NADPH oxidase pathway and Nrf2 in human tracheal smooth muscle cells**. *J Immunol.* 181:5098-110.
86. Bucki, R., Byfield, F. J., Kulakowska, A., McCormick, M. E., Drozdowski, W., Namiot, Z., Hartung, T., Janmey, P. A. (2008) **Extracellular gelsolin binds lipoteichoic acid and modulates cellular response to proinflammatory bacterial wall components**. *J Immunol.* 181:4936-44.
87. Wang, Q., Xie, Y., Du, Q. S., Wu, X. J., Feng, X., Mei, L., McDonald, J. M., Xiong, W. C. (2003) **Regulation of the formation of osteoclastic actin rings by proline-rich tyrosine kinase 2 interacting with gelsolin**. *J Cell Biol.* 160:565-75.
88. Jacquin, C., Gran, D. E., Lee, S. K., Lorenzo, J. A., Aguila, H. L. (2006) **Identification of multiple osteoclast precursor populations in murine bone marrow**. *J Bone Miner Res.* 21:67-77.
89. Kobayashi, N., Kadono, Y., Naito, A., Matsumoto, K., Yamamoto, T., Tanaka, S., Inoue, J. (2001) **Segregation of TRAF6-mediated signaling pathways clarifies its role in osteoclastogenesis**. *EMBO J.* 20:1271-80.
90. Mandal, P., Pratt, B. T., Barnes, M., McMullen, M. R., Nagy, L. E. (2011) **Molecular mechanism for adiponectin-dependent M2 macrophage polarization: link between the metabolic and innate immune activity of full-length adiponectin**. *J Biol Chem.* 286:13460-9.
91. Ohashi, K., Parker, J. L., Ouchi, N., Higuchi, A., Vita, J. A., Gokce, N., Pedersen, A. A., Kalthoff, C., Tullin, S., Sams, A., Summer, R., Walsh, K. (2010) **Adiponectin promotes macrophage polarization toward an anti-inflammatory phenotype**. *J Biol Chem.* 285:6153-60.
92. Francke, A., Herold, J., Weinert, S., Strasser, R. H., Braun-Dullaeus, R. C. (2011) **Generation of mature murine monocytes from heterogeneous bone**

marrow and description of their properties. *J Histochem Cytochem.* 59:813-25.

93. Fleetwood, A. J., Dinh, H., Cook, A. D., Hertzog, P. J., Hamilton, J. A. (2009) **GM-CSF- and M-CSF-dependent macrophage phenotypes display differential dependence on type I interferon signaling**. *J Leukoc Biol.* 86:411-21.
94. Ji, J. D., Park-Min, K. H., Shen, Z., Fajardo, R. J., Goldring, S. R., McHugh, K. P., Ivashkiv, L. B. (2009) **Inhibition of RANK expression and osteoclastogenesis by TLRs and IFN-gamma in human osteoclast precursors**. *J Immunol.* 183:7223-33.
95. Nakayama, M., Kurokawa, K., Nakamura, K., Lee, B. L., Sekimizu, K., Kubagawa, H., Hiramatsu, K., Yagita, H., Okumura, K., Takai, T., Underhill, D. M., Aderem, A., Ogasawara, K. (2012) **Inhibitory receptor paired Ig-like receptor B is exploited by Staphylococcus aureus for virulence**. *J Immunol.* 189:5903-11.
96. Hashimoto, Y., Tabuchi, Y., Sakurai, K., Kutsuna, M., Kurokawa, K., Awasaki, T., Sekimizu, K., Nakanishi, Y., Shiratsuchi, A. (2009) **Identification of lipoteichoic acid as a ligand for draper in the phagocytosis of Staphylococcus aureus by Drosophila hemocytes**. *J Immunol.* 183:7451-60.
97. Zhang, P., Liu, J., Xu, Q., Harber, G., Feng, X., Michalek, S. M., Katz, J. (2011) **TLR2-dependent modulation of osteoclastogenesis by Porphyromonas gingivalis through differential induction of NFATc1 and NF-kappaB**. *J Biol Chem.* 286:24159-69.
98. Chang, E. J., Kim, H. J., Ha, J., Kim, H. J., Ryu, J., Park, K. H., Kim, U. H., Lee, Z. H., Kim, H. M., Fisher, D. E., Kim, H. H. (2007) **Hyaluronan inhibits osteoclast differentiation via Toll-like receptor 4**. *J Cell Sci.* 120:166-76.
99. Shigeoka, A. A., Holscher, T. D., King, A. J., Hall, F. W., Kiosses, W. B., Tobias, P. S., Mackman, N., McKay, D. B. (2007) **TLR2 is constitutively expressed within the kidney and participates in ischemic renal injury through both MyD88-dependent and -independent pathways**. *J Immunol.* 178:6252-8.
100. Long, E. M., Klimowicz, A. C., Paula-Neto, H. A., Millen, B., McCafferty, D. M., Kubes, P., Robbins, S. M. (2011) **A subclass of acylated anti-inflammatory mediators usurp Toll-like receptor 2 to inhibit neutrophil recruitment through peroxisome proliferator-activated receptor gamma**. *Proc Natl Acad Sci U S A* 108:16357-62.

101. Polotsky, V. Y., Fischer, W., Ezekowitz, R. A., Joiner, K. A. (1996) **Interactions of human mannose-binding protein with lipoteichoic acids**. *Infect Immun.* 64:380-3.
102. Schroder, N. W., Morath, S., Alexander, C., Hamann, L., Hartung, T., Zahringer, U., Gobel, U. B., Weber, J. R., Schumann, R. R. (2003) **Lipoteichoic acid (LTA) of Streptococcus pneumoniae and Staphylococcus aureus activates immune cells via Toll-like receptor (TLR)-2, lipopolysaccharide-binding protein (LBP), and CD14, whereas TLR-4 and MD-2 are not involved**. *J Biol Chem.* 278:15587-94.
103. Mitsui, Y., Gotoh, M., Fukushima, N., Shirachi, I., Otabe, S., Yuan, X., Hashinaga, T., Wada, N., Mitsui, A., Yoshida, T., Yoshida, S., Yamada, K., Nagata, K. (2011) **Hyperadiponectinemia enhances bone formation in mice**. *BMC Musculoskelet Disord.* 12:18.
104. Parhami, F., Tintut, Y., Beamer, W. G., Gharavi, N., Goodman, W., Demer, L. L. (2001) **Atherogenic high-fat diet reduces bone mineralization in mice**. *J Bone Miner Res.* 16:182-8.
105. Nagy, T. R., Krzywanski, D., Li, J., Meleth, S., Desmond, R. (2002) **Effect of group vs. single housing on phenotypic variance in C57BL/6J mice**. *Obes Res.* 10:412-5.
106. Ostrowska, Z., Kos-Kudla, B., Marek, B., Kajdaniuk, D. (2003) **Influence of lighting conditions on daily rhythm of bone metabolism in rats and possible involvement of melatonin and other hormones in this process**. *Endocr Regul.* 37:163-74.
107. Yokota, T., Meka, C. S., Medina, K. L., Igarashi, H., Comp, P. C., Takahashi, M., Nishida, M., Oritani, K., Miyagawa, J., Funahashi, T., Tomiyama, Y., Matsuzawa, Y., Kincade, P. W. (2002) **Paracrine regulation of fat cell formation in bone marrow cultures via adiponectin and prostaglandins**. *J Clin Invest.* 109:1303-10.
108. Tamura, T., Yoneda, M., Yamane, K., Nakanishi, S., Nakashima, R., Okubo, M., Kohno, N. (2007) **Serum leptin and adiponectin are positively associated with bone mineral density at the distal radius in patients with type 2 diabetes mellitus**. *Metabolism* 56:623-8.
109. Hofbauer, L. C., Khosla, S., Dunstan, C. R., Lacey, D. L., Boyle, W. J., Riggs, B. L. (2000) **The roles of osteoprotegerin and osteoprotegerin ligand in the paracrine regulation of bone resorption**. *J Bone Miner Res.* 15:2-12.
110. Dalle Carbonare, L., Valenti, M. T., Zanatta, M., Donatelli, L., Lo Cascio, V. (2009) **Circulating mesenchymal stem cells with abnormal osteogenic differentiation in patients with osteoporosis**. *Arthritis Rheum.* 60:3356-65.

111. Cao, J., Venton, L., Sakata, T., Halloran, B. P. (2003) **Expression of RANKL and OPG correlates with age-related bone loss in male C57BL/6 mice**. *J Bone Miner Res*. 18:270-7.
112. Lovren, F., Pan, Y., Quan, A., Szmitko, P. E., Singh, K. K., Shukla, P. C., Gupta, M., Chan, L., Al-Omran, M., Teoh, H., Verma, S. (2010) **Adiponectin primes human monocytes into alternative anti-inflammatory M2 macrophages**. *Am J Physiol Heart Circ Physiol.* 299:656-63.
113. Takayanagi, H., Kim, S., Matsuo, K., Suzuki, H., Suzuki, T., Sato, K., Yokochi, T., Oda, H., Nakamura, K., Ida, N., Wagner, E. F., Taniguchi, T. (2002) **RANKL maintains bone homeostasis through c-Fos-dependent induction of interferon-beta**. *Nature* 416:744-9.
114. Zhao, B., Takami, M., Yamada, A., Wang, X., Koga, T., Hu, X., Tamura, T., Ozato, K., Choi, Y., Ivashkiv, L. B., Takayanagi, H., Kamijo, R. (2009) **Interferon regulatory factor-8 regulates bone metabolism by suppressing osteoclastogenesis**. *Nat Med.* 15:1066-71.
115. Wan, Y., Chong, L. W., Evans, R. M. (2007) **PPAR-gamma regulates osteoclastogenesis in mice**. *Nat Med.* 13:1496-503.
116. Nakashima, Y. and Haneji, T. (2013) **Stimulation of osteoclast formation by RANKL requires interferon regulatory factor-4 and is inhibited by simvastatin in a mouse model of bone loss**. *PLoS One* 8:e72033.
117. Duque, G. and Troen, B. R. (2008) **Understanding the mechanisms of senile osteoporosis: new facts for a major geriatric syndrome**. *J Am Geriatr Soc.* 56:935-41.
118. Dalle Carbonare, L., Arlot, M. E., Chavassieux, P. M., Roux, J. P., Portero, N. R., Meunier, P. J. (2001) **Comparison of trabecular bone microarchitecture and remodeling in glucocorticoid-induced and postmenopausal osteoporosis**. *J Bone Miner Res.* 16:97-103.
119. Krakauer, J. C., McKenna, M. J., Buderer, N. F., Rao, D. S., Whitehouse, F. W., Parfitt, A. M. (1995) **Bone loss and bone turnover in diabetes**. *Diabetes* 44:775-82.
120. Viljakainen, H., Ivaska, K. K., Paldanius, P., Lipsanen-Nyman, M., Saukkonen, T., Pietilainen, K. H., Andersson, S., Laitinen, K., Makitie, O. (2014) **Suppressed bone turnover in obesity: a link to energy metabolism? A case-control study**. *J Clin Endocrinol Metab.* 99:2155-63.

국문초록

리포테이코산과 아디포넥틴에 의한 파골세포의 분화 조절

양지현

서울대학교 치의학대학원
치의과학과 면역 및 분자미생물 전공

(지도교수 한 승 현)

목적

골조직은 불필요한 골을 파괴시키는 파골세포와 새로운 골을 생성하는 조골세포의 균형에 의해 골 항상성이 유지된다. 골 흡수를 담당하는 파골세포는 선천성 면역세포인 대식세포로부터 분화하며, 파골세포의 비정상적 분화는 다양한 골질환의 발병과 밀접하게 연관되기 때문에 파골세포 분화를 조절하는 것은 골질환의 예방과 치료에 매우 중요하다. 파골세포의 분화는 골 미세환경에 존재하는 세포와 내인성 인자들 뿐만 아니라 미생물 또는 미생물 유래 인자들에 의해 영향을 받는다. 특히, 감염성 골질환의 주요 원인균인 그람양성세균은 세포 표면에 리포테이코산을 발현하는데 현재까지 파골세포 분화 조절에 리포테이코산이 미치는 영향에 대해서는 전혀 보고된 바 없다. 또한 대표적 골질환인 골다공증은 골량의 감소와 함께 골조직 내 지방세포가 증가되는 특성을 가지는데, 지방세포에서 주로 분비되는 아디포넥틴은 면역 및 대사과정에 중요한 역할을 한다고 보고되었으나 골 항상성과 파골세포의 분화 조절에 미치는 영향에 대해서는 아직 명확하지 않다. 따라서 본 연구에서는 파골세포의 분화 조절에 리포테이코산과 아디포넥틴이 미치는 영향에 대해 알아보고 그 작용기전을 규명하고자 하였다.

실험방법

리포테이코산이 골 항상성에 관여하는지 확인하기 위해, 야생형 황색포도상구균 또는 리포테이코산-결여 균을 쥐의 복강 내 주입하거나 황색포도상구균에서 분리한 리포테이코산을 지질펩타이드와 단독 또는 복합으로 쥐의 두개골 위에 이식하였다. 파골세포의 분화는 기질세포를 제거한 골수세포를 macrophage colony-stimulating factor (M-CSF)와 배양하여 얻은 대식세포를 이용해 M-CSF 와 receptor activator of NF-κB ligand (RANKL)과 추가 배양하여 유도하였으며, 이 때 황색포도상구균 또는 리포테이코산을 함께 처리하였다. 또한 후기 파골전구세포인 RANKL 이 전처리 된 대식세포를 이용하여 M-CSF 만 존재하는 상태에서 리포테이코산을 황색포도상구균, 지질펩타이드, 내독소, 종양괴사인자-알파, 또는 RANKL 과 단독 또는 복합 처리하였다.

파골세포 분화 조절에 아디포넥틴의 역할을 규명하기 위해, 야생형 쥐와 아디포넥틴-결여 쥐를 이용하였다. 두개골에서 조골전구세포를 분리한 후 조골세포 또는 지방세포로 분화를 유도하였으며, 골수 유래 대식세포를 이용하여 파골세포로 분화를 유도하였다. 아디포넥틴 결핍 시 파골세포 분화능의 차이가 대식세포 아형과 관련되는지 확인하기 위해, granulocyte/macrophage colony-stimulating factor 에 의해 분화된 M1 대식세포와 M-CSF 에 의해 분화된 M2 대식세포를 사용하였다. 골 미세환경을 대변하는 시험관 내 방법인 조골전구세포-대식세포 공배양을 통해 파골세포 분화를 유도하였다. 생체 내 골 소실 정도를 확인하기 위해, RANKL 을 쥐의 복강 내 주입 또는 두개골 위에 이식하였다.

미세단층촬영기법을 이용해 대퇴골 내 소주골 또는 두개골의 골량을 분석하였다. 헤마톡실린/에오신 또는 tartrate-resistant acid phosphatase (TRAP)이 염색된 조직절편에서 골흡수, 골생성, 지방생성 관련 인자들을 측정하였다. 파골세포 분화는 TRAP 염색 시 세 개 이상의 핵을 갖는 TRAP-양성 다핵세포의 수를 측정하여 확인하였다. 파골세포

활성은 칼슘인산-부착 판에서 세포배양 후 생성된 흡수 면적을 측정하여 평가하였다. 신호전달인자의 인산화와 c-Fos 와 NFATc1 의 발현 정도를 Western blotting 으로 확인하였고, AP-1 과 NFATc1 의 DNA-결합 활성은 electrophoric mobility shift assay 를 통해 확인하였다. 조골세포 분화는 alkaline phosphatase 또는 Alizarin Red S 염색으로, 지방세포 분화는 Oil Red O 염색을 통해 확인하였다. RANKL 과 osteoprotegerin (OPG)의 발현은 세포 배양액, 혈청, 골수 내 세포외액을 사용해 효소면역측정법으로 확인하였다.

결과

리포테이코산-결여 황색포도상구균은 야생형 황색포도상구균에 비해 더 강한 골 소실을 유발했고, 후기 파골전구세포로부터 파골세포의 분화를 강하게 유도하였다. 하지만 리포테이코산 단독은 생체 내/외 모두에서 골 소실 또는 파골세포 분화에 영향을 주지 않았다. 대신 리포테이코산은 RANKL 에 의한 대식세포의 파골세포 분화 억제하였으며, 이 억제기전은 톨유사수용체-2 (toll-like receptor 2, TLR2)를 경유하여 MyD88 의존/비의존적 경로를 통해 일어났다. 또한 리포테이코산은 황색포도상구균, 지질펩타이드, 내독소, 종양괴사인자-알파에 의해 유도되는 후기 파골전구세포로부터의 파골세포 분화 역시 강하게 억제하였다. 이 억제기전은 TLR2 를 경유하지 않으며 파골세포 분화와 활성 과정 중 액틴 결합반응에 필수적인 액틴-젤솔린의 해리를 억제하였다. 따라서 리포테이코산은 파골세포 분화를 직접적으로 억제하는 핵심 인자임을 확인하였다.

아디포넥틴-결여 쥐는 대퇴골 또는 두개골의 골량이 정상 쥐에 비해 감소되어 있었고, 대퇴골 내 골흡수의 증가, 골생성의 감소, 골 내 지방 증가되어 있었다. 생체 내 현상과 동일하게, 아디포넥틴-결여 쥐에서 분리한 조골전구세포는 정상세포와 비교 시 조골세포의 분화는 억제된 반면 지방세포의 분화는 향상되었다. 하지만 파골세포의 분화를 확인한 결과 아디포넥틴-결여 대식세포가 정상세포에 비해 TRAP-양성 다핵세포의 생성, 골 흡수능, AP-1 과 NFATc1 의 DNA-결합 활성이

현저히 억제되었다. 또한 저해된 파골세포 분화능을 가진 아디포넥틴 결여 쥐의 대식세포는 M1 대식세포의 특성을 가지고 있었는데, M1 대식세포 분화의 핵심 인자인 인터페론 조절인자 5 의 발현 증가가 RANKL 신호전달을 억제하기 때문인 것을 확인하였다. 다른 한편으로 골 미세환경을 대변하는 조골전구세포와 대식세포의 공배양 시, 파골세포 분화가 아디포넥틴-결여 조골전구세포와 공배양한 경우 증가함을 확인하였다. 특히, 파골세포 활성지표인 RANKL/OPG 비율의 증가가 아디포넥틴-결여 조골세포의 배양액과 아디포넥틴-결여 쥐의 골수 내 세포외액에서 동일하게 관찰되었다. 또한 생체 내 골소실의 정도가 아디포넥틴-결여 쥐에서 정상 쥐와 비교 시 증가하였다. 이를 통해 아디포넥틴이 파골세포와 조골세포의 분화를 모두 조절하는 인자임을 확인하였다.

결론

이상의 연구결과들로부터 다음과 같은 결론을 얻을 수 있었다. 리포테이코산은 직접적으로 파골세포 분화에 영향을 주지 않으나, 파골세포 활성화 인자들에 의해 유도되는 파골세포의 분화를 억제하는 것을 알 수 있었다. 아디포넥틴은 직접적으로 파골세포 분화를 향상시키나 조골세포로부터 분비되는 RANKL/OPG 비율을 억제하여 궁극적으로 파골세포 분화를 억제하며, 복합적으로 조골세포의 분화는 활성화시켜 골량을 증가시킨다. 결론적으로 리포테이코산과 아디포넥틴은 파골세포의 분화를 억제함으로써 궁극적으로 골대사를 조절하는데 기여한다.

주요어: 파골세포, 대식세포, 후기 파골전구세포, 아디포넥틴, 리포테이코산

학번: 2008-30634